doi : 10.17596/0003706

R/V Mirai Cruise Report

MR00-K04

June 13 - July 6, 2000

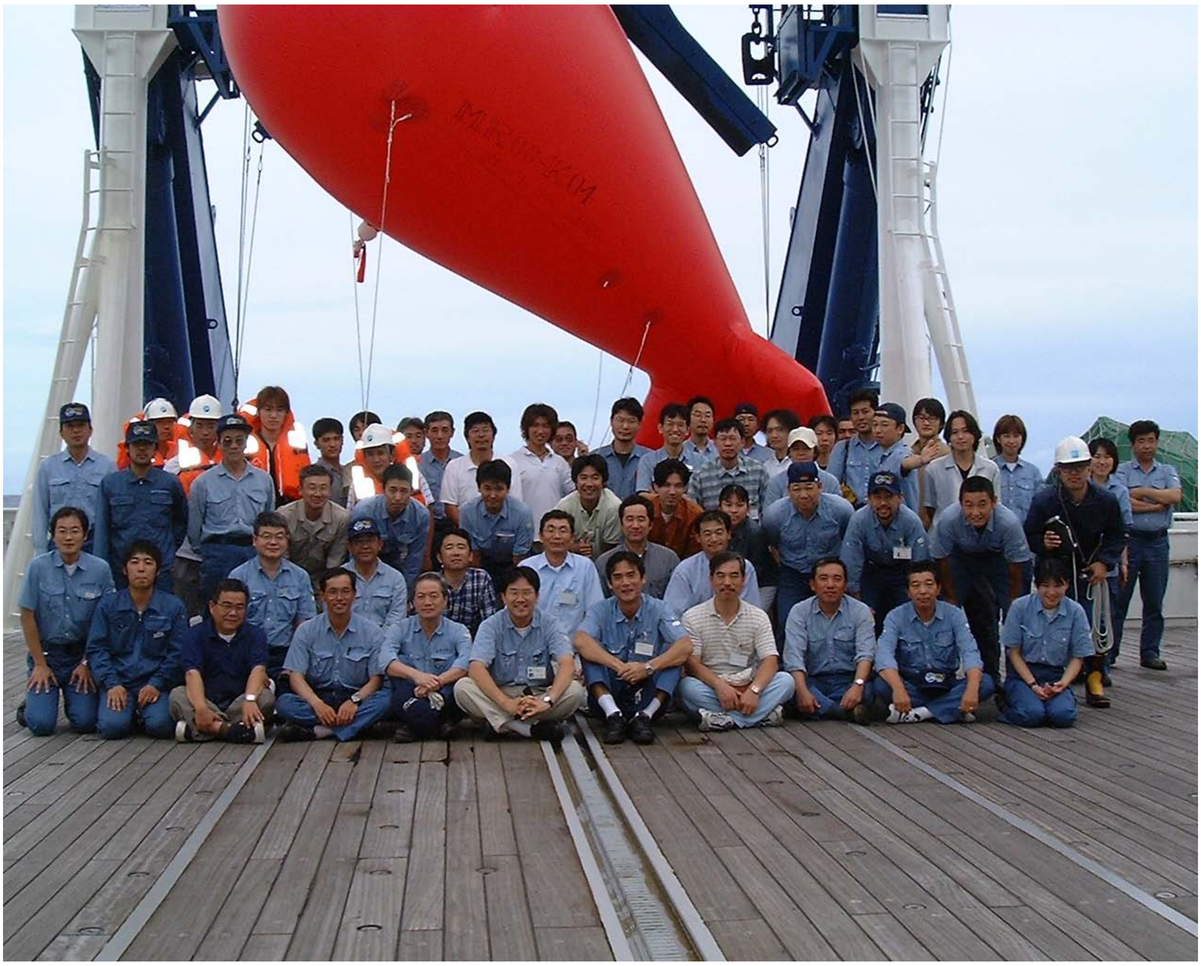

Japan Marine Science and Technology Center
(JAMSTEC)

MR00-K04 Cruise Report

[Contents]

7. Appendix

A. Data Policies on R/V Mirai

B. GMS Full Disk Images

C. Atmospheric Profiles (Emagram) on Radiosonde Observations

D. Daily Sky Images from Total Sky Imager

E. Oceanic Profiles on CTD Observations

F. Oceanic Profiles on Shallow Water CTD Observations

G. Obtained Data / Sample Inventory Information

1. Introduction

The intertropical convergence zone (ITCZ), where north-easterly and south-easterly trade winds encounter, is well known as convectively active region and produce much precipitation over the Ocean whole the year. It can be easily seen on the satellite cloud images as a zonal band of deep clouds between 5N and 15N. Usually, it consists of a number of cloud clusters with order of 100km and it is thought that they play key role for the heat balance over not only the Tropics but also the entire globe. As for the vertical heat balance, cumulonimbus clouds effectively bring the heat vertically through the pseudoadiabatic ascent. But these are “qualitative” ideas.

The R/V Mirai MR00-K04 cruise is designed to carry out the observation of deep convections developed in the ITCZ to reveal the internal structure of ITCZ “quantitatively” using shipboard C-band Doppler radar and other many measurement systems. Usually, ITCZ is easily defined in the central and eastern Pacific and Atlantic, and sometimes ambiguous in the tropical western Pacific. However, the relation between ITCZ and the warm water pool is also one important goal of this cruise.

The R/V Mirai departed Sekinehama in the very early morning of June 13, 2000 and called at Hachinohe on the same day. After leaving Hashinohe, it cruised southward along the 140E line from 30N to 5N. To surely get the clouds, we decided the stationary observation site during this cruising period using latest satellite data. We conducted the stationary observation at 7N, 140E from June 20 through June 30. During the twelve days, we could have many kinds of clouds developed in the ITCZ.

In addition to this main mission, various observations were carried out. We can say that this cruise consists of three major components; one is observation of precipitation, second is the air-sea interaction, and the third is the study of the aerosol and atmospheric chemistry. Especially, some scientists joined this cruise as part of preparation for the international project ACE Asia(Asian Pacific Regional Aerosol Characterization Experiment) to explore the shipboard observation of atmospheric chemistry.

This cruise report summarizes briefly these various observation items including personnel, objectives, methods, and preliminary results in addition to the cruise basic information. Please enjoy with this, as someone can recall the cruise, and someone can imagine the cruise.

2. Cruise Summary

2.1 Ship

Name	R/V MIRAI
L×B×D	128.6 m × 19.0 m × 13.2 m
Gross Tonnage	8,672 tons
Call sign	JNSR
Mother Port	Mutsu, Aomori Pref.

2.2 Cruise Code

MR00-K04

2.3 Project Name

The Study of Air-Sea Interaction in the Tropics

2.4 Undertaking Institute

Japan Marine Science and Technology Center (JAMSTEC)
2-15, Natsushima, Yokosuka 237-0061, JAPAN

2.5 Chief Scientist

Kunio Yoneyama (Ocean Research Department / JAMSTEC)

2.6 Periods and Ports of call

June 13, 2000	departed Mutsu, Aomori, Japan
June 13, 2000	called at Hachinohe, Aomori, Japan
July 6, 2000	arrived at Yokosuka, Kanagawa, Japan

2.7 Observation Summary

C-band Doppler radar		continuously (10minutes interval volume scan)
Radiosonde launching		94 times (every 3 hours during June 19-30)
Ceilometer		continuously (every 1 minutes)
Total Sky Imager		continuously (every 5 minutes)
LIDAR		continuously (every 10 seconds)
Surface Meteorology		continuously (every 6 seconds for Mirai Weather Station) (every 10 seconds for SOAR system)
Skin Sea Surface Temperature		continuously (every 10 seconds)
Turbulent Measurement		continuously (every 3 hours, 1 hour duration)
Aerosol sampling	by sampler on deck	continuously (vary with target)
	by kytoon	23 times

Sky radiometer	continuously
Spectral radiometer	occasionally in daytime
Sunphotometer	occasionally in daytime
Satellite receiving (SeaWiFS)	once a day
Wet and Dry deposition	collected once a day
CTD	48 times (down to 1000m) (every 5deg from 30N to 5N along 140E, and every 6 hours during June 20-30)
CTD with chlorophyll sensor	48 times (down to 200m)
ADCP	continuously (every 5 minutes)
Sea Surface Water Monitoring	continuously (every 1 minute)
PCO_2/pCO_2 measurement	continuously (surface) 7 times (vertical)
N_2O and CO_2 measurement	continuously (surface, every 6 hours during June 16-20, every 3 hours during June 26-28) 3 times (vertical)

2.8 Overview

During the stationary observation period, sea surface temperatures show higher than 30C.

In the lower troposphere, easterly trade winds were dominant and their 12 days mean wind speed of 1000-700 hPa layer was 6.7m/s.

In the earlier days of the stationary observation period, we observed well organized convections that could be identified to be accompanied with westward propagating equatorial Rossby wave from satellite cloud images. However, they are relatively shallow (7~8km) than we expected. It was relatively stable condition for convection in the following two days after above cloud system passed by observation area. Slightly dry layer can be seen above 0C level. In the last few days(June 26-30), deep convections often developed and produced much rain. They showed early morning maxima. On July 2 after we left the observation area, tropical depression occurred around 14N, 132E.

In addition to the main mission whose aim is precipitation measurement, various observations including solar radiation measurement, flux measurement, aerosol sampling/measuremnt were actively conducted during whole the cruise.

2.9 Acknowledgment

We'd like to express our special thanks to Cpatain T. Hashimoto and his crew for the skillful ship operation. Technical staff of Global Ocean Development Inc. and Marine Works Japan Ltd. provided highly assured data to obtain.

Personally, as a chief scientist of the cruise, I deeply appreciate all participants as I could enjoy the rainy days under the ITCZ with their collaboration and effort.

3. List of Instruments

3.1 Surface Meteorological Parameters

(a) JAMSTEC / Mirai Met System
- Anemometer: KE-500, Koshin Denki
- Thermometer: FT, Koshin Denki
- Dewpoint Meter DW-1, Koshin Denki
- Barometer: F-451, Yokogawa Co.
- Rain Gauge: 50202, R.M. Young
- Optical Rain Gauge: ORG-115DR, SCTI
- Wave Height Meter: MW-2, Tsurumi-seiki

(b) JAMSTEC / SOAR system
- Anemometer: 05106, R. M. Young
- Thermometer / Hygrometer: HMP45A, Vaisala
  (with 43408 Gill aspirated radiation shield, R.M.Young)
- Barometer: 61201, R. M. Young
- Rain Gauge: 50202, R. M. Young
- Optical Rain Gauge: ORG-115DA, ScTi
- Sea Surface Skin Tempreature Sensor: SST-100, Brookhaven National Lab.
- Shortwave Radiometer: PSP, Eppley Labs.
- Longwave Radiometer: PIR, Eppley Labs.
- Fast Rotating Shadowband Radiometer: Yankee Engineering Systems

(c) JAMSTEC / Total Sky Imager System
- Total Sky Imager: Yankee Engineering System

3.2 Radiosonde Observation

(a) JAMSTEC
- GPS radiosonde: RS-80-G, Vaisala
- Receiver: DigiCORA MW11, Vaisala

3.3 Doppler Radar Observation

(a) JAMSTEC
- C-band Doppler Radar: RC-52B, Mitsubishi Electric Co.
- Signal Processor: RVP-6, Sigmet
- Antenna Controller: RCP-02, Sigmet
- Control and Processing Software: IRIS/Open, Sigmet
- Inertial Navigation Unit: DRUH, Honeywell

3.4 Lidar Observation

(a) NIES and Tohoku Institute of Technology
- Compact Mie Scattering Lidar

(b) JAMSTEC
- Ceilometer: CT-25K, Vaisala

3.5 Surface Flux Measurement system

(a) MUK, FORSGC and Okayama Univ.

Supersonic Thermoanemometer: DA-600, Kaijo Co.
Infrared Hygrometer: AH-300, Kaijo Co.
Inclinometer: MD-900-T, Appied Geomechanics
Accelerometer: OA700-020, Applied Signal Inc.
Rate Gyros: QRS11-0050-100, Sytron Donner
Data Logging System: Labview, National Intsruments Co.
Infrared Radiation Thermometer: THI-700, TASCO
Data Logging System: CR-23X, Campbell Scientific Co.

3.6 Aerosol Sampling and Measurement

(a) SUT

Sampling Tower
Scanning Mobility Particle Sizer: 3936N25 (3085 + 2025A), TSI Inc.
Optical Particle Counters: KC18 and KC01, Rion Co. Ltd.
Radon Daughter Monitor: ES-7269, Japan Radiation Engineering Co., Ltd.
Kytoon: K. Y. S., Kikyu Seisakusyo
Optical Particle Counter: KR12, Rion Co. Ltd.
Portable Sunphotometer: MS-120(S), Eko Co.
Low Volume Sampler
Cascade Impactor: Model I-1L, PIXE Int.Corp.
SO_2 , NOX meter: GFS-32, DKK Co.

(b) ORI, Univ. of Tokyo

Ambient Carbon Particulate Monitor: Model 5400, Rupprechet & Patashnick Co. Inc.,
Ozone Monitor: Model 1150, Dylec,
Cellulose Acetate Filters: Whatman 41
High-Volume Air Sampler: Model SS-1003A, Kimoto Electric Co. Inc.
Quartz Fiber Filters: 2500QAT-UP, Pallflex
High-volume Virtual Impactor: Model AS9, Kimoto Electric Co. Inc.
Low-Volume Impactor
Low Pressure Impactor: Model LP-20, Tokyo Dylec

(c) ILTS, Hokkaido Univ. (group-a)

High Volume Air Sampler: HVC-1000N, Shibata
High Volume Air Sampler: Model-120F, Kimoto
Andersen-type High Volume Air Sampler: HVC-1000N, Shibata + Model AH-600Z, Dylec
Micro-Orifice Uniform Deposit Impactor: Model 110, MSP corp.
UV ozone monitor: Model 1150, Dylec
Quartz Fiber Filters: 2500QAT-UP, Pallflex

(d) ILTS, Hokkaido Univ. (group-b)
Sky Radiometer: POM-01MKII, PREDE
Particle Soot / Absorption Photometer: Radiance Research
Integrating Nephelometer: M903, Radiance Research
Optical Particle Counter: KC-01C, RION

3.7 Ocean Color Measurement

(a) MUK, Toba-CMT
Sunphotometer: MS120, Eiko Seiki Corp.
Polarization Spectral Radiometer: PSR1000, Opto Research Corp.
Multi-Spectral Radiometer: MSR7000, Opto Research Corp.
Spectroradiometer: GER1500, Geophysical & Environmental Research Corp.

3.8 CTD

(a) JAMSTEC
CTD Unit: 9 plus, Sea-Bird
Temperature Sensor: SBE3-04/F, Sea-Bird
Conductivity Sensor: SBE-4-04/0, Sea-Bird
Oxygen Sensor: SBE13-04-B, Sea-Bird.
Deck Unit: 11plus, Sea-Bird
Altimeter 2110-2, Benthos
Guildline Autosal Salinometer: model 8400B
Peristalitic-type Sample Intake Pump: Ocean Science International
Quartz Thermometer: model 2804A, Hewlett Packard
Quartz Probes: 18111A, Hewlett Packard

(b) MUK
Shallow Water Observation Unit: Chlorothec ACL-200DK, Alec Electronics Co. Ltd.
Secchi Disk

3.9 Current Profiling

(a) JAMSTEC
Broad-Band ADCP: VM-75, RD Instrument.

3.10 Sea Surface Water Monitoring

(a) JAMSTEC
Thermosalinograph: SEACAT SBE-21
Dissolved Oxygen Sensor: Oubisufair Laboratories
Fluorometer: 10-AU-005, Turner Designs
Particle Size Sensor: P-05, Nippon Kaiyo

3.11 N_2O and CO_2 Measurement

(a) MUK

CO_2 Infrared Gas Analyzer: VIA-510, HORIBA Ltd.
N_2O Infrared Gas Analyzer: 46C, Thermo Environmental Instruments Inc.

3.12 pCO_2/PCO_2 Measurement

(a) Okayama University of Science
CO2 Analyzer: LI-6252 LI-COR ,INC.
Gas Mixing Unit: SO96NL-T, S-ONE, INC.
Equilibrumeter: SO96NL-T, S-ONE, INC.

3.13 Miscellaneous

(a) JAMSTEC
Navigation System: SAINS19, Sena Co.
GMS Receiving System: Nippon Hakuyo
HRPT Receiving System: Terascan
Observation Data Acquisition System: SCS (Scientific Computer System), NOAA

4. Cruise Track and Log

4.1 Cruise Track

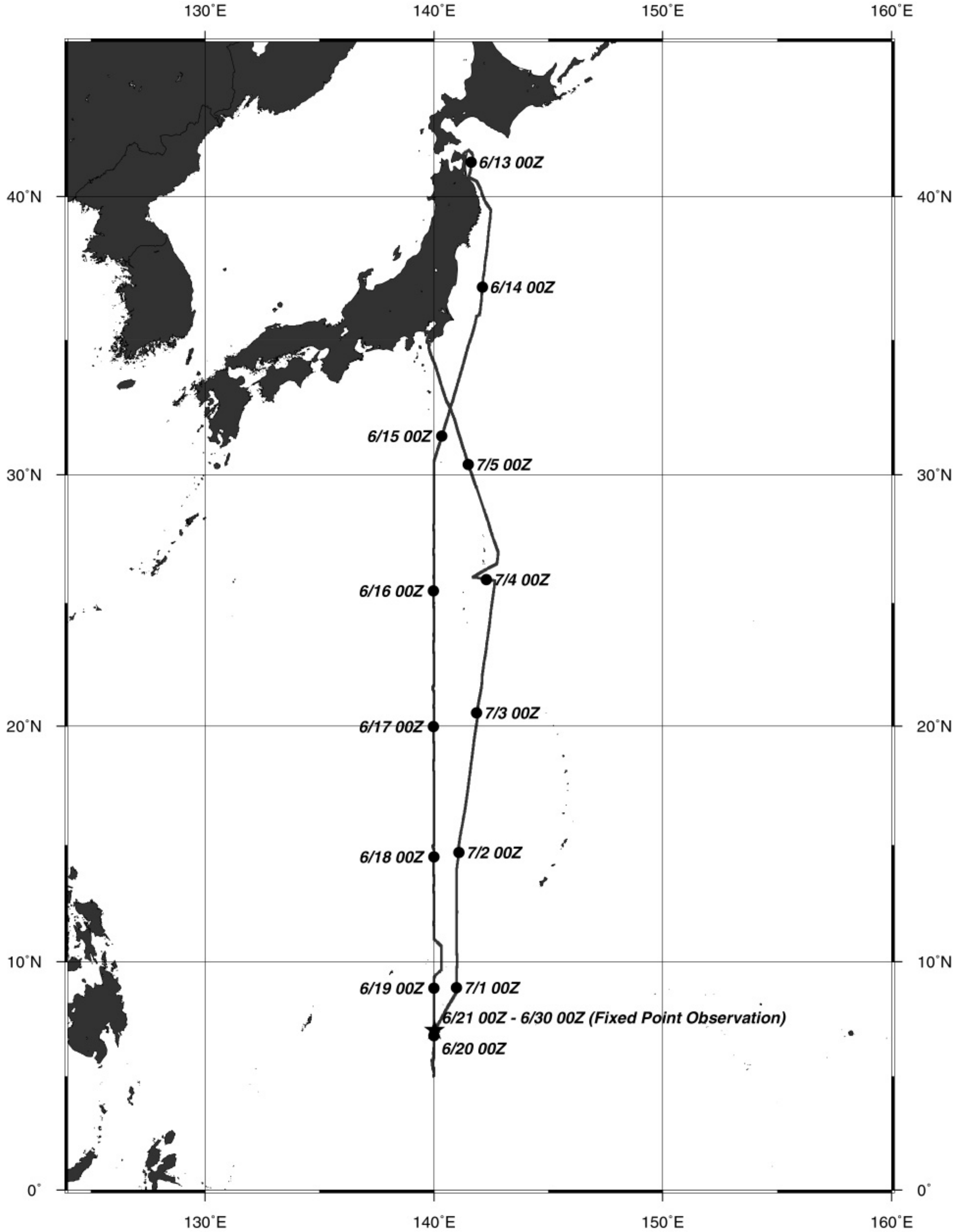

Fig.4.1-1: Cruise Track on MR00-K04.

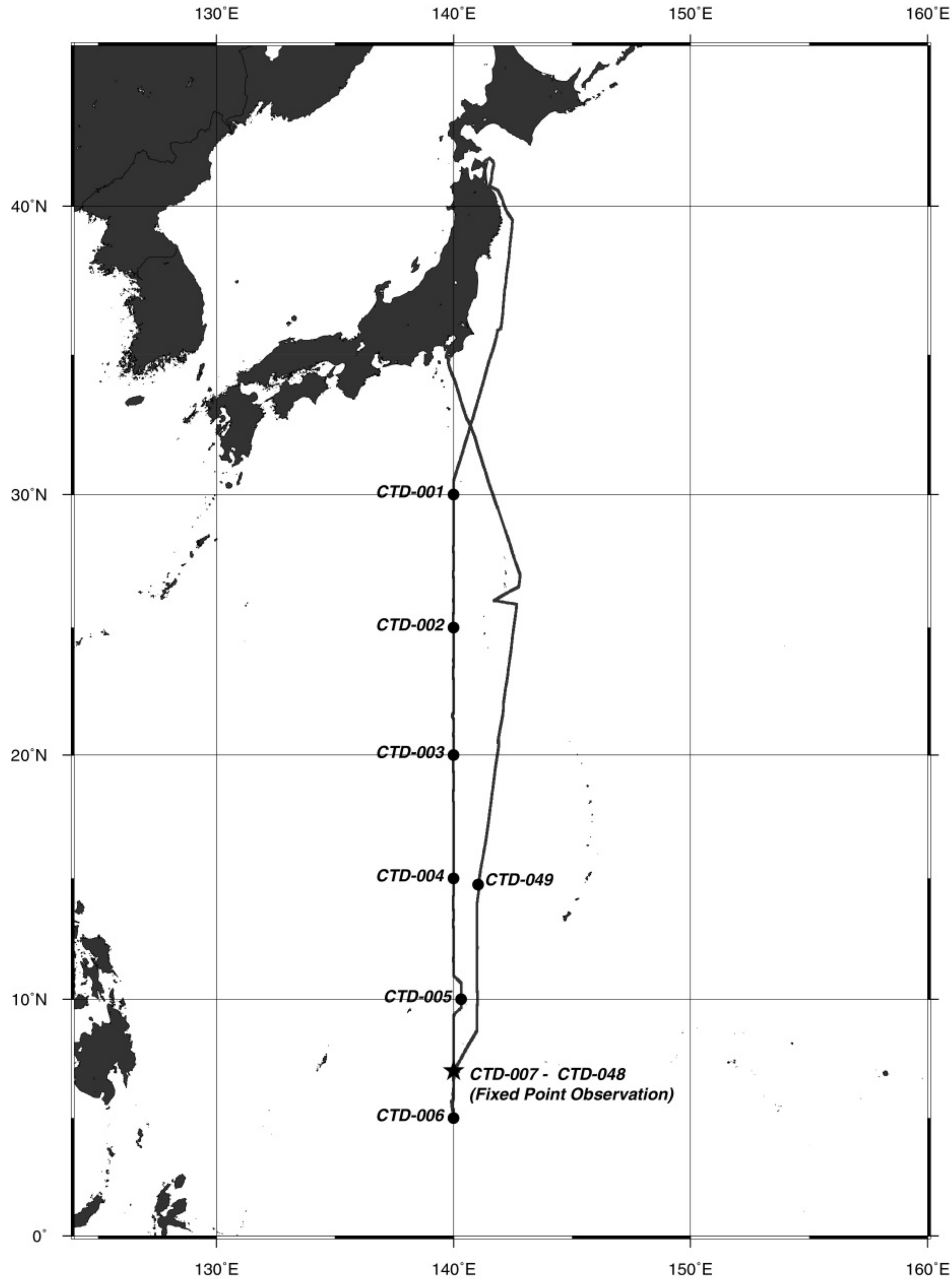

Fig.4.1-2: Locations of CTD casting in MR00-K04. The number corresponds to the observation number in Cruise Log.

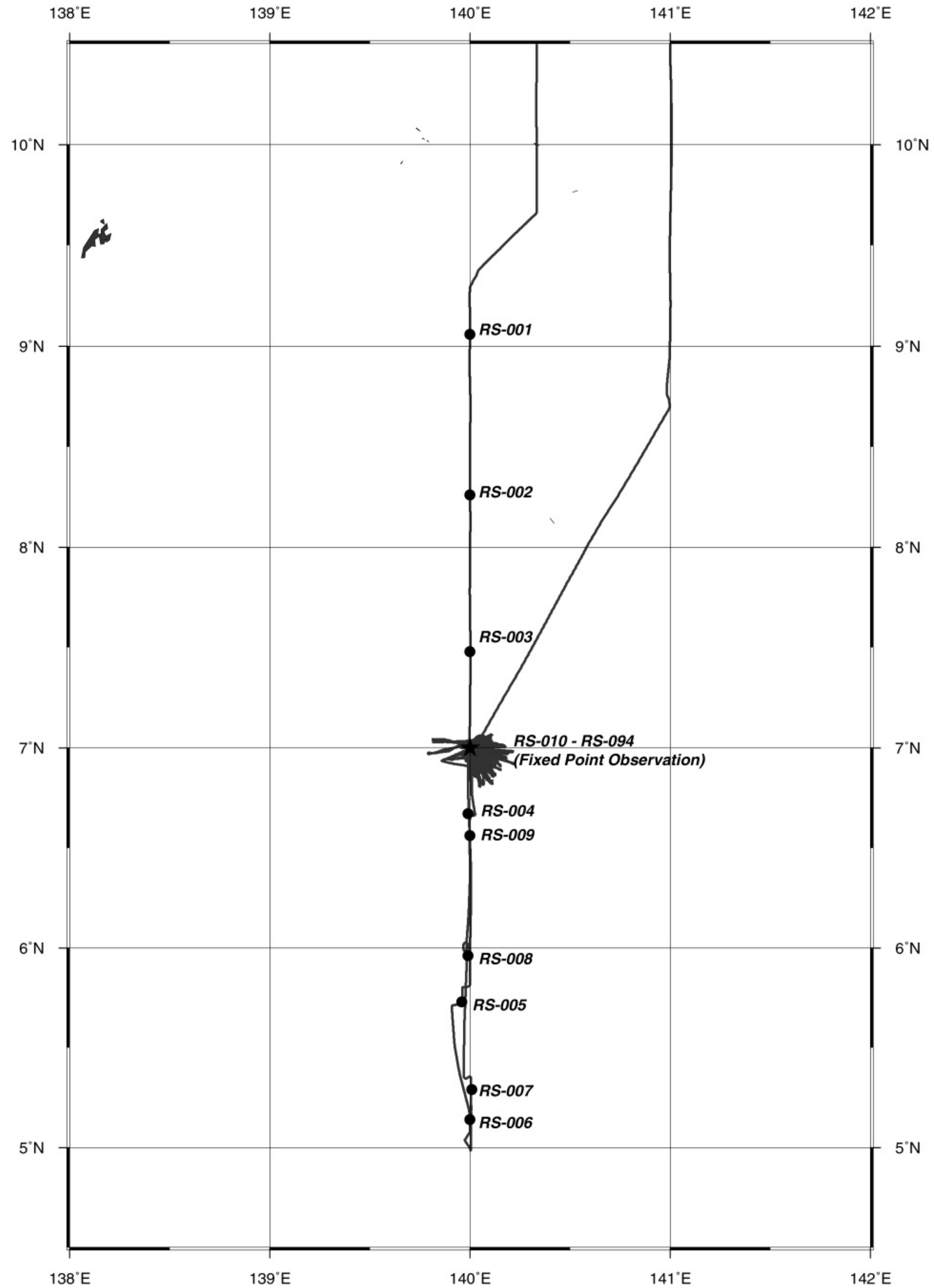

Fig.4.1-3: Locations of radiosonde launch in MR00-K04. The number corresponds to the observation number in Cruise Log.

4.2 Cruise Log

Date	LST	Event	Lat.(deg.)		Lon. (deg.)	
13-Jun		Cloudy / Rainy				
	06:00	Depart Sekinehama	41.36	N	141.24	E
		Arrive Hachinohe	40.55	N	141.50	E
		Depart Hachinohe	40.55	N	141.50	E
	18:10	Start surface sea water monitoring	40.56	N	141.72	E
14-Jun		Cloudy / Rainy				
	09:45	Briefing				
	13:00	Fire Drill				
	13:45	PI meeting				
	21:00	Start Doppler radar observation	34.18	N	141.30	E
15-Jun		Cloudy / Rainy				
	14:54	Arrive (30N, 140E)	30.00	N	140.00	E
	14:56	CTD-001 : CTD casting to 1000 m (with 12-layer water samp	30.00	N	140.00	E
	15:05	Test for tethered balloon	30.00	N	140.00	E
	15:42	ChT-001: "Chlorotec" observation	30.00	N	140.00	E
	16:00	Depart (30N, 140E)				
16-Jun		Fine				
	10:40	Test for "Sea Snake" sensor	25.04	N	140.00	E
	10:54	Arrive (25N, 140E)	25.00	N	140.00	E
	11:00	CTD-002 (1000 m, with 12-layer water sampling)	25.00	N	140.00	E
	11:04	Tethered balloon observation (300 m)	25.00	N	140.00	E
	11:46	ChT-002	25.00	N	140.00	E
	11:58	Tethered balloon observation (300 m)	25.00	N	140.00	E
	12:30	Depart (25N, 140E)				
17-Jun		Fine				
	08:00	Arrive (20N, 140E)	20.00	N	140.00	E
	08:00	CTD-003 (1000 m)	20.00	N	139.99	E
	08:46	ChT-003	19.99	N	139.99	E
	09:38	Depart (20N, 140E)				
18-Jun		Fine				
	04:29	Arrive (15N, 140E)	15.00	N	140.00	E
	04:29	CTD-004 (1000 m, with 12-layer water sampling)	15.00	N	140.00	E
	05:18	ChT-004	15.01	N	139.99	E
	05:28	Tethered balloon observation (1050m)	15.01	N	139.99	E
	06:42	Tethered balloon observation (300m)	15.01	N	139.99	E
	07:06	Depart (15N, 140E)				
19-Jun		Fine				
	02:48	Arrive (10N, 140E)	10.00	N	140.00	E
	02:55	CTD-005 (1000 m, with 12-layer water sampling)	10.00	N	140.33	E
	03:47	ChT-005	10.00	N	140.33	E
	04:00	Depart (10N, 140E)				
	08:31	RS-001 : Radiosonde observation	8.97	N	140.00	E
	11:37	RS-002	8.16	N	140.00	E
	14:36	RS-003	7.38	N	140.00	E
	17:34	RS-004	6.58	N	140.00	E
	20:29	RS-005	5.80	N	139.97	E
	20:59	RS-005-2	5.71	N	139.99	E
	23:32	RS-006	5.02	N	139.98	E
	23:42	Arrive (5N, 140E)	5.00	N	140.00	E

	23:48	CTD-006 (1000 m, with 12-layer water sampling)	4.99	N	140.00	E
20-Jun		Rainy				
	00:36	ChT-006	4.98	N	140.00	E
	00:48	Depart (5N, 140E)				
	02:30	RS-007	5.35	N	139.99	E
	05:33	RS-008	5.99	N	139.97	E
	08:31	RS-009	6.66	N	140.02	E
	08:45	Start "Sea Snake" SSST sensor monitoring	6.71	N	140.02	E
	09:48	Arrive (7N, 140E)	7.00	N	140.00	E
	11:07	Tethered balloon observation (800 m)	6.96	N	140.05	E
	11:24	RS-010	6.95	N	140.05	E
	11:50	Tethered balloon observation (600 m)	6.95	N	140.05	E
	12:28	Start turbulance flux observation	6.89	N	140.09	E
	14:24	RS-011	6.98	N	140.02	E
	14:30	CTD-007 (1000 m)	6.97	N	140.02	E
	14:37	Secchi disk obserbation	6.97	N	140.02	E
	15:10	ChT-007	6.97	N	140.01	E
	15:25	Turbulance flux observation	6.47	N	140.02	E
	17:26	RS-012	7.00	N	140.01	E
	17:27	Turbulance flux observation	6.99	N	140.01	E
	20:29	RS-013	7.00	N	139.99	E
	20:33	CTD-008 (1000 m)	7.00	N	139.98	E
	21:13	ChT-008	7.00	N	139.98	E
	21:25	Turbulance flux observation	7.00	N	139.98	E
	23:27	RS-014	7.00	N	140.00	E
	23:28	Turbulance flux observation	7.00	N	140.00	E
21-Jun		Rainy				
	02:24	RS-015	6.99	N	140.00	E
	02:29	CTD-009 (1000 m)	6.99	N	140.00	E
	03:11	ChT-009	6.99	N	139.99	E
	03:26	Turbulance flux observation	7.00	N	140.00	E
	05:24	RS-016	7.00	N	140.00	E
	05:26	Turbulance flux observation	7.00	N	140.01	E
	08:29	RS-017	6.99	N	140.01	E
	08:32	CTD-010 (1000 m, , with 12-layer water sampling)	7.00	N	140.01	E
	08:36	Secchi disk obserbation	7.00	N	140.01	E
	09:17	ChT-010	7.00	N	140.01	E
	09:29	Turbulance flux observation	7.00	N	140.01	E
	10:56	Test for tethered balloon (50m)	7.03	N	140.07	E
	11:01	Tethered balloon observation (1300 m)	7.03	N	140.07	E
	11:29	RS-018	7.03	N	140.07	E
	12:11	Tethered balloon observation (600 m)	7.03	N	140.05	E
	12:55	Turbulance flux observation	7.03	N	140.05	E
	14:29	RS-019	7.00	N	140.00	E
	14:33	CTD-011 (1000 m)	7.00	N	140.00	E
	14:39	Secchi disk obserbation	7.00	N	140.00	E
	15:12	ChT-011	7.00	N	140.00	E
	15:25	Turbulance flux observation	7.00	N	140.00	E
	17:29	RS-020	7.01	N	140.02	E
	17:30	Turbulance flux observation	7.01	N	140.02	E
	20:29	RS-021	7.02	N	140.01	E
	20:32	CTD-012 (1000 m)	7.02	N	140.01	E
	21:14	ChT-012	7.02	N	140.01	E
	21:27	Turbulance flux observation	7.02	N	140.01	E
	23:29	RS-022	7.02	N	140.01	E
	23:30	Turbulance flux observation	7.02	N	140.01	E

22-Jun		Rainy				
	02:29	RS-023	7.02	N	140.00	E
	02:32	CTD-013 (1000 m)	7.02	N	140.00	E
	03:11	ChT-013	7.02	N	139.99	E
	03:25	Turbulance flux observation	7.02	N	140.00	E
	06:05	RS-024	7.02	N	140.01	E
	06:05	Turbulance flux observation	7.02	N	140.01	E
	08:29	RS-025	7.03	N	140.01	E
	08:35	CTD-014 (1000 m, with 12-layer water sampling)	7.03	N	140.01	E
	09:23	ChT-014	7.03	N	140.02	E
	09:35	Turbulance flux observation	7.03	N	140.02	E
	11:29	RS-026	7.02	N	140.02	E
	12:20	Turbulance flux observation	7.02	N	140.02	E
	14:29	RS-027	7.03	N	140.01	E
	14:32	CTD-015 (1000 m)	7.03	N	140.01	E
	14:39	Secchi disk obserbation	7.03	N	140.01	E
	15:13	ChT-015	7.03	N	140.01	E
	15:25	Turbulance flux observation	7.03	N	140.01	E
	17:29	RS-028	7.02	N	140.02	E
	17:29	Turbulance flux observation	7.02	N	140.02	E
	20:30	RS-029	7.01	N	139.96	E
	20:37	CTD-016 (1000 m)	7.02	N	139.96	E
	21:16	ChT-016	7.02	N	139.95	E
	21:27	Turbulance flux observation	7.02	N	139.95	E
	23:29	RS-030	7.01	N	140.00	E
	23:30	Turbulance flux observation	7.01	N	140.00	E
23-Jun		Fine				
	02:30	RS-031	7.01	N	140.01	E
	02:33	CTD-017 (1000 m)	7.01	N	140.01	E
	03:13	ChT-017	7.01	N	140.00	E
	03:30	Turbulance flux observation	7.01	N	140.00	E
	05:29	RS-032	7.02	N	140.06	E
	05:30	Turbulance flux observation	7.02	N	140.06	E
	08:29	RS-033	7.01	N	140.00	E
	08:32	CTD-018 (1000 m, with 6-layer water sampling)	7.01	N	139.99	E
	08:37	Secchi disk obserbation	7.01	N	139.99	E
	09:17	ChT-018	7.01	N	139.99	E
	09:28	Turbulance flux observation	7.01	N	139.99	E
	11:10	Tethered balloon observation (1300 m)	7.02	N	140.02	E
	11:29	RS-034	7.00	N	139.94	E
	12:20	Turbulance flux observation	6.97	N	139.80	E
	14:29	RS-035	7.03	N	140.00	E
	14:38	CTD-019 (1000 m)	7.03	N	140.00	E
	14:35	Secchi disk obserbation	7.03	N	140.00	E
	15:12	ChT-019	7.03	N	140.00	E
	15:25	Turbulance flux observation	7.03	N	140.00	E
	17:29	RS-036	7.00	N	140.01	E
	17:29	Turbulance flux observation	7.00	N	140.01	E
	20:29	RS-037	7.00	N	139.99	E
	20:40	CTD-020 (1500 m)	6.99	N	139.99	E
	21:33	ChT-020	6.99	N	139.98	E
	21:45	Turbulance flux observation	6.99	N	139.98	E
	23:29	RS-038	6.97	N	140.01	E
	23:30	Turbulance flux observation	6.97	N	140.01	E
24-Jun		Fine				
	02:29	RS-039	6.92	N	140.00	E
	02:32	CTD-021 (1000 m)	6.99	N	140.00	E

	03:11	ChT-021	6.99	N	140.00	E
	03:30	Turbulance flux observation	6.99	N	140.00	E
	05:29	RS-040	7.01	N	140.01	E
	05:29	Turbulance flux observation	7.01	N	140.01	E
	08:29	RS-041	6.99	N	140.00	E
	08:38	CTD-022 (1000 mwith 6-layer water sampling)	6.99	N	140.00	E
	08:41	Secchi disk obserbation	6.99	N	140.00	E
	09:22	ChT-022	6.99	N	139.99	E
	09:33	Turbulance flux observation	6.99	N	139.99	E
	11:02	Tethered balloon observation (800 m)	7.03	N	140.04	E
	11:29	RS-042	7.03	N	140.04	E
	11:42	Tethered balloon observation (800 m)	7.02	N	140.03	E
	12:30	Turbulance flux observation	7.01	N	140.02	E
	14:29	RS-043	6.99	N	140.00	E
	14:32	CTD-023 (1000 m)	6.99	N	140.01	E
	14:36	Secchi disk observation (50m)	6.99	N	140.01	E
	15:11	ChT-023	6.99	N	140.01	E
	15:25	Turbulance flux observation	6.99	N	140.01	E
	17:29	RS-044	7.00	N	140.01	E
	17:29	Turbulance flux observation	7.00	N	140.01	E
	20:29	RS-045	7.00	N	139.99	E
	20:32	CTD-024 (1000 m)	7.00	N	139.99	E
	21:14	ChT-024	7.00	N	139.99	E
	21:26	Turbulance flux observation	7.00	N	139.99	E
	23:30	RS-046	6.99	N	140.00	E
	23:30	Turbulance flux observation	6.99	N	140.00	E
25-Jun		Fine / Cloudy				
	02:29	RS-047	6.99	N	140.02	E
	02:33	CTD-025 (1000 m)	6.98	N	140.02	E
	03:12	ChT-025	6.98	N	140.02	E
	03:25	Turbulance flux observation	6.98	N	140.02	E
	05:29	RS-048	7.00	N	140.00	E
	05:29	Turbulance flux observation	7.00	N	140.00	E
	08:29	RS-049	7.00	N	139.99	E
	08:35	CTD-026 (1000 m, with 6-layer water sampling)	7.00	N	139.99	E
	08:39	Secchi disk obserbation	7.00	N	139.99	E
	09:20	ChT-026	7.00	N	139.99	E
	09:32	Turbulance flux observation	6.99	N	139.99	E
	11:16	Tethered balloon observation (600 m)	7.03	N	139.97	E
	11:29	RS-050	7.03	N	139.99	E
	11:42	Tethered balloon observation (600 m)	7.03	N	139.90	E
	12:20	Turbulance flux observation	7.03	N	139.82	E
	14:29	RS-051	7.02	N	140.00	E
	14:32	CTD-027 (1000 m)	7.02	N	140.00	E
	14:35	Secchi disk obserbation	7.02	N	140.00	E
	15:11	ChT-027	7.02	N	140.00	E
	15:25	Turbulance flux observation	7.02	N	140.00	E
	17:29	RS-052	6.99	N	140.01	E
	17:29	Turbulance flux observation	6.99	N	140.01	E
	20:29	RS-053	7.00	N	139.95	E
	20:32	CTD-028 (1000 m)	7.00	N	139.99	E
	21:11	ChT-028	7.00	N	139.99	E
	21:22	Turbulance flux observation	7.00	N	139.99	E
	23:29	RS-054	7.00	N	140.01	E
	23:29	Turbulance flux observation	7.00	N	140.01	E
26-Jun		Cloudy / Rainy				
	02:29	RS-055	6.99	N	140.01	E

	02:33	CTD-029 (1000 m)	6.99	N	140.01	E
	03:12	ChT-029	6.99	N	140.01	E
	03:25	Turbulance flux observation	6.99	N	140.01	E
	05:29	RS-056	6.98	N	140.01	E
	05:29	Turbulance flux observation	6.98	N	140.01	E
	08:29	RS-057	7.00	N	140.00	E
	08:33	CTD-030 (1000 m)	7.00	N	140.00	E
	08:37	Secchi disk obserbation	7.00	N	140.00	E
	09:13	ChT-030	7.00	N	140.00	E
	09:24	Turbulance flux observation	7.00	N	140.00	E
	11:05	Tethered balloon observation (1000 m)	7.00	N	140.06	E
	11:29	RS-058	7.00	N	140.07	E
	11:55	Tethered balloon observation (1000 m)	7.03	N	139.92	E
	12:40	Turbulance flux observation	7.04	N	139.82	E
	14:29	RS-059	7.01	N	140.01	E
	14:32	CTD-031 (1000 m)	7.01	N	140.01	E
	14:25	Secchi disk obserbation	7.01	N	140.01	E
	15:10	ChT-031	7.01	N	140.01	E
	15:25	Turbulance flux observation	7.01	N	140.01	E
	17:29	RS-060	7.00	N	139.99	E
	17:33	Turbulance flux observation	6.99	N	140.11	E
	20:29	RS-061	6.99	N	140.00	E
	20:32	CTD-032 (1000 m)	6.99	N	140.01	E
	21:12	ChT-032	6.99	N	140.01	E
	21:24	Turbulance flux observation	6.99	N	140.01	E
	23:29	RS-062	6.99	N	139.99	E
	23:33	Turbulance flux observation	6.99	N	139.99	E
27-Jun		Cloudy / Rainy				
	02:29	RS-063	6.96	N	140.00	E
	02:38	CTD-033 (1000 m)	6.96	N	140.01	E
	03:18	ChT-033	6.95	N	140.01	E
	03:35	Turbulance flux observation	6.95	N	140.01	E
	05:29	RS-064	6.97	N	139.98	E
	05:35	Turbulance flux observation	6.97	N	139.98	E
	08:29	RS-065	7.00	N	139.99	E
	08:30	CTD-034 (1000 m)	7.00	N	139.99	E
	08:33	Secchi disk obserbation	7.00	N	139.99	E
	09:08	ChT-034	7.00	N	139.99	E
	09:25	Turbulance flux observation	6.99	N	139.99	E
	11:00	Tethered balloon observation (1000 m)	6.91	N	140.06	E
	11:40	RS-066	6.91	N	140.02	E
	11:52	Tethered balloon observation (600 m)	6.91	N	139.96	E
	12:35	Turbulance flux observation	6.93	N	139.87	E
	14:29	RS-067	7.00	N	140.00	E
	14:32	CTD-035 (1000 m)	7.00	N	140.00	E
	14:37	Secchi disk obserbation	7.00	N	140.00	E
	15:11	ChT-035	7.00	N	140.00	E
	15:25	Turbulance flux observation	6.92	N	140.00	E
	17:29	RS-068	7.00	N	139.99	E
	17:29	Turbulance flux observation	7.00	N	139.99	E
	20:39	RS-069	7.00	N	140.00	E
	20:26	CTD-036 (1000 m)	7.00	N	140.00	E
	21:05	ChT-036	6.99	N	140.00	E
	21:17	Turbulance flux observation	7.01	N	140.00	E
	23:39	RS-070	6.97	N	139.96	E
	23:43	Turbulance flux observation	6.97	N	139.95	E
28-Jun		Rainy / Cloudy				

	02:29	RS-071	6.98	N	140.04	E
	02:33	CTD-037 (1000 m)	6.98	N	140.04	E
	03:13	ChT-037	6.97	N	140.04	E
	03:30	Turbulance flux observation	6.97	N	140.04	E
	05:29	RS-072	6.99	N	140.01	E
	05:29	Turbulance flux observation	6.99	N	140.01	E
	08:39	RS-073	6.99	N	140.00	E
	08:41	CTD-038 (1000 m)	6.99	N	139.99	E
	08:45	Secchi disk obserbation	6.99	N	139.99	E
	09:20	ChT-038	6.99	N	139.99	E
	09:32	Turbulance flux observation	6.99	N	139.99	E
	11:29	RS-074	7.01	N	140.04	E
	11:36	Turbulance flux observation	7.01	N	140.03	E
	14:30	RS-075	6.97	N	140.03	E
	14:34	CTD-039 (1000 m)	6.97	N	140.03	E
	14:38	Secchi disk obserbation	6.97	N	140.03	E
	15:13	ChT-039	6.97	N	140.03	E
	15:30	Turbulance flux observation	6.97	N	140.03	E
	17:29	RS-076	7.00	N	139.99	E
	17:32	Turbulance flux observation	6.99	N	139.99	E
	20:29	RS-077	7.00	N	139.99	E
	20:33	CTD-040 (1000 m)	7.00	N	139.99	E
	21:11	ChT-040	7.00	N	139.99	E
	21:22	Turbulance flux observation	7.00	N	139.99	E
	23:39	RS-078	7.03	N	139.99	E
	23:33	Turbulance flux observation	7.02	N	139.99	E
29-Jun		Rainy				
	02:29	RS-079	6.99	N	139.99	E
	02:35	CTD-041 (1000 m)	6.99	N	139.99	E
	03:13	ChT-041	6.99	N	139.99	E
	03:30	Turbulance flux observation	6.99	N	140.00	E
	05:28	RS-080	6.99	N	140.00	E
	05:31	Turbulance flux observation	6.97	N	140.00	E
	08:29	RS-081	7.00	N	140.00	E
	08:33	CTD-042 (1000 m)	7.00	N	140.00	E
	08:36	Secchi disk obserbation	7.00	N	140.00	E
	09:12	ChT-042	7.00	N	139.99	E
	09:24	Turbulance flux observation	7.00	N	139.99	E
	10:58	Tethered radiosonde observation	7.00	N	139.99	E
	11:39	RS-082	7.04	N	140.02	E
	11:45	Turbulance flux observation	7.05	N	140.03	E
	13:43	Tethered radiosonde observation	6.95	N	140.12	E
	14:29	RS-083	6.98	N	140.08	E
	14:32	CTD-043 (1000 m)	6.98	N	140.07	E
	14:36	Secchi disk obserbation	6.98	N	140.07	E
	15:11	ChT-043	6.98	N	140.07	E
	15:25	Turbulance flux observation	6.98	N	140.08	E
	16:43	Tethered radiosonde observation	6.93	N	140.03	E
	17:29	RS-084	6.98	N	140.00	E
	17:30	Turbulance flux observation	6.98	N	139.99	E
	19:48	Tethered radiosonde observation	6.93	N	140.02	E
	20:31	RS-085	7.00	N	139.99	E
	20:37	CTD-044 (1000 m)	7.00	N	139.99	E
	21:15	ChT-044	7.00	N	139.99	E
	21:27	Turbulance flux observation	7.00	N	139.99	E
	23:30	RS-086	7.00	N	139.96	E
	23:35	Turbulance flux observation	7.00	N	139.96	E

30-Jun		Rainy				
	02:29	RS-087	7.00	N	140.00	E
	02:33	CTD-045 (1000 m)	7.00	N	140.00	E
	03:13	ChT-045	7.00	N	140.00	E
	03:30	Turbulance flux observation	6.99	N	140.01	E
	05:29	RS-088	6.98	N	140.00	E
	05:29	Turbulance flux observation	7.00	N	140.00	E
	08:29	RS-089	7.00	N	140.00	E
	08:33	CTD-046 (1000 m)	7.00	N	140.00	E
	08:36	Secchi disk obserbation	7.00	N	140.00	E
	09:10	ChT-026	6.99	N	139.99	E
	09:23	Turbulance flux observation	6.99	N	140.00	E
	11:00	Tethered balloon observation	6.93	N	140.06	E
	11:39	RS-090	6.93	N	140.06	E
	11:45	Turbulance flux observation	6.88	N	140.10	E
	14:30	RS-091	7.01	N	140.00	E
	14:33	CTD-047 (1000 m)	7.01	N	140.01	E
	14:37	Secchi disk obserbation	7.01	N	140.01	E
	15:14	ChT-047	7.01	N	140.01	E
	15:30	Turbulance flux observation	7.01	N	140.01	E
	17:29	RS-092	7.00	N	140.00	E
	17:29	Turbulance flux observation	7.00	N	140.00	E
	20:39	RS-093	7.00	N	139.99	E
	20:43	CTD-048 (2000 m)	7.00	N	139.99	E
	21:50	ChT-048	7.00	N	140.00	E
	22:01	Turbulance flux observation	7.00	N	140.00	E
	23:29	RS-094	7.00	N	140.00	E
1-Jul		Rainy / Cloudy				
	00:15	End of "Sea Snake" sensor observation	7.00	N	140.00	E
	00:24	Left obspit for Yokosuka	7.00	N	140.00	E
2-Jul		Rainy / Cloudy				
	08:00	CTD-049 (2000m)	14.69	N	141.09	E
3-Jul		Fine				
4-Jul		Fine				
	08:16	Tethered balloon observation (1000m)	25.91	N	142.57	E
	10:13	Tethered balloon observation (1000m)	25.98	N	142.08	E
5-Jul		Fine				
	18:30	Stop Doppler radar observation	32.53	N	140.70	E
6-Jul						
	08:00	Arrive Yokosuka	35.28	N	139.68	E

5. List of Participants

5.1 On board Scientists / Engineers / Technical Staff

Name	Affiliation	e-mail
Yoneyama, Kunio	JAMSTEC	
Katsumata, Masaki	JAMSTEC	
Shibayama, Ken-ichi	JAMSTEC	
Moriwaki, Kaichi	JAMSTEC	
Ushiyama, Tomoki	FORSGC	
Ishida, Hiroshi	MUK / FORSGC	
Kozai, Katsutoshi	MUK	
Hayashi, Mitsuru	MUK	
Kusakari, Masanao	MUK	
Ishida, Kunimitsu	Toba-CMT	
Nojima, Kunikazu	Kinki Univ.	
Takemi, Tetsuya	Osaka Univ.	
Tsukamoto, Osamu	Okayama Univ.	
Takahashi, Satoshi	Okayama Univ.	
Kono, Takehiko	Okayama Univ.	
Nakanishi, Ayako	Okayama Univ.	
Yamashita, Eiji	Okayama Univ. of Science	
Iwata, Jun	Okayama Univ. of Science	
Hirose, Masafumi	IHAS, Nagoya Univ.	
Miura, Kazuhiko	Science Univ. of Tokyo	
Hara, Takeshi	Science Univ. of Tokyo	
Ui, Takeshi	Science Univ. of Tokyo	
Kishida, Takeshi	Science Univ. of Tokyo	
Matsumoto, Kiyoshi	ORI, Univ. of Tokyo	
Matsui, Ichiro	NIES	
Narukawa, Masahiro	ILTS, Hokkaido Univ.	
Mochida, Michihiro	ILTS, Hokkaido Univ.	
Fujitani, Yuji	D. of Eng., Hokkaido Univ.	
Hanyu, Masaki	GODI	
Yoshiura, Fumitaka	GODI	
Kozuma, Kiyotake	GODI	
Sueyoshi, Soichiro	GODI	
Ozawa, Satoshi	MWJ	
Inoue, Asako	MWJ	
Sagishima, Katsunori	MWJ	
Yasuda, Ai	MWJ	
Akizawa, Kaori	MWJ	
Ooyama, Kentaro	MWJ	

Japan Marine Science and Technology Center (JAMSTEC)
Natsushima-cho 2-15, Yokosuka 237-0061 JAPAN
TEL : +81-468-66-3811
FAX : +81-468-65-3202

Frontier Observational Research System for Global Change (FORSGC)
Sumitomo Hamamatsu-cho bld. 4F, Hamamatsu-cho 1-18-16, Minato-ward, Tokyo 105-0013 JAPAN

Maritime University of Kobe (MUK)
5-1-1, Fukae-minami, Higashi-Nada-ku, Kobe 658-0022 JAPAN

Toba National College of Marine Technology (Toba-CMT)
1-1, Ikegami, Toba, Mie 517-8501 JAPAN

Kinki University
3-4-1, Kowakae, Higashi-Osaka, Osaka 577-8502 JAPAN

Osaka University
2-1, Yamadaoka, Suita, Osaka 565-0871 JAPAN

Okayama University
3-1-1, Tsushimanaka, Okayama 700-8530 JAPAN

Okayama University of Science
1-1, Ridai-cho, Okayama 700-0005 JAPAN

Institute of Hydrology and Atmospheric Science (IHAS), Nagoya University,
Furo-cho, Chikusa-ward, Nagoya 464-8601 JAPAN

Science University of Tokyo
1-3, Kagurazaka, Shinjuku-ward, Tokyo 162-8601 JAPAN

Ocean Research Institute (ORI), University of Tokyo
1-15-1, Minamidai, Nakano-ward, Tokyo 164-8639 JAPAN

National Institute of Environmental Studies (NIES)
16-2, Onogawa, Tsukuba, Ibaraki 305-0053 JAPAN

Institute of Low Temperature Science, Hokkaido Univ.
N19W8, Kita-ward, Sapporo 060-0819 JAPAN

Department of Engineering, Hokkaido University
N13W8, Kita-ward, Sapporo 060-8628 JAPAN

Global Ocean Development Inc.
3-65, Oppamahigashi-cho, Yokosuka 237-0063 JAPAN

Marine Works Japan Ltd.
1-1-7, Mutsuura, Kanazawa-ward, Yokohama 236-0031 JAPAN

5.2 Ship Crew

Master	Hashimoto, Takaaki
Chief Officer	Dowaki, Yukio
1st Officer	Shibata, Yuji
2nd Officer	Maruyama, Hiroki
3rd Officer	Asanuma, Mitsunobu
Chief Engineer	Watanabe, Yoichiro
1st Engineer	Inoue, Toru
2nd Engineer	Narumi, Hiroaki
3rd Engineer	Masuno, Koji
Chief Radio Officer	Nakabayashi, Shuji
2nd Radio Officer	Morioka, Naoto
Boatswain	Suzuki, Tadao
Able Seaman	Ishikawa, Ken-etsu
Able Seaman	Yamamoto, Yasuyuki
Able Seaman	Kinoshita, Hirokazu
Able Seaman	Kawata, Seiichiro
Able Seaman	Iwamura, Yukihiro
Able Seaman	Horita, Kazunori
Able Seaman	Oguni, Hisao
Able Seaman	Kuwahara, Yosuke
Able Seaman	Monzawa, Tsuyoshi
Able Seaman	Yamamoto, Nobuhiro
Able Seaman	Komata, Shuji
No.1 Oiler	Horiuchi, Yukitoshi
Oiler	Yoshikawa, Toshimi
Oiler	Inoue, Fumio
Oiler	Araki, Sunao
Oiler	Sugimoto, Yoshihiro
Oiler	Matsuo, Toshio
Chief Steward	Koga, Yasuaki
Steward	Ota, Hitoshi
Steward	Hamabe, Tatsuya
Steward	Uemura, Kozo
Steward	Hiraishi, Hatsuji
Steward	Yoshizawa, Hiroyuki

6. Summary of Observations

6.1 Surface Meteorological Parameters

(1) Personnel
Kunio Yoneyama (JAMSTEC): Principal Investigator
Masaki Katsumata (JAMSTEC)
Masaki Hanyu (GODI): Operation Leader
Fumitaka Yoshiura (GODI)
Kiyotake Kouzuma (GODI)
Souichiro Sueyoshi (GODI)

(2) Objective
The surface meteorological parameters are observed as a basic dataset of the meteorology. These parameters bring us the information about temporal variation of the meteorological condition surrounding the ship.

(3) Methods
The surface meteorological parameters were observed throughout MR00-K04 cruise from the departure of Sekinehama on 13 June 2000 to the arrival of Yokosuka on 6 July 2000.
This cruise, we used 3 systems for the surface meteorological observation.

1. Mirai meteorological observation system
2. Shipboard Oceanographic and Atmospheric Radiation (SOAR) system
3. Total Sky Imager (TSI)

The measured parameters of each systems are listed in Table 6.1-1, 6.1-2 and 6.1-3.

(4-1) Mirai meteorological observation system
Instruments and archived parameters of Mirai met system are listed in the table below. Data was collected and processed by KOAC-7800 weather data processor made by Koshin Denki, Japan. The data set has 6-second averaged every 6-second record and 10-minute averaged every 10-minute record.

Table 6.1-1: Instrument installation locations of Mirai met system

Sensors	type	manufacturer	location (altitude from surface)
Anemometer	KE-500	Koshin Denki, Japan	foremast (24m)
Thermometer	FT	Koshin Denki, Japan	compass deck (21m)
dewpoint meter	DW-1	Koshin Denki, Japan	compass deck (21m)
Barometer	F451	Yokogawa, Japan	weather observation room captain deck (13m)
rain gauge	50202	R. M. Young, USA	compass deck (19m)
optical rain gauge	ORG-115DR	SCTI, USA	compass deck (19m)
radiometer (short wave)	MS-801	Eiko Seiki, Japan	radar mast (28m)
radiometer (long wave)	MS-200	Eiko Seiki, Japan	radar mast (28m)
wave height meter	MW-2	Tsurumi-seiki, Japan	Bow

Table 6.1-2: Parameters of Mirai meteorological observation system

	parameters	units	remarks
1	latitude	degree	
2	longitude	degree	
3	ship's speed	knot	Mirai log
4	ship's heading	degree	Mirai gyro
5	relative wind speed	m/s	6 sec. / 10 min. averaged
6	relative wind direction	degree	6 sec. / 10 min. averaged
7	true wind speed	m/s	6 sec. / 10 min. averaged
8	true wind direction	degree	6 sec. / 10 min. averaged
9	barometric pressure	hPa	adjusted to the sea surface level 6 sec. / 10 min. averaged
10	air temperature (starboard side)	degC	6 sec. / 10 min. averaged
11	air temperature (port side)	degC	6 sec. / 10 min. averaged
12	dewpoint temperature (stbd side)	degC	6 sec. / 10 min. averaged
13	dewpoint temperature (port side)	degC	6 sec. / 10 min. averaged
14	Relative humidity (starboard side)	%	6 sec. / 10 min. averaged
15	Relative humidity (port side)	%	6 sec. / 10 min. averaged
16	rain rate (optical rain gauge)	mm/hr	6 sec. / 10 min. averaged
17	rain rate (capacitive rain gauge)	mm/hr	6 sec. / 10 min. averaged
18	downwelling shortwave radiometer	W/m^2	6 sec. / 10 min. averaged
19	downwelling infra-red radiometer	W/m^2	6 sec. / 10 min. averaged
20	sea surface temperature	degC	-5m
21	significant wave height (fore)	m	3 hourly
22	significant wave height (aft)	m	3 hourly
23	Significant wave period (fore)	second	3 hourly
24	Significant wave period (aft)	second	3 hourly

(4-2) Shipboard Oceanographic and Atmospheric Radiation (SOAR) system

SOAR system, designed by BNL (Brookhaven National Laboratory, USA), is consisted of 3 parts.

1. Portable Radiation Package (PRP) designed by BNL – short and long wave down welling radiation
2. Zeno meteorological system designed by BNL – wind, Tair/RH, pressure and rainfall measurement
3. Scientific Computer System (SCS) designed by NOAA (National Oceanographic and Atmospheric Administration, USA) – centralized data acquisition and logging of all data sets

SCS recorded PRP data every 6.5 seconds and Zeno met data every 10 seconds.
Instruments and their locations are listed in Table 6.1-3. The archived parameters are in Table 6.1-4.

Table 6.1-3: Instrument installation locations of SOAR system

Sensors	type	manufacturer	location (altitude from surface)
Anemometer	05106	R. M. Young, USA	foremast (24m)
Tair/RH	HMP45A	Vaisala, USA	foremast (24m)
	with 43408 Gill aspirated radiation shield (R. M. Young)		
Barometer	61201	R. M. Young, USA	foremast (24m)
	with 61002 Gill pressure port (R. M. Young)		
rain gauge	50202	R. M. Young, USA	foremast (24m)
optical rain gauge	ORG-115DA	ScTi, USA	foremast (24m)
sea surface temperature	SST-100	BNL, USA	bow, 3m extention (-1cm)
radiometer (short wave)	PSP	Eppley labs, USA	foremast (24m)
radiometer (long wave)	PIR	Eppley labs, USA	foremast (24m)
Fast ratating shadowband radiometer		Yankee, USA	foremast (24m)

Table 6.1-4: Parameters of SOAR System

	parameters	units	remarks
1	latitude	degree	
2	longitude	degree	
3	sog	knot	
4	cog	degree	
5	relative wind speed	m/s	
6	relative wind direction	degree	
7	barometric pressure	hPa	
8	air temperature	degC	
9	relative humidity	%	
10	sea surface temperature	degC	-1cm, Seasnake
11	rain rate (optical rain gauge)	mm/hr	
12	precipitation (capacitive rain gauge)	mm	reset at 50mm
13	down welling shortwave radiation	W/m^2	
14	down welling infra-red radiation	W/m^2	
15	defuse irradiation	W/m^2	

(4-3) Total Sky Imager (TSI)

The Total Sky Imager (TSI) was installed at the top deck midship, altitude of 17m from sea level. TSI was developed jointly by Penn State University, BNL and Yankee Environmental Systems, Inc. and manufactured by YES Inc. TSI recorded every 5 minutes from dawn to sunset. The archived parameters are in Table 6.1-5.

Table 6.1-5: Parameters of TSI system

	parameters	units
1	opaque cloud cover	%
2	thin cloud cover	%

(4) Preliminary results

The daytime cloud cover ratio obtained from TSI during the cruise from 14 June to 3 July is shown in Fig 6.1-1. Precipitation, Tair/RH/SSST and pressure observed during Intensive Observation Period (IOP) from SOAR system are shown in Fig 6.1-2, Fig 6.1-3 and Fig 6.1-4 respectively. In the figures, accumulated precipitation data from SOAR capacitive rain gauge was converted to the amount of every minute and obvious noises were eliminated but not calibrated. SSST in Fig 6.1-3 shows re-calculated values because temperature deriving parameter for SSST sensor was set wrong. Other figures are showing uncorrected data.

(5) Data archives

These raw data will be submitted to the Data Management Office (DMO) in JAMSTEC just after the cruise.

Remarks concerning about data quality are as follows;

1. Air tube from outside to the barometer of Mirai met system was connected on 0152UTC June 29. Pressure data of Mirai met system might be affected by indoor air conditioning until that time.
2. Radiometers for upwelling of Mirai met system were not used during this cruise.
3. SST data of Mirai met system is effective from 1315UTC June 13 to 0000UTC July 5.
4. Lat/Long data of Mirai met system from 1635UTC to 1833UTC July 4 is not effective because of bad GPS receiver condition.
5. PRP software and hardware were reset on the morning of June 16, 18, 20, 22, 24, 26, 28, and 30. FRSR, PIR and PSP sensors of SOAR system and long-wave/short-wave radiometers of Mirai met system were cleaned up at those times.
6. PRP stopped from 0848UTC July 1 probably caused by the Control Data Unit problem. It started again on 0922UTC by power reset at the foremast. PRP sensors were cleaned up at that time.
7. PRP stopped from 2248UTC to 2341UTC July 2 by same situation as above. PRP sensors were cleaned up at that time.
8. Wind meter of SOAR system was installed about 20 degrees tilted to ship's starboard side. Data needs correction.
9. SSST sensor of SOAR system was deployed on 2339UTC June 19 and recovered on 0112UTC June 22 because of the mounting boom trouble. It re-deployed on 0152UTC same day and recovered on 1500UTC June 30.
10. SSST deriving parameter was set wrong. Sensor No.2 was used but the parameter was set for sensor No.1.

    $T = a*v+b$ where v is measured voltage in volts

#1:	a=110.78774	b=-15.17399
#2:	a=112.38104	b=-17.306849

11. SOAR data acquisition was stopped from 0000UTC to 0005UTC June 27 for the configuration work.

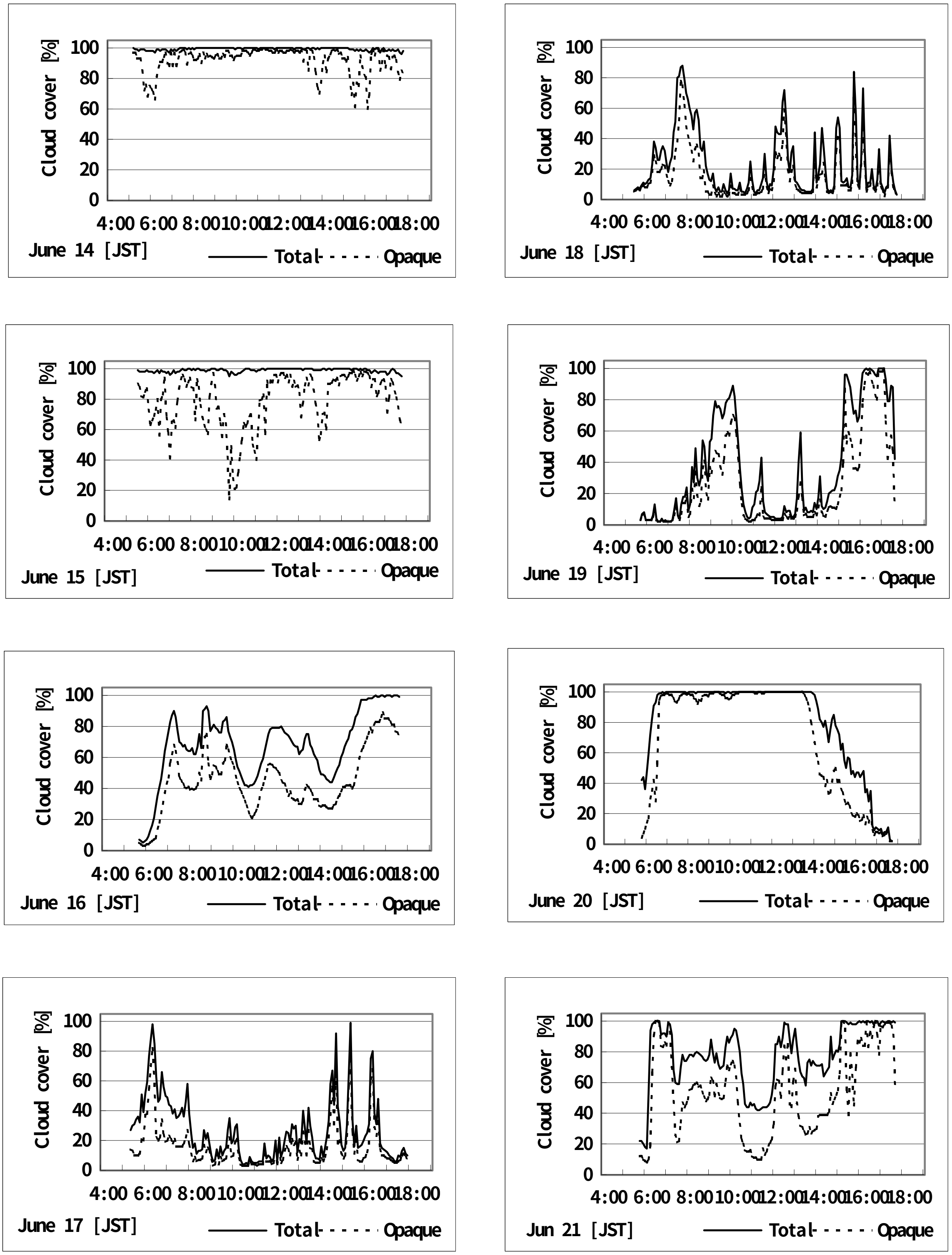

Fig 6.1-1: Daytime cloud cover ratio from TSI (1/3)

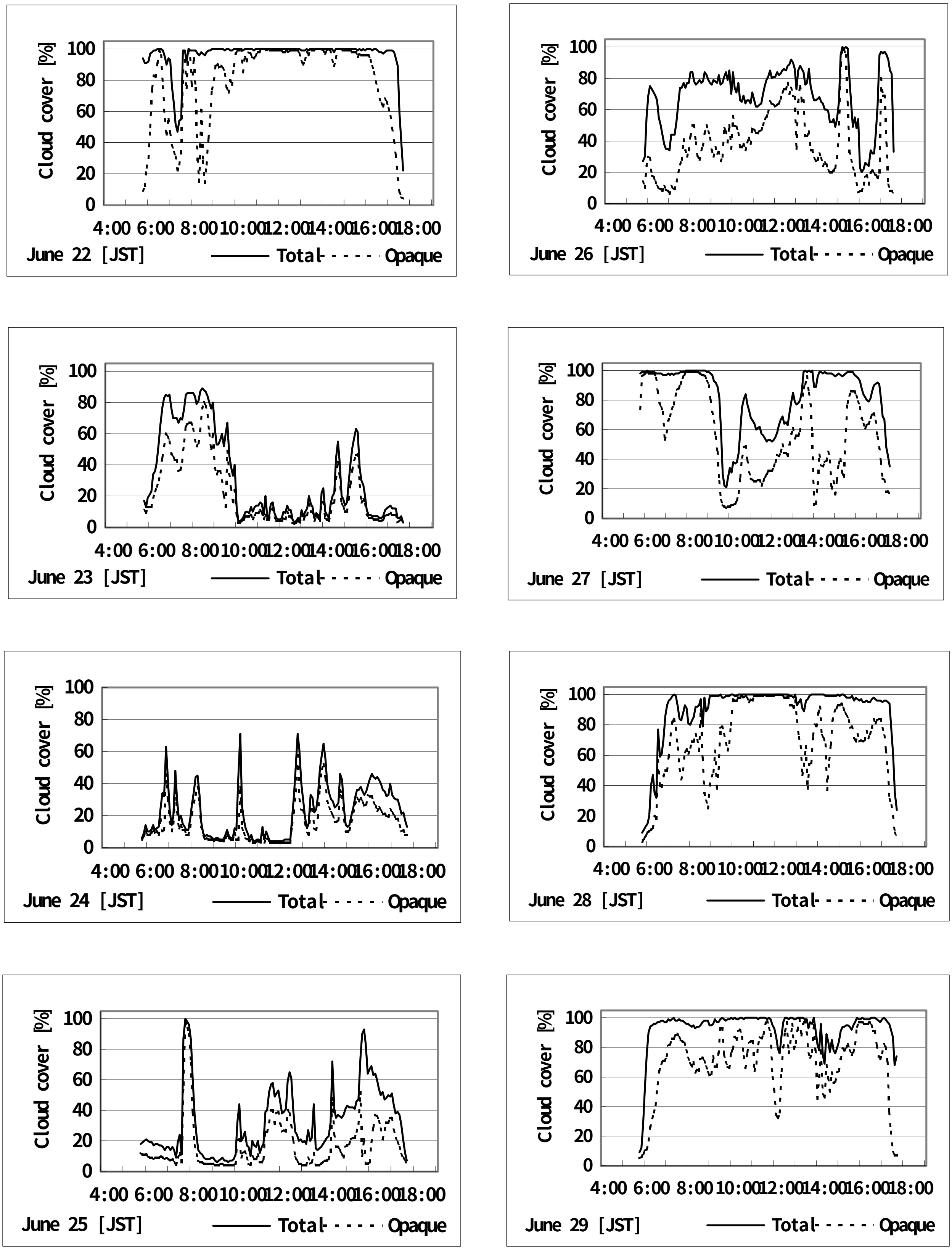

Fig 6.1-1: Daytime cloud cover ratio from TSI (2/3)

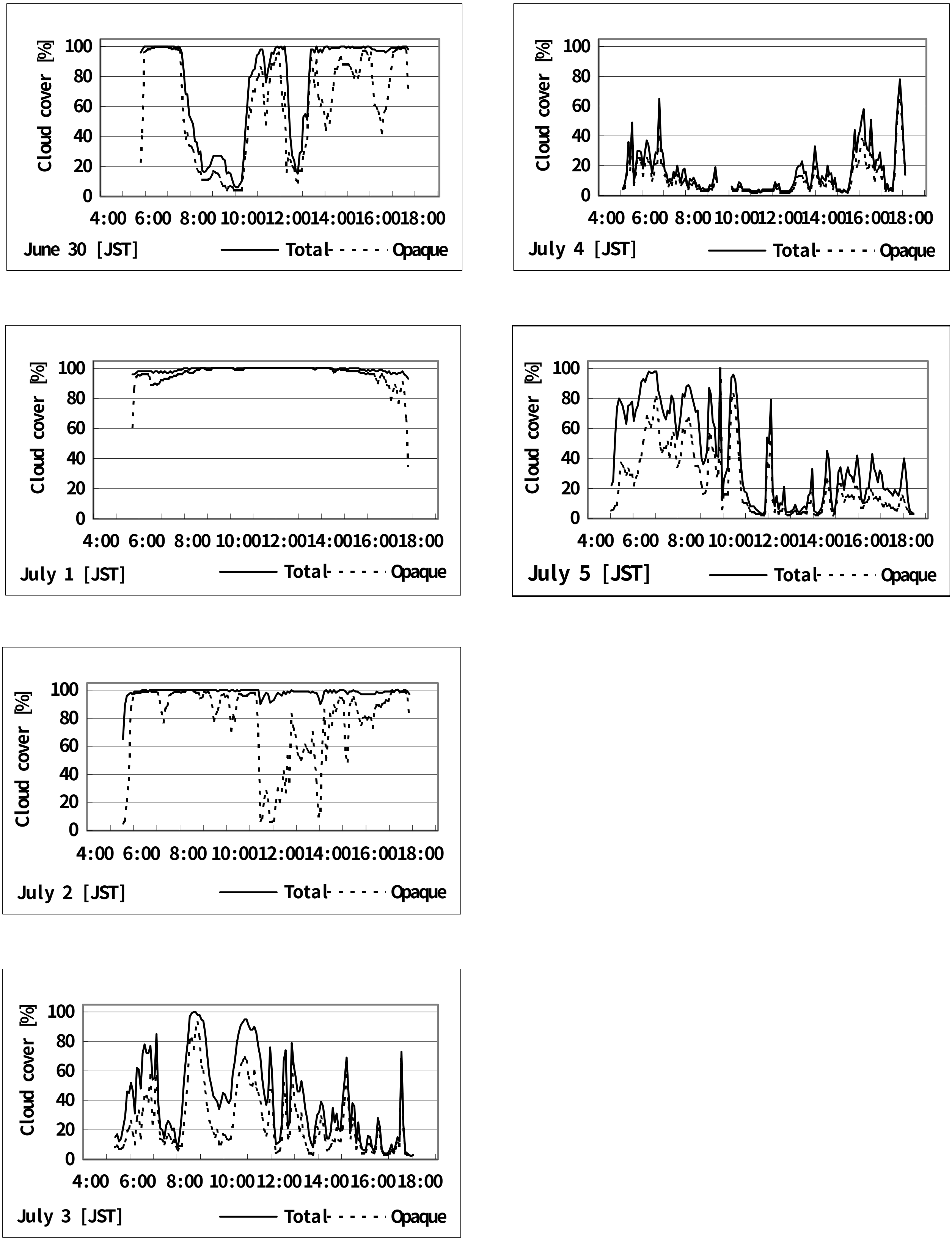

Fig 6.1-1: Daytime cloud cover ratio from TSI (3/3)

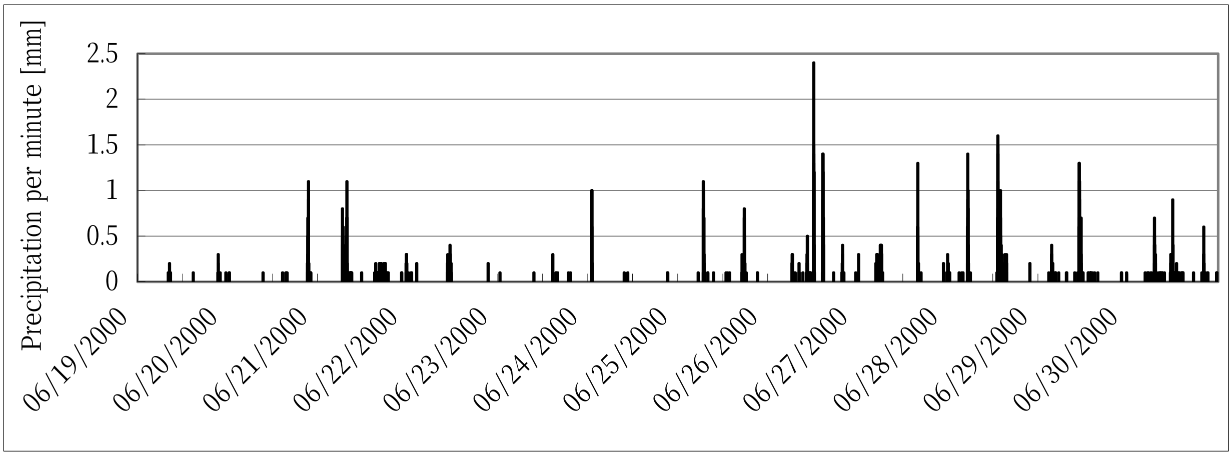

Fig 6.1-2: Precipitation during IOP (SOAR capacitive rain gauge). Dates are shown in UTC.

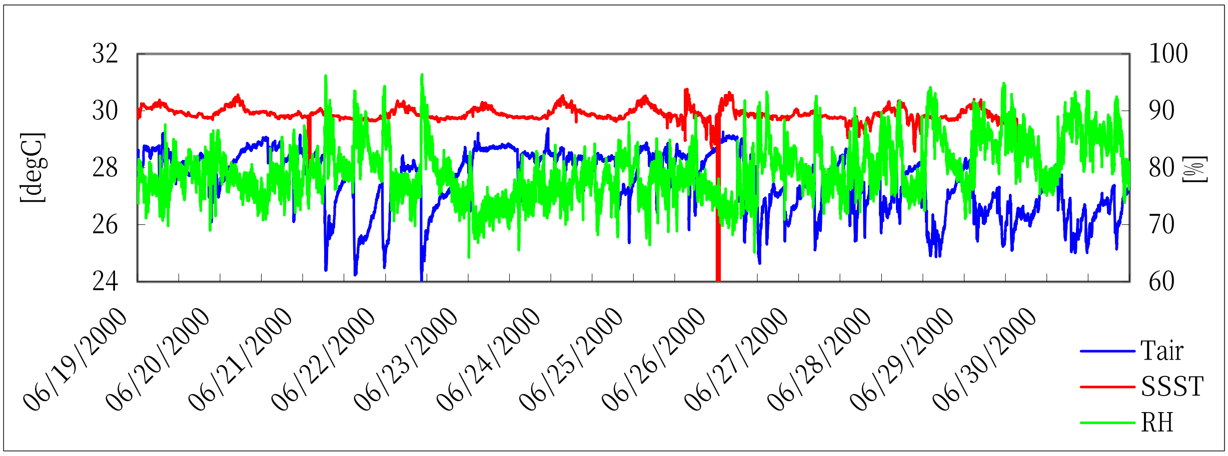

Fig 6.1-3: Tair/RH/SSST during IOP (SOAR sensors). Dates are shown in UTC.

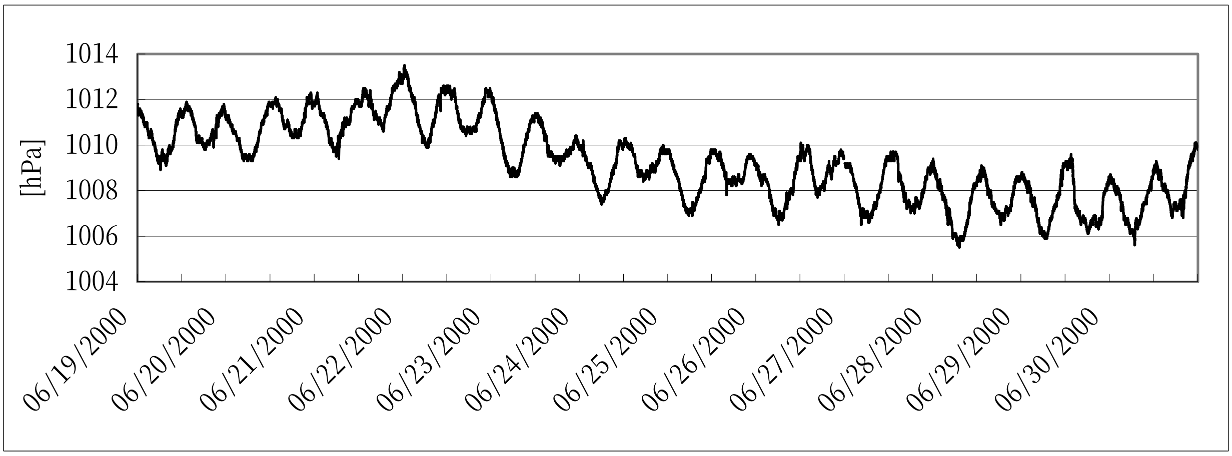

Fig 6.1-4: Pressure during IOP (SOAR). Dates are shown in UTC.

6.2 Radiosonde Observation

(1) Personnel

Kunio Yoneyama	(JAMSTEC)	Principal Investigator
Fumitaka Yoshiura	(GODI)	Operation Leader
Kiyotake Kouzuma	(GODI)	
Souichiro Sueyoshi	(GODI)	
Tomoki Ushiyama	(FORSGC)	
Masaki Katsumata	(JAMSTEC)	
Kenichi Shibayama	(JAMSTEC)	
Kaichi Moriwaki	(JAMSTEC)	

(2) Objective

To survey atmospheric conditions (vertical profile of temperature, humidity, and wind speed/direction)

(3) Method

Atmospheric sounding by radiosonde was carried out every three hours (00, 03, 06, 09, 12, 15, 18, 21 UTC) during June 19 and June 30. In total, 94 radiosondes were launched. The system consists of Main processor (Vaisala DigiCORA MW11), Balloon Launcher (Vaisala ASAP), GPS antenna (GA20), UHF telemetry antenna (RB21), PC (Toshiba Dynabook 430CDT), and GPS sonde (RS80-15G, A-type sensor).

Before launching, temperature and humidity were calibrated using Humidity calibrator (Digilog Instruments VAPORPAK H-31). However, since the temperature of calibrator became unstable in the end of the cruise(in spite of the fact that the calibrator itself was calibrated just before the cruise), we used another thermometer (Vaisala HM34) as reference. Surface 30m data were affected by ship body warming/cooling in daytime/nighttime. By conducting tethered sonde measurement for the surface 100m layer, we confirmed that these data could be corrected by linear extrapolation using above layer data(not shown here).

(4) Preliminary results

The log file of sonde launching is listed in Table 6.2.1-1.

Time-height cross section of potential temperature, mixing ratio, zonal and meridional wind components are shown in Fig.6.2.1-1, respectively. Profiles of temperature and dew point temperature are plotted on the thermodynamic chart (EMAGRAM) and attached in the Appendix. Wind profile is also shown there.

During whole the cruise, easterly trade wind prevailed in the lower troposphere, but it was relatively weak. Strong inversion layer that is typical under the trade wind condition was not observed. Instead, in the middle of the stationary observation period, namely on June 24 and 25, relatively dry layer could be found just above 0°C layer.

From sounding data, several basic parameters to describe atmospheric conditions such as Convective Available Potential Energy (CAPE), Convective Inhibition (CIN), total precipitable water(TPW), and lifted condensation level (LCL) are calculated. For CAPE, in the first 2 days it shows higher values of order of 2000J/kg. But gradually it decreased and reached 500J/kg in the last 3 days. As twelve days mean of CAPE was 1072J/kg. Twelve days mean of other parameters were CIN; -34J/kg, TPW; 54mm, and LCL 930hPa, respectively.

(5) Data Archive

All data were immediately sent to the world through GTS by Japan Meteorological Agency, immediately after the each observation.

Raw data is stored as ASCII format every 2 seconds during ascending. Data near the surface are corrected and all data are converted onto every 5 hPa from 1000 hPa through 100 hPa. Both (raw ASCII and corrected 5hPa interval data) are archived and available from K.Yoneyama of JAMSTEC.

Table 6.2-1: Logs for radiosonde observation in MR00-K04.

No.	Time (UTC) YY	MM	DD	HH	Position Lat.	Lon.	Surface State P (hPa)	T (deg. C)	RH (%)	WD (deg)	WS (m/s)	Max Altitude (hPa)	(m)	Cloud Amount	Cloud Type
1	00	06	19	0	9.06N	140.00E	1009.5	28.8	77	128	8.6	75.0	18238	6	Cu,Cb,As,Ci
2	00	06	19	3	8.26N	140.00E	1008.5	29.2	72	115	3.8	94.8	16876	1	Cu,Ac
3	00	06	19	6	7.48N	140.00E	1007.2	29.0	78	106	3.9	28.9	24018	6	Ac,Ci,Ns,Cu,Cb
4	00	06	19	9	6.67N	139.99E	1007.5	28.3	73	34	3.1	240.7	11206	7	Cu,Cb,As
5	00	06	19	12	5.73N	139.96E	1009.1	27.3	82	145	2.3	62.7	19294	9	Cu,Cb
6	00	06	19	15	5.14N	140.00E	1009.2	27.5	82	130	2.0	56.7	19896	10	As
7	00	06	19	18	5.29N	140.01E	1007.8	29.1	76	140	2.6	46.9	21049	5	Cu,As
8	00	06	19	21	5.96N	139.99E	1008.1	27.8	79	76	2.1	38.1	22339	8	Cu,Cb,Ac,As
9	00	06	20	0	6.56N	140.00E	1009.3	27.4	83	6	6.9	75.2	18211	10	Ns,Ac
10	00	06	20	3	6.96N	140.05E	1008.0	29.5	70	107	2.2	294.9	9834	10	St,Cu
11	00	06	20	6	6.95N	140.04E	1007.0	29.4	74	95	3.3	36.7	22567	8	Cu,As,Ac,Cs
12	00	06	20	9	6.99N	140.04E	1007.4	28.7	75	80	3.5	37.4	22463	5	Cu,Cb,As,Cc,Sc
13	00	06	20	12	7.00N	139.99E	1009.2	28.3	80	69	4.3	36.6	22632	2	As,Cu
14	00	06	20	15	7.02N	140.03E	1009.3	26.9	83	57	2.6	41.8	21772	6	Cu
15	00	06	20	18	7.00N	140.02E	1008.1	28.0	80	85	4.4	33.1	23209	5	Cu,Cb
16	00	06	20	21	7.03N	140.03E	1007.9	27.6	85	35	3.1	30.1	23811	8	Cb,Cu,As,Ac
17	00	06	21	0	7.01N	140.03E	1009.2	29.0	76	71	4.7	49.3	20761	6	Cb,Ns,Cu,Ac,As
18	00	06	21	3	7.03N	140.07E	1008.7	29.4	76	29	2.7	36.6	22579	8	Ci,As,Cu
19	00	06	21	6	7.00N	140.01E	1007.2	29.6	71	118	2.9	26.4	24660	8	Ns,Cb,Cu
20	00	06	21	9	6.99N	140.04E	1008.6	25.9	86	100	6.4	608.3	4299	10	St,Ns,Cu
21	00	06	21	12	7.01N	140.04E	1009.4	26.7	86	98	4.8	42.3	21677	10	St,As,Ns
22	00	06	21	15	7.03N	140.05E	1009.7	27.4	83	100	8.1	78.0	17993	10	Ns,Cu
23	00	06	21	18	7.03N	140.04E	1008.6	26.6	70	147	4.6	574.8	4759	10	Ns
24	00	06	21	21	7.01N	140.01E	1009.6	26.5	80	109	2.7	44.6	21322	9	Cu,Sc,As,Ac
25	00	06	22	0	6.99N	140.06E	1010.5	25.4	90	156	8.6	524.5	5514	10	Cu,Ns,Sc
26	00	06	22	3	7.01N	140.07E	1009.7	26.9	76	123	7.4	33.1	23225	10	Sc,Ac,Cu,Ns
27	00	06	22	6	7.03N	140.01E	1007.7	28.4	75	117	6.3	25.8	24768	10	Cu,As
28	00	06	22	9	7.02N	140.05E	1008.4	28.3	77	112	7.2	43.7	21481	9	Cu,Cb,As
29	00	06	22	12	7.02N	140.02E	1009.9	25.5	88	100	8.5	124.9	15251	10	As,St
30	00	06	22	15	7.03N	140.03E	1009.6	26.1	84	59	4.6	31.6	23505	10	N/A
31	00	06	22	18	7.02N	140.04E	1008.1	27.0	80	52	5.1	38.5	22262	10	Ns
32	00	06	22	21	7.06N	140.05E	1008.6	27.6	76	81	5.7	33.1	23167	7	Cu,Sc,Ac
33	00	06	23	0	7.01N	140.01E	1009.7	28.6	73	57	5.4	26.8	24523	8	Cu,Ac,Cb,Ns
34	00	06	23	3	7.02N	140.02E	1007.9	29.4	65	76	6.6	31.0	23564	3	Cu,As,Ci
35	00	06	23	6	7.03N	139.99E	1006.2	29.1	73	63	4.1	26.3	24646	4	Cu,Ci,As
36	00	06	23	9	7.03N	140.03E	1006.7	28.7	77	68	3.8	37.6	22393	4	As,Cb,Cc,Cs,As,Ac
37	00	06	23	12	7.00N	140.01E	1008.6	28.3	75	69	5.8	32.5	23346	2	As,Sc
38	00	06	23	15	6.95N	140.04E	1008.1	28.4	78	60	11.9	28.2	24218	2	Cu
39	00	06	23	18	6.96N	140.02E	1006.8	28.2	77	76	5.1	28.0	24222	3	Cu
40	00	06	23	21	7.04N	140.04E	1007.0	28.0	81	72	6.2	43.9	21415	5	Cu,Cb,Ci
41	00	06	24	0	7.01N	140.02E	1007.6	29.0	72	69	7.6	34.7	22891	2	Cu,Cb,Ac
42	00	06	24	3	7.03N	140.05E	1006.5	29.6	74	71	3.7	28.1	24194	2	Cb,Cu,Ci,As
43	00	06	24	6	7.01N	140.04E	1005.1	29.5	73	61	4.9	36.9	22481	6	St,Cu,Cb
44	00	06	24	9	7.02N	140.03E	1005.8	28.3	77	87	3.7	150.7	14201	4	Cu,Cb,As,Ci
45	00	06	24	12	7.00N	140.01E	1007.4	27.9	82	67	5.2	34.8	22890	4	As,St,Sc
46	00	06	24	15	7.00N	140.04E	1007.3	27.9	77	98	5.6	32.6	23310	1 -	N/A
47	00	06	24	18	6.97N	140.07E	1005.9	28.0	79	105	5.5	27.4	24391	2	Cb,Cu
48	00	06	24	21	6.98N	140.02E	1006.5	27.0	80	149	3.6	27.1	24459	3	Cu,St,Cb,As
49	00	06	25	0	7.01N	140.00E	1007.1	28.4	72	143	2.9	25.1	24902	3	Cb,Cu,Cs,Ci
50	00	06	25	3	7.02N	140.06E	1006.0	29.6	71	77	4.9	258.0	10726	6	Cu,As,Ci
51	00	06	25	6	7.03N	139.97E	1004.4	29.0	77	93	1.9	27.1	24447	5	Cb,Cu,As
52	00	06	25	9	7.02N	140.03E	1005.2	28.0	78	112	5.1	38.2	22287	6	Cu,Cb,As
53	00	06	25	12	7.00N	140.01E	1006.7	27.8	81	112	5.5	29.5	23946	4	Sc,As,Cu
54	00	06	25	15	7.01N	140.04E	1007.1	27.6	86	98	5.0	N/A	N/A	1	N/A
55	00	06	25	18	6.99N	140.05E	1005.7	27.4	82	142	4.7	29.1	24011	7	N/A
56	00	06	25	21	6.96N	140.04E	1005.7	27.7	79	111	3.1	28.1	24208	6	Cb,Cu,As,Ci
57	00	06	26	0	6.99N	140.01E	1006.6	25.9	64	90	3.9	31.8	23462	8	Cu,Sc
58	00	06	26	3	7.00N	140.14E	1005.8	30.7	63	88	5.5	23.4	25375	8	Cu,As
59	00	06	26	6	7.01N	140.00E	1004.3	29.4	71	96	5.2	23.5	25360	9	Cu,As,Cb,Ci
60	00	06	26	9	6.99N	140.03E	1005.2	26.3	85	132	9.5	36.5	22595	7	Cb,Cu
61	00	06	26	12	6.98N	140.01E	1006.7	26.8	76	111	2.2	39.4	22151	3	Cu,As
62	00	06	26	15	6.95N	140.01E	1007.3	26.9	82	344	2.1	269.5	10454	10	Cu
63	00	06	26	18	6.91N	140.02E	1005.4	27.0	81	260	2.4	28.7	24117	7	Cu
64	00	06	26	21	6.98N	139.95E	1006.1	26.1	81	194	2.1	32.2	23332	10	As,Ac,St,Cb,Cu
65	00	06	27	0	7.01N	140.01E	1006.9	27.1	77	201	0.3	26.1	24581	9	Ac,Cu,Ns
66	00	06	27	3	6.91N	140.06E	1005.6	28.7	74	90	4.2	163.3	13610	8	Cb,Cu,As
67	00	06	27	6	7.00N	140.02E	1004.3	26.2	85	159	2.2	568.6	4814	10 -	Cb,Cu
68	00	06	27	9	6.98N	140.02E	1004.8	27.7	77	104	5.8	32.1	23383	8	Cb,Cu,As,Sc
69	00	06	27	12	6.99N	140.04E	1006.7	27.5	81	85	5.6	31.8	23482	5	Cu,As,Sc
70	00	06	27	15	7.00N	140.05E	1006.5	27.2	80	82	12.6	34.6	22954	7	N/A
71	00	06	27	18	6.97N	140.10E	1004.8	26.8	79	131	5.7	35.7	22729	6	N/A
72	00	06	27	21	6.99N	140.01E	1004.7	27.2	81	91	6.4	23.4	25385	8	Cb,Cu,St,As,Ac,Ci
73	00	06	28	0	6.99N	140.04E	1006.5	28.7	76	81	10.2	30.3	23786	10	Cu,Ac,As,Cb
74	00	06	28	3	7.02N	140.10E	1005.5	27.1	81	109	7.2	31.6	23489	10	Ns,Cu,As
75	00	06	28	6	6.96N	140.09E	1003.4	26.9	86	115	9.8	245.4	11058	10	Ns,Cb,As,Cu
76	00	06	28	9	6.98N	140.02E	1003.2	27.9	79	149	6.9	87.9	17261	9	Sc,As
77	00	06	28	12	6.97N	140.01E	1005.4	28.0	79	140	5.8	576.2	4719	9	As,Sc
78	00	06	28	15	7.00N	140.05E	1005.8	25.2	93	161	4.4	67.9	18779	10	Cu,Ns
79	00	06	28	18	6.98N	140.02E	1004.4	25.4	85	158	1.1	34.8	22872	9	N/A
80	00	06	28	21	6.94N	140.04E	1004.4	26.9	81	134	4.6	27.8	24267	8	Cu,As,Ac,Cb

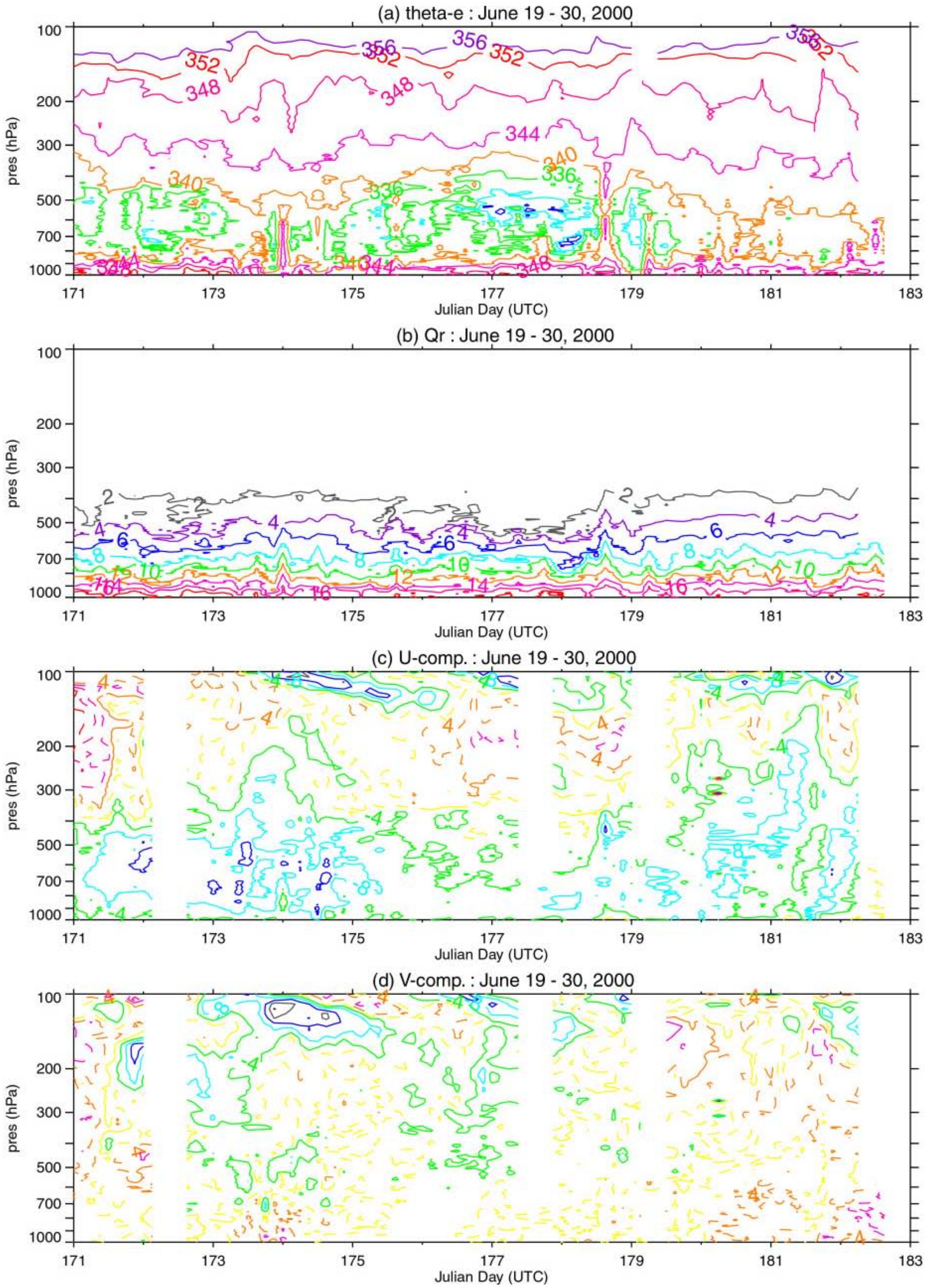

Fig.6.2-1: Time-height cross sections of (a) equivalent potential temperature (K), (b) mixing ratio (g/kg), (c) zonal, and (d) meridional wind components (m/s), respectively. Contour intervals are (a) 4K, (b) 2 g/kg, (c) and (d) 4 m/s.

6.3 Doppler Radar Observation

(1) Personnel

Masaki Katsumata (JAMSTEC): Principle Investigator
Masaki Hanyu (GODI): Operation Leader
Kunio Yoneyama (JAMSTEC)
Tomoki Ushiyama (Frontier Observational Research System for Global Change)
Masafumi Hirose (Nagoya Univ.)
Ken-ichi Shibayama (JAMSTEC)
Kaichi Moriwaki (JAMSTEC)
Fumitaka Yoshiura (GODI)
Souichiro Sueyoshi (GODI)
Kiyotake Kouzuma (GODI)

(2) Objectives

The Doppler radar is operated to obtain spatial and temporal distribution of rainfall amount, and structure of precipitating cloud systems.

(3) Methods

The hardware specifications of the shipborne Doppler radar (RC-52B, made by Mitsubishi Electric Co. Ltd., Japan) are

Frequency:	5290 MHz
Beam Width:	better than 1.5 degrees
Output Power:	250 kW (PEP)
Signal Processor:	RVP-6 (Sigmet Inc., U.S.A.)
Inertial Navigation Unit:	DRUH (Honeywell Inc., U.S.A.)
Application Software:	IRIS / Open (Sigmet Inc., U.S.A.).

The hardware is calibrated by checking (1) frequency, (2) mean power output, (3) transmitting pulse width, (4) pulse repetition frequencies, and (5) receiver linearity for once par a day, at least.

Spatial and temporal distribution of two parameters, radar reflectivity and Doppler velocity, were obtained for 120 km radius and 10 minutes intervals by volume scan, which consists of PPIs (Plan Position Indicator) for 21-elevations. The horizontal radar reflectivity fields were also obtained for 200 km radius and 10 minute intervals by surveillance PPI scan at one elevation of 0.5 degrees. In addition, a few vertical cross sections were observed by RHI (Range Height Indicator) scans to obtain detailed vertical structure of characteristic precipitating systems. The RHI scans obtain Doppler velocity and radar reflectivity, same as volume scan.

The parameters are summarized in Table 6.3-1.

Table 6.3-1: Parameters for each tasks.

	Surveillance PPI	Volume Scan	RHI
Pulse Width	2 [μs]	0.5 [μs]	
Scan Speed	18 [deg./sec.]		automatically determined
PRF	260 [Hz]	900 / 720 [Hz] (dual PRF)	
Sweep Integration	32 samples		
Ray Spacing	about 1.0 [deg.]		0.2 [deg.]
Bin Spacing	250 [m]	125 [m]	
Elevations	0.5	0.5, 1.2, 2.0, 3.0, 4.0, 5.0, 6.0, 7.0, 8.0, 9.0, 10.1, 11.3, 12.8, 14.6, 16.6, 18.9, 21.6, 25.0, 29.0, 34.0, 40.0	0.0 to 85.0 (continuous)
Azimuths	Full Circle		Optional
Filters	None	Dual-PRF velocity unfolding for Doppler velocity	

(4) Results

Figure 6.3-1 shows the time series of the echo area, obtained by surveillance PPI. As shown in the figure, we met two huge precipitating event in the beginning and the end of the observation period. An example of observed meso-scale precipitating system in the former event is shown in Figs. 6.3-1 and 6.3-2. As shown in Fig.6.3-1, this system had north-south oriented leading edge with strong (convective) precipitation and trailing stratiform precipitating area. The vertical cross section (Fig. 6.3-2) of the system shows strong rear-to-front wind which reached in front of the leading strong precipitation. (The strong gust was observed at Mirai at around 15UTC, after 1 hour of the figure.) This structure is similar to the “squall line” structure in the previous studies.

The detailed and integrated analyses on the various precipitating events are in the future works.

(5) Data Archives

The inventory information of the Doppler radar data obtained in this cruise will be submitted to the DMO (Data Management Office) of JAMSTEC. The original data will be archived at Ocean Research Department of JAMSTEC (Contact Masaki Katsumata)

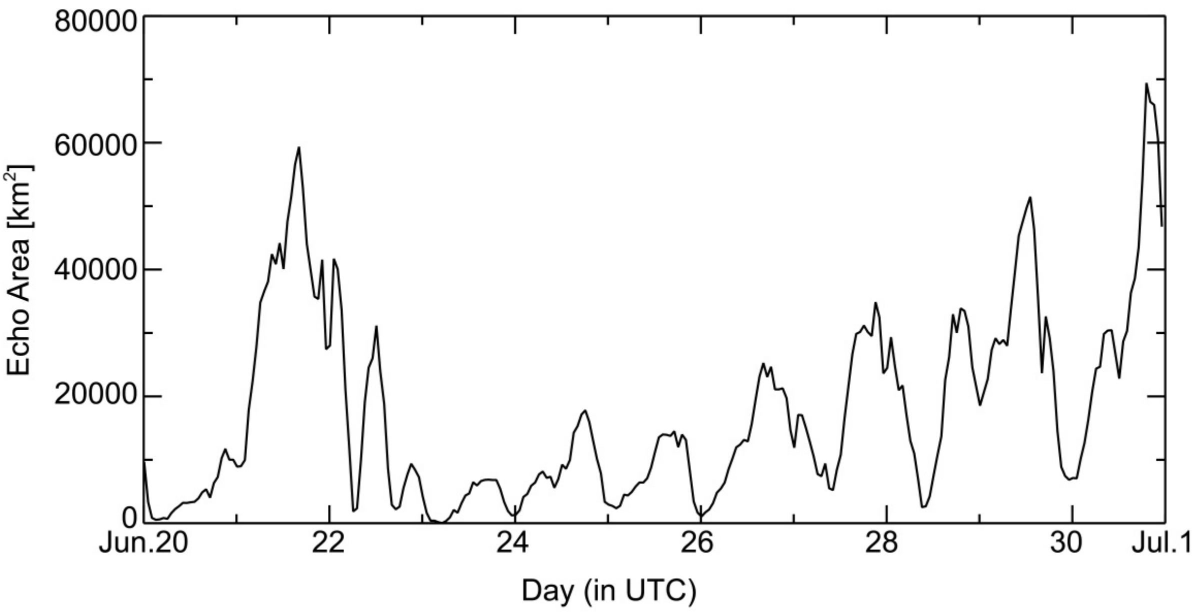

Fig. 6.3-1: Time series of the radar echo area (> 15dBZ) which is obtained by surveillance PPI (for 200 km radius area; about 125000 km^2), for the period of the "fixed-point observation".

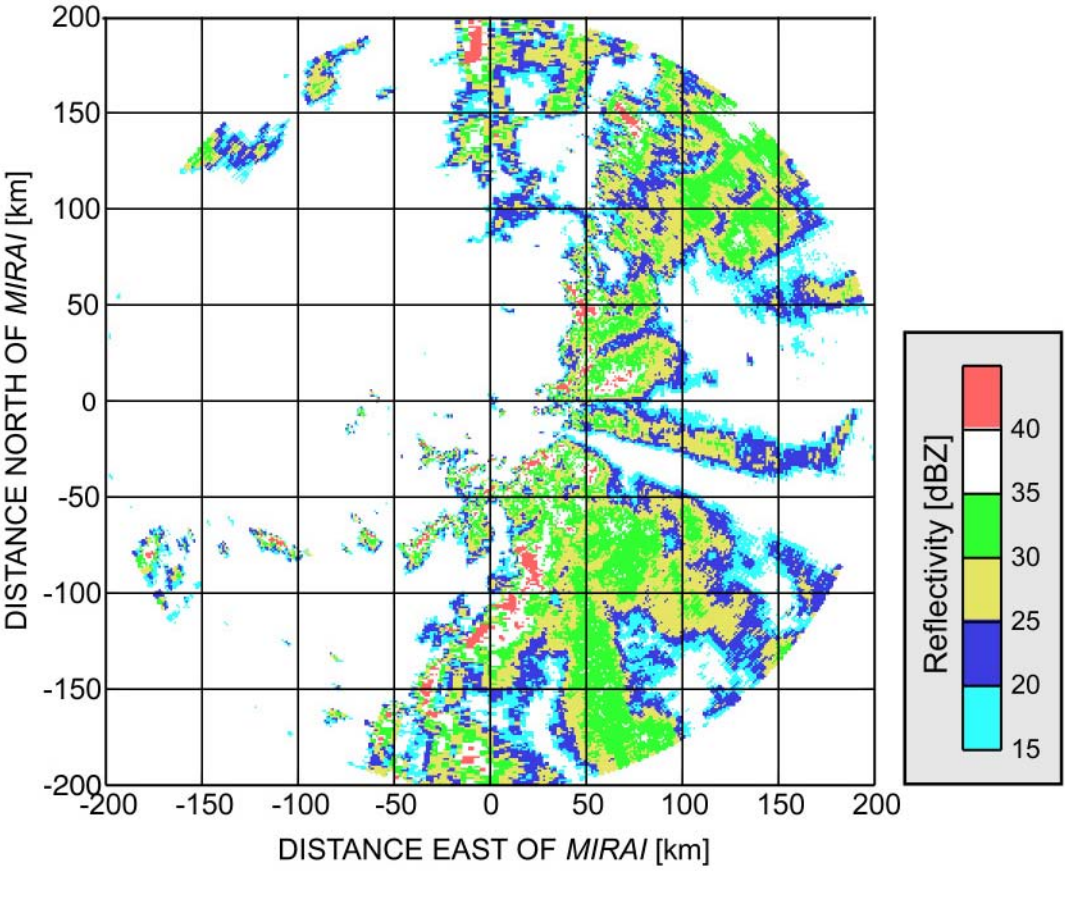

Fig. 6.3-2: The horizontal distribution of radar reflectivity image at 1408UTC, June 21, 2000, obtained by surveillance PPI.

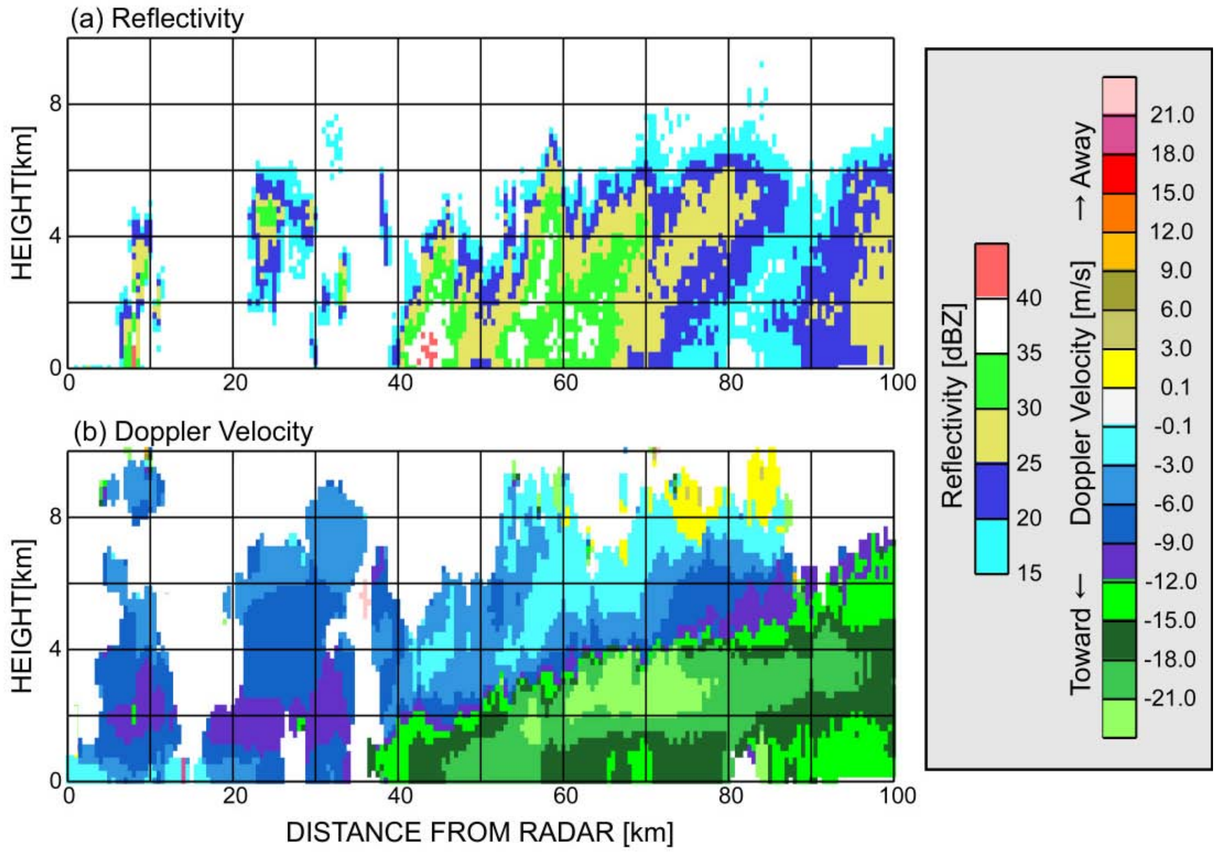

Fig. 6.3-3: The vertical cross section of (a) radar reflectivity and (b) Doppler velocity for the azimuth of 120° at 1408 UTC, June 21, 2000, obtained by RHI scan.

6.4 Lidar Observation

6.4.1 Mie Scattering Lidar

(1) Personnel (* indicates on board personnel)
Ichiro Matsui (NIES)*
Nobuo Sugimoto (NIES)
Osamu Takahashi (TIT)
Kazuhiro Asai (TIT)

(2) Objectives
Shipborne Mie scattering lidar observation of aerosols and clouds have been started using R/V Mirai. The purposes of the observation are to obtain global distribution and optical characteristics of aerosols and clouds which are used in the climatological study and in the study on the data reduction algorithms and data methods for space borne lidars.

(3) Method
The lidar employs a compact flashlamp pumped second-harmonics Nd:YAG laser. Mie scattering at 1064 nm and 532 nm, and depolarization ratio at 532 nm were recorded. System parameters are as follows.

Laser:	Big Sky Laser CFR-200
Output power:	532nm 50mJ/Pulse, 1064nm 100mJ/pulse
Repetition rate:	10Hz
Beam div.:	0.5mrad
Receiver:	Schmidt cassegrainian
Diameter:	280 mm
Field of view:	1mrad
Detector:	PMT(532nm) , APD(1064nm)
Data collection:	LeCroy LC574AL
Measurement range:	0-24km Range resolution: 6m
Sampling rate:	10sec

(4) Results
Figure 6.4.1-1 shows a temporal variation of vertical profile. The range-corrected lidar signal at 532 nm is indicated with a color scale. Diurnal variation of boundary layer is not significant as seen in Fig.1. Low clouds are frequently observed at the top of the planetary boundary layer. Cirrus clouds are also frequently observed in an altitude range of 10 to 15 km.

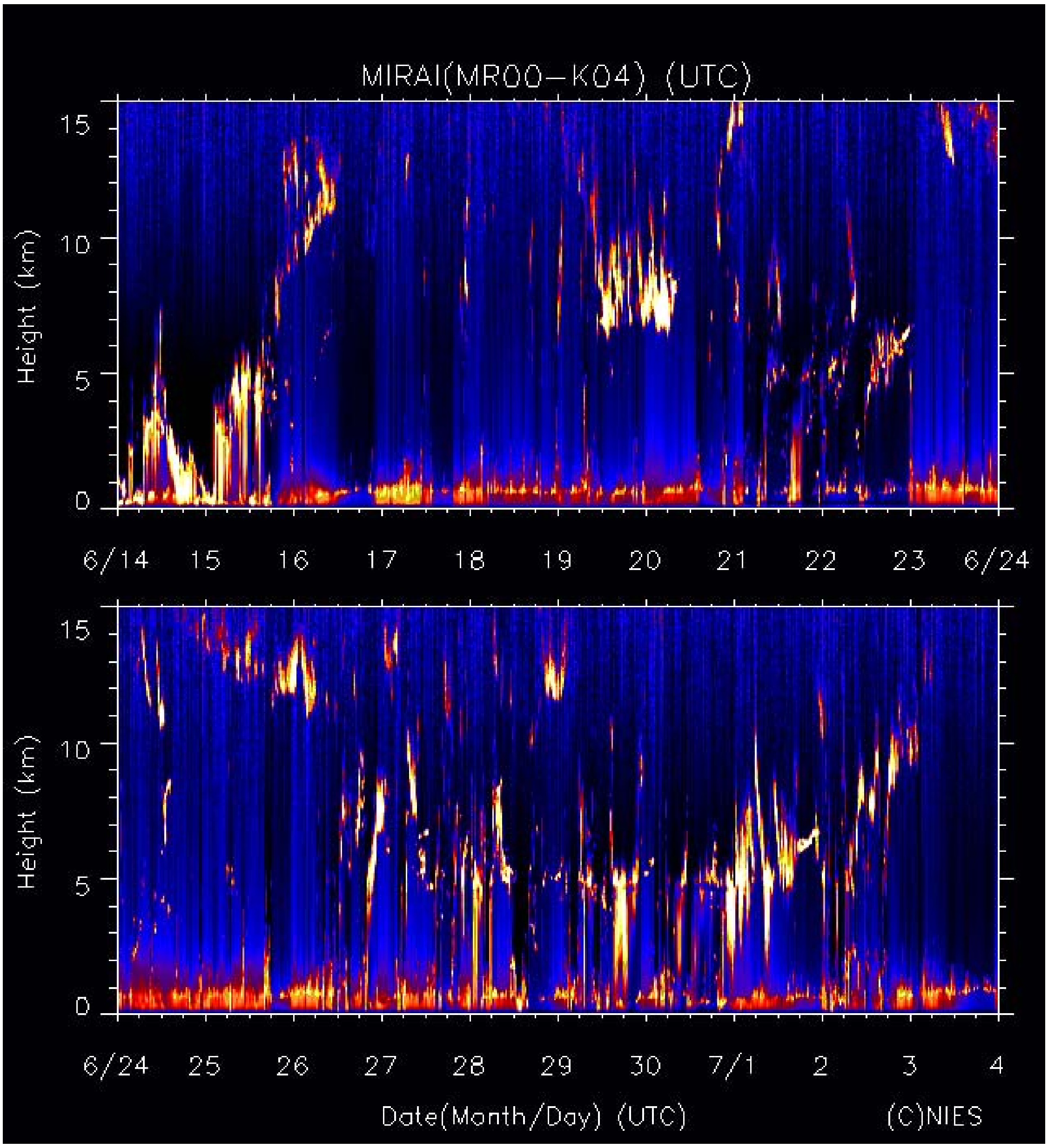

Fig.6.4-1: Temporal variation of range-corrected lidar signal at 532 nm.

(6) Data archive

All data will be archived at NIES and TIT. The data is also submitted to and archived at JAMSTEC DMO.

6.4.2 Ceilometer Observation

(1) Personnel

Masaki Hanyu (GODI) : Operation Leader
Kunio Yoneyama (JAMSTEC)
Masaki Katsumata (JAMSTEC)
Souichiro Sueyoshi (GODI)
Fumitaka Yoshiura (GODI)
Kiyotake Kouzuma (GODI)

(2) Objectives

The information of the cloud base height and the liquid water amount around cloud base is important to understand the processes on the formation of the cloud. As few method to measure them, the ceilometer observation was carried out.

(3) Methods

We measured cloud base height and backscatter profiles using CT-25K ceilometer (Vaisala, Finland) throughout MR00-K04 cruise from the departure of Sekinehama on 13 June 2000, to the arrival of Yokosuka on 6 July 2000.

Major parameters for the measurement configuration are as follows;

Laser source:	Indium Gallium Arsenide (InGaAs) Diode
Transmitting wave length:	905 +-5 nm at 25 deg-C
Transmitting average power:	8.9 mW
Repetition rate:	5.57 kHz
Detector:	Silicon avalanche photodiode (APD)
	Responsibility at 905 nm : 65 A/W
Measurement range:	0 - 7.5 km
Resolution:	50 ft in full range
Sampling rate:	60 sec.

On the archived dataset, cloud base height and backscatter profile are recorded with the resolution of 30 m (100 ft.).

(4) Preliminary results

An example of observed backscatter is shown in Fig. 6.6.2-1. The signal reaching ground before 11:30 UTC corresponds to the precipitating clouds passed over Mirai. After that, the significant signals are in two height: one is at about 500 m height, and other is in upper layer. The former is recognized as the cloud base of small cumulus. In contrast, the latter is recognized as the stratiformed non-precipitating cloud (or precipitating cloud but the rain did not reached ground) following the precipitating leading cloud, which passed Mirai before 11:30 UTC. The further and detailed analyses with radiosonde data, Doppler radar data, etc. are future works.

(5) Data archives

Ceilometer data obtained during this cruise will be submitted to the DMO (Data Management Office) of JAMSTEC, and will be under their control.

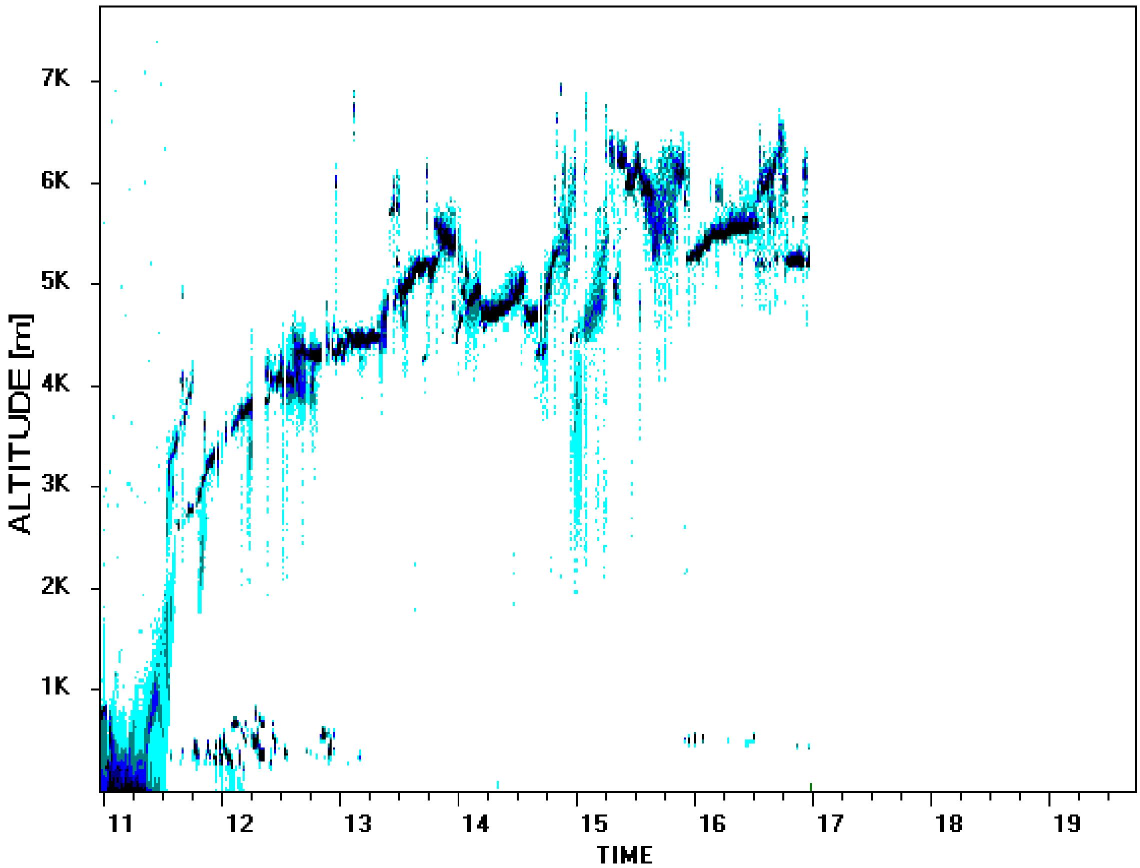

Fig. 6.4.2-1: Time height cross section of backscatter coefficient observed by ceilometer on Jun. 22, 2000. Time is in UTC.

6.5 Surface Turbulent Flux Measurement

(1) Personnel

Osamu Tsukamoto (Okayama University): Principal Investigator
Hiroshi Ishida (Maritime University of Kobe /
Frontier Observational Research system for Global Change)
Tetsuya Takemi (Osaka University)
Satoshi Takahashi (Okayama University)
Ayako Nakanishi (Okayama University)

(2) Objectives

For the understanding of air-sea interaction, accurate measurements of surface heat and fresh water budgets are necessary as well as the momentum exchange through the sea surface. The surface turbulent fluxes of momentum, sensible heat and latent heat (water vapor) were measured with the eddy correlation method. These flux measurement data are combined with radiation and CTD measurements to lead the surface energy budget.

(3) Methods

A new flux measurement system was supplied by Frontier Observational Research system for Global Change. It consists of a turbulence measurement system (Kaijo Co.,Ltd) and a ship motion measurement system(Kanto Aircraft Instrument Co.,Ltd). A three dimensional sonic anemometer-thermometer (Kaijo, DA-600) and an infrared hygrometer (Kaijo, AH-300) were mounted on the top of the foremast. These turbulence instruments output signals of turbulent fluctuations of three components of wind velocity, air temperature and specific humidity. The anemometer measures relative wind velocities effected by the ship motion. The motions were measured with the motion sensors, such as an inclinometer (Applied Geomechanics, MD-900-T), accelerometers (Applied Signal Inc.,QA700-020) and rate gyros (Systron Donner, QRS11-0050-100). Fig. 6.5-1 and Fig. 6.5-2 show the installation and block diagram.

During the present cruise, it is found that high frequency noise were found in the motion signals when R/V Mirai stayed the point or cruising in dead slow. It is found that bow/astern thruster induce mechanical vibrations on the ship including the foremast. So she cruised at 8knot during the time of eddy flux measurement after 26 June.

These signals were sampled at 10 Hz with a PC based data logging system (Labview, National Instruments Co.,Ltd). The turbulent fluxes of momentum, sensible heat and latent heat (water vapor) are calculated with the eddy correlation method including the ship motion correction. This complicated data processing is carried out after the cruise.

Sea surface temperature was continuously measured with a infrared radiation thermometer (TASCO. THI-700) at the bow of the ship during the period of IOP. 1 minute mean values were recorded with a data logging system (CR-23X, Campbell Scientific Co.,Ltd).

(4) Results

The continuous measurements of turbulent fluctuations were carried out throughout the cruise (Sekinehama – 7N,140E – Yokosuka). Three-hourly flux observation was carried out during the period of IOP (20-30 Jun) at 7N,140E, as a sequence of the radio sonde sounding and CTD cast. Favorable wind conditions are selected and analyzed later. The time of the flux measurements is listed in Table 6.5-1.

(5) Data archives

The raw data of turbulent fluctuation time series were archived in MO disks. All raw data are submitted to JAMSTEC DMO. The processed data of turbulent fluxes will be archived in Okayama University and open to public after the data processing and quality check.

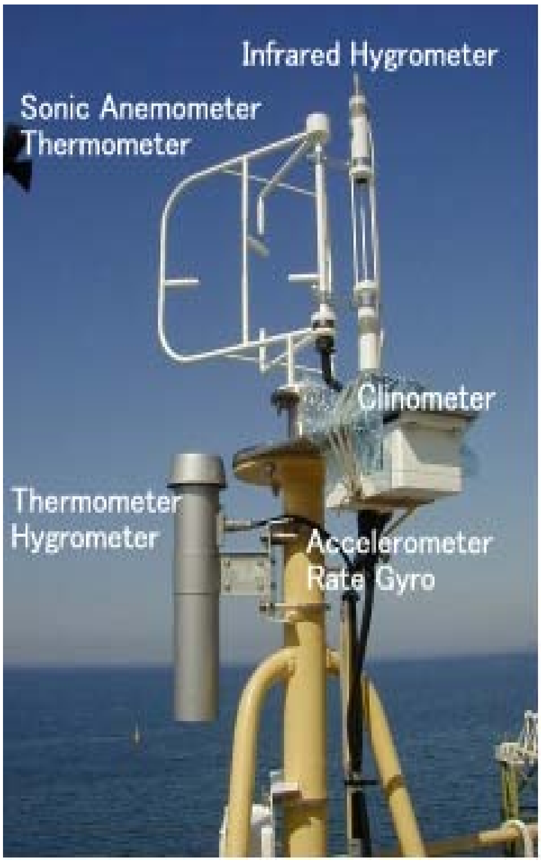

Fig.6.5-1

Installation at the top of the foremast

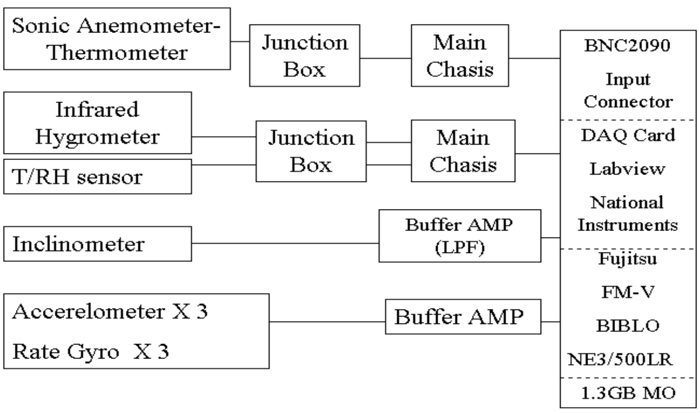

Fig.6.5-2 Block diagram of the observation

Table 6.5-1 List of turbulent flux measurements at 7N,140E

Date(JST) (day-Mon)	Start Time(JST) (hr:min)	End Time(JST) (hr:min)	Duration (hr:min)	Remarks and Memo
20-Jun	12:28	13:40	1:12	cloudy
	15:25	16:49	1:24	fine
	17:27	19:20	1:53	
	21:25	22:50	1:25	fine
	23:28	1:35	2:07	fine
21-Jun	3:26	4:51	1:25	
	5:26	7:38	2:12	cloudy
	9:29	11:00	1:31	fine
	12:55	13:42	0:47	fine
	15:25	16:50	1:25	shower
	17:30	19:30	2:00	cloudy
	21:27	22:48	1:21	
	23:30	1:37	2:07	shower
22-Jun	3:25	4:55	1:30	shower
	6:05	7:51	1:46	cloudy
	9:35	11:00	1:25	cloudy
	11:34	13:30	1:56	cloudy
	15:25	16:45	1:20	cloudy
	17:29	19:20	1:51	cloudy
	21:27	23:00	1:33	cloudy
	23:30	1:40	2:10	cloudy
23-Jun	3:30	5:02	1:32	cloudy
	5:30	7:20	1:50	fine
	9:28	10:52	1:24	fine
	12:20	13:40	1:20	fine
	15:25	16:45	1:20	fine
	17:20	19:20	2:00	fine
	21:45	23:00	1:15	fine
	23:30	1:30	2:00	fine
24-Jun	3:30	5:10	1:40	
	5:29	7:33	2:04	fine
	9:33	10:50	1:17	cloudy
	12:30	13:45	1:15	fine
	15:25	16:50	1:25	fine
	17:29	19:24	1:55	fine
	21:26	22:55	1:29	fine
	23:30	1:40	2:10	fine
25-Jun	3:25	4:41	1:16	fine
	5:29	7:22	1:53	cloudy
	9:32	10:53	1:21	fine
	12:20	13:50	1:30	fine

	15:25	16:51	1:26	cloudy
	17:29	19:25	1:56	
	21:22	22:55	1:33	fine
	23:29	1:40	2:11	
26-Jun	3:25	4:50	1:25	fine
	5:29	7:22	1:53	cloudy
	9:24	10:56	1:32	cloudy, MAST vibration test
	12:40	14:15	1:35	fine, 8 knot cruise started
	15:25	16:33	1:08	cloudy
	17:33	19:10	1:37	
	21:24	22:35	1:11	cloudy
	23:33	1:30	1:57	cloudy
27-Jun	3:35	4:33	0:58	
	5:35	7:47	2:12	cloudy
	9:25	10:55	1:30	cloudy
	12:35	14:00	1:25	fine
	15:25	16:31	1:06	cloudy
	17:29	19:03	1:34	cloudy
	21:17	22:35	1:18	
	23:03	1:40	2:37	shower
28-Jun	3:30	4:17	0:47	shower
	5:29	6:59	1:30	cloudy
	9:32	10:54	1:22	cloudy
	11:36	13:20	1:44	cloudy
	15:30	16:24	0:54	cloudy
	17:32	18:59	1:27	cloudy
	21:22	22:35	1:13	
	23:33	1:20	1:47	
29-Jun	3:30	4:41	1:11	
	5:31	6:59	1:28	cloudy
	9:24	10:50	1:26	cloudy
	11:45	13:20	1:35	cloudy
	15:25	16:43	1:18	cloudy
	17:30	19:09	1:39	
	21:27	22:35	1:08	
	23:35	1:25	1:50	
30-Jun	3:30	4:39	1:09	shower
	5:29	7:12	1:43	cloudy
	9:23	10:51	1:28	fine
	11:45	13:20	1:35	fine
	15:30	16:36	1:06	shower
	17:29	19:10	1:41	shower
	22:01	22:50	0:49	shower

6.6 Aerosol Sampling and Measurement by pre-ACE Asia Group

Kazuhiko Miura (SUT)

Atmospheric aerosol particles affect the Earth's radiative balance directly by scattering or absorbing light, and indirectly by acting as cloud condensation nuclei (CCN), thereby influencing the albedo and life-time of clouds. The natural aerosol has been substantially perturbed by anthropogenic activities, particularly by increases of sulfates, nitrates, organic condensates, soot, and soil dust. The present day global mean radiative forcing due to anthropogenic aerosol particles is estimated to be between - 0.3 and -3.5 Wm^{-2}, which must be compared with the present day forcing by greenhouse gases of between +2.0 and +2.8 Wm^{-2} (IPCC, 1995).

Although aerosol particles have this potential climatic importance, they are poorly characterized in global climate models. This is a result of a lack of both comprehensive global data and a clear understanding of the processes linking aerosol particles, aerosol precursor emissions, and radiative effects. At this time, tropospheric aerosols pose the largest uncertainty in model calculations of the climate forcing due to man-made changes in the composition of the atmosphere. Clearly there is an urgent need to quantify the processes controlling the natural and anthropogenic aerosol, and to define and minimize the uncertainties in the calculated climate forcings. Among the largest sources of uncertainty is the climate forcing by Asian aerosols.

The Aerosol Characterization Experiments (ACE), which are sponsored by the International Global Atmospheric Chemistry Program (IGAC), are envisioned as a series of international field studies aimed at understanding the combined chemical and physical processes that control the evolution of those aerosol properties that are relevant to radiative forcing and climate. The ultimate goal of this series of studies is to provide the necessary data to incorporate aerosols into global climate models and to reduce the overall uncertainty in the climate forcing by aerosols.

The strategy of ACE is to investigate the multiphase atmospheric system in key areas of the globe. ACE-1, conducted in late 1995, was aimed at the minimally polluted marine troposphere in the Southern Ocean near Tasmania. TARFOX, conducted in June of 1996, studied continental aerosol off the eastern coast of North America. ACE-2, conducted in June of 1997, focused on anthropogenic aerosols from the European continent and desert dust from the African continent as they move over the North Atlantic Ocean.

ACE Asia (ACE-3), of which intensive observations are planned in spring of 2001 and 2003, will focus on the outflow of both desert dust and anthropogenic aerosol from Eastern Asia to the Pacific. The goal of ACE Asia is to determine and understand the properties and controlling factors of the aerosol in the anthropogenically modified atmosphere of Eastern Asian and the Northwest Pacific and to assess their relevance for radiative forcing. (http://saga.pmel.noaa.gov/aceasia/)

MR00-K04 cruise is regarded as the Japanese pre-ACE Asia cruise. Principle Investigators of pre-ACE Asia group are shown in Table 6.6-1.

Table 6.6-1 Principle Investigators of pre-ACE Asia group.

PI	Participating Organizations
Kimitaka Kawamura	Institute of Low Temperature Science, Hokkaido University (ILTSa)
Tatsuo Endo	Institute of Low Temperature Science, Hokkaido University (ILTSb)
Mitsuo Uematsu	Ocean Research Institute, University of Tokyo (ORI)
Kazuhiko Miura	Faculty of Science, Science University of Tokyo (SUT)
Nobuo Sugimoto	National Institute for Environmental Studies (NIES)
Kunio Yoneyama	Japan Marine Science and Technology Center (JAMSTEC)

6.6.1 Study on the Transport Process and the Modification of Aerosols

(1) Personnel

Kazuhiko Miura (SUT): Principle Investigator
Takeshi Hara (SUT)
Takeshi Ui (SUT)
Takeshi Kishida (SUT)

(2) Objectives

In order to examine the transport process and the modification of aerosols, we measured the complete size distribution from 44nm to 5000nm in diameter and radon concentration and collected aerosols with filters and impactor. We also tested the kytoon observation up to 1300 m and the new sampling tower.

(3) Methods

- Sampling Tower (Fig. 6.6.1-1)
  80 x 3 m, main flow rate : 80 *l*/min, manifold with 5 inlets
- Continuous measurement of size distribution
  scanning mobility particle sizer : 3936N25 (3085 + 2025A), TSI Inc. (44<d<168nm)
  optical particle counters : KC18 and KC01, Rion Co. Ltd.
    (d>100, 150, 200, 250, 300, 500, 1000, 2000, 5000 nm)
- Continuous measurement of radon daughter concentration
  radon daughter monitor
- Measurement of particle concentration profile with kytoon system (Table 6.6.1-1, Fig. 6.6.1-2)
  kytoon : 10 m^3 in volume, up to 1300 m
  optical particle counter (d>300, 500, 700, 1000, 2000, 5000 nm) : KR12, Rion Co. Ltd.
- Measurement of particle concentration at various place (Table 6.6.1-2)
  optical particle counter (d>300, 500, 700, 1000, 2000, 5000 nm) : KR12, Rion Co. Ltd.
  place : for-mast, radar mast, inlet of sampling tower
- Observation of solar radiation
  portable sunphotometer (λ : 368, 500, 675, 778, and 862 nm) : MS-120(S), Eko Co.
- Sampling of aerosols and gasses
  low volume sampler (Table 6.6.1-3)
    aerosols : nuclepore filter (0.8 μm in pore size)
    acid gasses : Whatman-41 impregated with K_2CO_3
  cascade impactor (Table 6.6.1-4) : Model I-1L, PIXE Int. Corp.
    carbon-covered nitrocellulose film supported on an electron microscopic grid
  canister and bag : gasses (Table 6.6.1-5)
- Gas measurement
  SO_2 , NOX meter : GFS-32, DKK Co.

(4) Preliminary Results

An example of aerosol profile on 23 June 2000 with optical sonde on the kytoon system is shown in Fig. 6.6.1-3. This shows that there is a boundary at about 600 m in length and the concentration in the upper layer is lower than that in the under layer. The further analyses are in future work.

(5) Data Archives

The original data and samples will be archived at Department of Physics, Science University of Tokyo (Contact Kazuhiko Miura). The data are also submitted to JAMSTEC DMO.

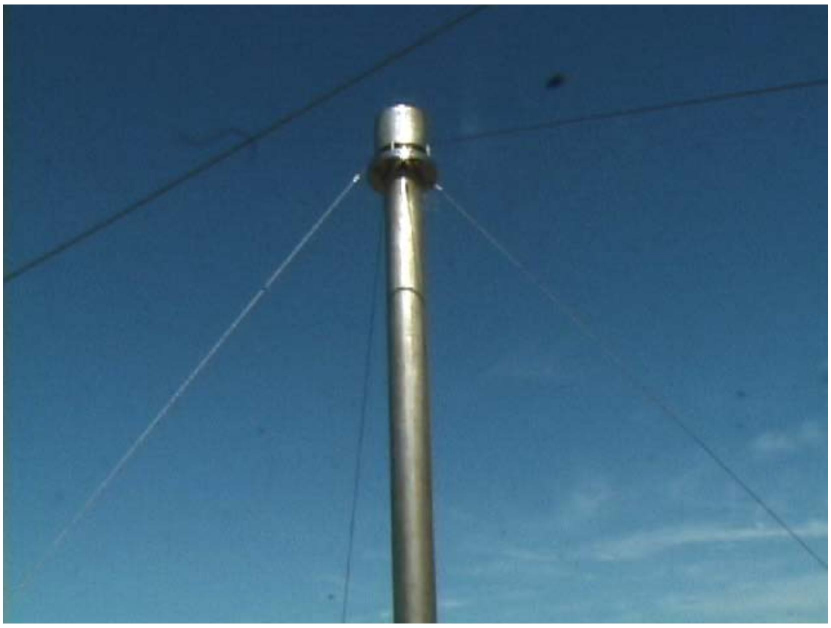

Fig. 6.6.1-1: Sampling tower.

Fig. 6.6.1-2: Kytoon.

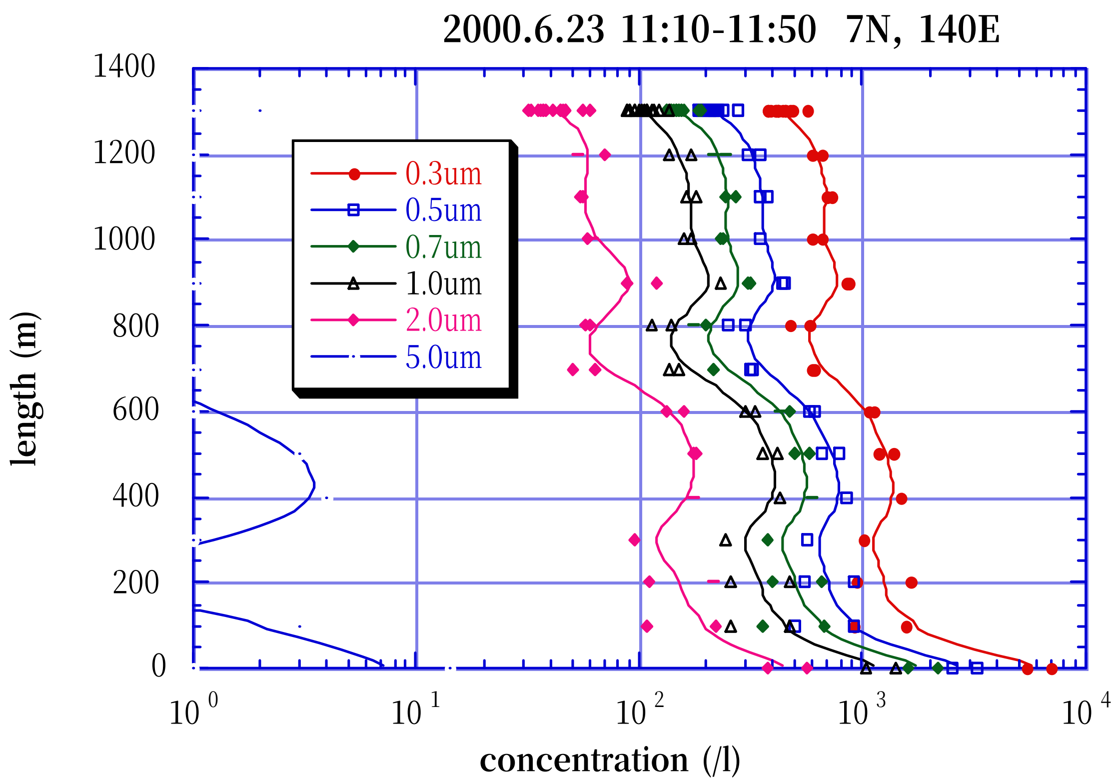

Fig. 6.6.1-3: An example of aerosol profile at 0210 to 0250 UTC on 23 June 2000, at (7N, 140E) with optical sonde on the kytoon system.

Table 6.6.1-1: Measuring list of the number concentration profile with OPC on the kytoon.

No.	date	start time	stop time	max. length (m)	latitude	longitude
1	2000.6.16	11:07	11:23	300	25-00N	140-00E
2	2000.6.18	5:27	6:03	1050	15-00N	140-00E
3	2000.6.20	11:07	11:28	800	7-00N	140-00E
4	2000.6.21	11:01	11:39	1300	7-00N	140-00E
5	2000.6.23	11:10	11:50	1300	7-00N	140-00E
6	2000.6.24	11:01	11:22	800	7-00N	140-00E
7	2000.6.25	11:19	11:32	600	7-00N	140-00E
8	2000.6.26	11:07	11:32	1000	7-00N	140-00E
9	2000.6.27	11:03	11:30	1000	7-00N	140-00E
10	2000.6.30	11:03	11:30	1000	7-00N	140-00E
11	2000.7.4	8:16	8:42	1000	25-??N	142-??E
12	2000.7.4	10:13	10:40	1000	26-??N	141-??E

Table 6.6.1-2: Measuring list of the number concentration with OPC at the various places.

No.	date	start time	stop time	place	latitude	longitude
1	2000.6.21	14:37	15:10	sampling tower	7-00N	140-00E
2	2000.6.22	13:07	13:32	FM,RM,ST	7-00N	140-00E
3	2000.6.22	13:39	13:59	FM,RM,ST	7-00N	140-00E
4	2000.6.23	13:39	16:44	sampling tower	7-00N	140-00E
5	2000.6.24	13:03	13:30	FM,RM,ST	7-00N	140-00E
6	2000.6.24	13:40	14:15	FM,RM,ST	7-00N	140-00E
7	2000.6.25	13:28	15:00	FM,RM,ST	7-00N	140-00E
8	2000.6.25	13:28	15:00	sampling tower	7-00N	140-00E
9	2000.6.26	13:33	14:00	FM,RM,ST	7-00N	140-00E
10	2000.6.26	14:00	15:06	sampling tower	7-00N	140-00E
11	2000.6.28	12:32	12:37	for-mast	7-00N	140-00E
12	2000.6.29	13:30	14:07	FM,RM,ST	7-00N	140-00E
13	2000.6.30	12:59	13:22	FM,RM,ST	7-00N	140-00E

Table 6.6.1-3: Sampling list of aerosols with filter holder.

Filter	date and time JST				sampling volume		sampling	total sampling	start point		stop point		remarks
No	start		stop		start	stop	period(min)	volume(little)	latitude	longitude	latitude	longitude	contamination
1	6/12	11:15	6/12	21:45	7.6 l/min	7.6 l/min	630	4788	41-21N	141-14E			
2	6/13	6:57	6/13	11:23	7.5 l/min	7.5 l/min	266	1995	41-28N	141-26E	40-33N	141-31E	
	6/13	17:54	6/14	8:02	7.5 l/min	7.5 l/min	848	6360					
3	6/14	8:30	6/14	20:06	7.5 l/min	7.5 l/min	696	5220	37-01N	142-08E	34-20N	141-21E	
4	6/14	21:01	6/15	8:23	7.5 l/min	7.0 l/min	683	4952	34-10N	141-17E	31-27N	140-21E	
5	6/15	8:53	6/15	20:14	7.5 l/min	7.5 l/min	681	5108	31-27N	140-21E	28-39N	139-59E	
6	6/15	20:44	6/16	8:04	7.5 l/min	7.5 l/min	680	5100	28-39N	139-59E	25-41N	140-00E	
7	6/16	8:29	6/16	10:40	7.6 l/min	7.6 l/min	131	996	25-41N	140-00E	25-01N	139-59E	
	6/16	20:30	6/17	7:52	7.6 l/min	7.5 l/min	682	5149	25-00N	139-59E	19-58N	139-59E	
8	6/17	9:14	6/17	22:30	7.5 l/min	7.5 l/min	676	5070	19-58N	139-59E			
	6/17	20:30	6/18	4:15	7.5 l/min	7.4 l/min	465	3464			16-57N	139-59E	
9	6/18	7:24	8/18	2:10	7.5 l/min	7.4 l/min	1128	8401	14-53N	139-58E	10-09N	140-19E	
10	6/19	7:35	6/19	20:00	7.5 l/min	7.4 l/min	745	5550	09-11N	139-59E	05-54N	140-00E	
	6/19	20:00	6/19	23:31	7.4 l/min	7.4 l/min	211	1561	05-54N	140-00E	05-00N	140-00E	
	6/20	1:07	6/20	12:31	7.4 l/min	7.4 l/min	684	5062	5-03N	140-00E	6-55N	140-03E	
	6/20	12:47	6/20	13:37	7.4 l/min	7.4 l/min	50	370	6-55N	140-03E	6-53N	140-05E	
	6/20	14:34	6/20	16:45	7.2 l/min	7.4 l/min	131	956					
11	6/20	17:48	6/20	19:16	7.4 l/min	7.5 l/min	88	556			7-00N	140-04E	
	6/20	19:16	6/20	22:46	7.4 l/min	7.4 l/min	210	1565	7-00N	140-04E	7-02N	140-03E	
	6/20	23:29	6/21	1:28	7.4 l/min	7.4 l/min	119	881	7-00N	140-00E	7-01N	140-05E	
	6/21	2:25	6/21	4:45	7.4 l/min	7.5 l/min	140	1043	6-59N	140-00E	7-12N	140-10E	
	6/21	5:35	6/21	7:22	7.5 l/min	7.0 l/min	107	776	7-00N	140-00E	7-03N	140-04E	
	6/21	8:31	6/21	11:27	7.4 l/min	7.4 l/min	176	1302	6-59N	140-00E			
	6/21	14:36	6/21	16:38	7.4 l/min	7.4 l/min	122	903			6-58N	140-03E	
	6/21	17:35	6/21	19:30	7.4 l/min	7.2 l/min	115	840	7-00N	140-00E			
12	6/21	20:32	6/21	22:35	7.4 l/min	7.4 l/min	123	910	7-00N	140-00E	7-01N	140-04E	
	6/21	23:31	6/22	1:38	7.4 l/min	7.4 l/min	127	940	7-01N	140-00E	7-01N	140-07E	

	6/22	2:32	6/22	4:26	7.5 l/min	7.5 l/min	114	855	7-00N	140-00E	7-00N	140-00E	
	6/22	6:15	6/22	7:42	7.4 l/min	7.4 l/min	87	644	7-00N	140-00E	6-58N	140-04E	
	6/22	8:45	6/22	11:01	7.4 l/min	7.4 l/min	136	1006	7-01N	140-00E	7-00N	140-04E	contamination
	6/22	11:38	6/22	13:25	7.4 l/min	7.4 l/min	107	792			6-57N	140-07E	probability
	6/22	14:30	6/22	16:42	7.5 l/min	7.5 l/min	132	990	7-01N	140-00E	7-00N	140-05E	
	6/22	17:34	6/22	19:14	7.5 l/min	7.4 l/min	100	745	7-07N	140-01E	6-59N	140-06E	
13	6/22	20:50	6/22	22:54	7.4 l/min	7.4 l/min	124	918	7-00N	139-57E	7-02N	140-01E	
	6/22	23:42	6/23	1:40	7.5 l/min	7.2 l/min	118	867	7-01N	140-00E	7-02N	140-06E	
	6/23	2:38	6/23	5:00	7.2 l/min	7.4 l/min	142	1051	7-00N	140-00E	7-03N	140-03E	
	6/23	5:41	6/23	7:18	7.4 l/min	7.4 l/min	97	718			7-01N	140-06E	
	6/23	8:29	6/23	8:47	7.4 l/min	7.4 l/min	18	133	7-00N	139-59E	7-00N	139-59E	
	6/23	9:03	6/23	11:54	7.4 l/min	7.4 l/min	171	1265	7-00N	139-59E	7-01N	140-03E	
	6/23	12:21	6/23	16:45	7.4 l/min	7.4 l/min	264	1954	6-58N	139-48E	7-03N	140-03E	
	6/23	17:38	6/23	19:20	7.4 l/min	7.4 l/min	102	755	6-59N	140-01E	7-00N	140-06E	
14	6/23	20:29	6/23	22:56	7.4 l/min	7.5 l/min	147	1095	6-59N	139-59E	6-57N	140-02E	
	6/23	23:34	6/24	1:29	7.5 l/min	7.5 l/min	115	863	6-58N	140-08E	6-56N	140-06E	
	6/24	2:35	6/24	4:57	7.4 l/min	7.4 l/min	144	1066	6-59N	140-00E	7-02N	140-02E	
	6/24	5:38	6/24	7:20	7.4 l/min	7.4 l/min	102	755	7-00N	140-01E	7-02N	140-05E	
	6/24	8:30	6/24	13:42	7.4 l/min	7.4 l/min	312	2309	7-00N	140-00E	7-01N	140-04E	
	6/24	14:35	6/24	16:41	7.4 l/min	7.4 l/min	126	932			7-01N	140-03E	
	6/24	17:37	6/24	19:20	7.4 l/min	7.4 l/min	104	762			6-59N	140-06E	
15	6/24	20:33	6/24	22:51	7.4 l/min	7.4 l/min	138	1021	7-00N	139-59E	6-59N	140-03E	
	6/24	23:40	6/25	1:30	7.4 l/min	7.4 l/min	110	814	6-59N	140-00E	6-58N	140-06E	
	6/25	2:39	6/25	4:35	7.4 l/min	7.2 l/min	116	847	6-59N	140-01E	6-56N	140-03E	
	6/25	5:36	6/25	7:18	7.2 l/min	7.4 l/min	102	745	6-59N	140-00E	6-55N	140-02E	
	6/25	8:25	6/25	11:12	7.5 l/min	7.4 l/min	167	1244	7-00N	139-59E	7-01N	139-54E	
	6/25	12:26	6/25	16:41	7.4 l/min	7.4 l/min	255	1887			7-02N	140-03E	
	6/25	17:49	6/25	19:19	7.4 l/min	7.4 l/min	90	666	6-58N	140-01E	6-57N	140-05E	
16	6/25	20:36	6/25	22:50	7.4 l/min	7.4 l/min	134	992	7-00N	140-00E	6-59N	140-04E	
	6/25	23:40	6/26	1:30	7.4 l/min	7.4 l/min	110	814	6-59N	140-01E	6-58N	140-06E	
	6/26	2:38	6/26	4:46	7.4 l/min	7.2 l/min	128	934	6-59N	140-00E	6-56N	140-03E	
	6/26	5:32	6/26	7:17	7.2 l/min	7.2 l/min	107	770	6-59N	140-01E	6-57N	140-06E	

	6/26	8:30	6/26	10:55	7.2 l/min	7.2 l/min	145	1044	6-59N	140-00E			
	6/26	12:45	6/26	16:32	7.2 l/min	7.2 l/min	227	1634	7-02N	139-49E	6-57N	140-07E	
	6/26	17:40	6/26	19:07	7.2 l/min	7.4 l/min	87	635	6-59N	140-00E	6-51N	140-06E	
17	6/26	21:08	6/26	22:31	7.4 l/min	7.4 l/min	83	614	6-59N	140-00E	6-51N	140-01E	
	6/26	23:53	6/27	1:34	7.2 l/min	7.2 l/min	101	727	6-59N	139-59E	6-48N	140-02E	
	6/27	2:50	6/27	4:33	7.2 l/min	7.2 l/min	103	741	6-57N	140-01E	6-56N	139-53E	
	6/27	5:40	6/27	7:34	7.2 l/min	7.4 l/min	116	847	6-57N	139-57E	7-01N	140-01E	
	6/27	9:34	6/27	10:54	7.4 l/min	7.4 l/min	80	592	6-58N	140-00E	6-53N	140-09E	
	6/27	12:52	6/27	13:54	7.2 l/min	7.2 l/min	62	446	6-57N	139-54E	6-59N	140-01E	
	6/27	14:29	6/27	16:21	7.2 l/min	7.2 l/min	112	806	6-59N	139-59E			
	6/27	17:35	6/27	18:57	7.2 l/min	7.4 l/min	87	635	6-58N	140-04E	6-58N	140-10E	
18	6/27	20:33	6/27	22:32	7.4 l/min	7.2 l/min	119	869	6-59N	139-59E	7-00N	140-08E	
	6/27	23:52	6/28	1:30	7.2 l/min	7.2 l/min	98	706	6-58N	139-59E	6-57N	140-11E	
	6/28	2:38	6/28	4:14	7.2 l/min	7.4 l/min	96	701	6-58N	140-02E	6-57N	140-08E	
	6/28	5:44	6/28	6:58	7.4 l/min	7.4 l/min	74	548	6-58N	140-11E			
	6/28	8:37	6/28	10:53	7.4 l/min	7.2 l/min	136	993	6-59N	139-59E	7-00N	140-08E	
	6/28	11:45	6/28	13:18	7.2 l/min	7.2 l/min	93	670	7-00N	140-03E	6-55N	140-13E	
	6/28	14:42	6/28	16:20	7.2 l/min	7.3 l/min	98	711	6-58N	140-01E	6-54N	140-06E	
	6/28	17:34	6/28	18:55	7.4 l/min	7.2 l/min	141	1029	6-59N	139-59E	6-50N	140-04E	
	6/28	20:41	6/28	22:34	7.2 l/min	7.2 l/min	113	814	7-00N	140-00E	6-57N	140-07E	
	6/28	23:39	6/29	1:19	7.2 l/min	7.2 l/min	100	814			6-51N	140-07E	
19	6/29	2:26	6/29	4:31	7.3 l/min	7.4 l/min	125	919	6-59N	139-59E	6-52N	140-04E	
	6/29	5:38	6/29	6:57	7.2 l/min	7.2 l/min	79	569	6-57N	140-01E	6-49N	140-06E	
	6/29	8:24	6/29	10:50	7.2 l/min	7.2 l/min	146	1051	7-00N	140-00E	6-55N	140-07E	
	6/29	12:22	6/29	13:16	7.4 l/min	7.4 l/min	54	400	7-00N	140-05E	6-54N	140-08E	
	6/29	15:39	6/29	16:40	7.4 l/min	7.4 l/min	61	451	6-58N	140-04E	6-55N	140-01E	
	6/29	17:35	6/29	19:09	7.4 l/min	7.4 l/min	94	696	6-57N	139-59E	6-53N	140-07E	
	6/29	20:43	6/29	22:31	7.2 l/min	7.2 l/min	108	778			7-03N	140-05E	
	6/29	23:46	6/30	1:15	7.2 l/min	7.2 l/min	89	641	7-00N	139-58E	7-00N	140-00E	
	6/30	2:34	6/30	4:37	7.4 l/min	7.2 l/min	123	886	7-00N	139-59E	6-51N	140-02E	
20	6/30	5:37	6/30	7:07	7.2 l/min	7.2 l/min	90	648	6-58N	140-00E	6-46N	140-00E	
	6/30	8:34	6/30	10:49	7.2 l/min	7.4 l/min	135	986	6-59N	139-59E	6-49N	140-03E	

	6/30	12:30	6/30	13:22	7.4 l/min	7.2 l/min	52	380			6-52N	140-05E	
	6/30	15:32	6/30	16:32	7.2 l/min	7.2 l/min	60	432	6-59N	140-00E	6-53N	140-04E	
	6/30	17:30	6/30	7:05	7.2 l/min	7.4 l/min	815	5950	7-00N	140-00E	6-58N	140-12E	
21	6/30	21:07	6/30	22:47	7.4 l/min	7.4 l/min	100	740	7-00N	139-59E	6-55N	140-03E	
	7/1	0:35	6/30	8:03	7.2 l/min	7.4 l/min	448	3270	7-00N	140-02E	6-59N	140-06E	
22	7/1	8:23	7/1	11:52	7.4 l/min	7.2 l/min	210	1533	8-44N	140-59E	9-42N	141-00E	contamination
23	7/1	14:10	7/2	8:08	7.4 l/min	7.2 l/min	1078	7869	10-14N	141-00E	14-41N	141-05E	
24	7/2	8:27	7/2	14:28	7.2 l/min	7.4 l/min	361	2635	14-41N	141-05E	16-01N	141-16E	contamination
25	7/2	14:46	7/3	8:11	7.4 l/min	7.4 l/min	1045	7733	16-06N	141-16E	20-26E	141-54E	
26	7/3	8:53	7/3	20:11	7.4 l/min	7.4 l/min	678	5017	20-31N	141-52E	23-07E	142-17E	

Table 6.6.1-4: Sampling list of aerosols with impactor.

No	date (JST)	start time	stop time	latitude	longitude	place	case No	remarks
1	2000.6.12	11:35	11:55	41-20N	141-14E	compass	No1-1	sekinehama
2	2000.6.13	9:25	9:45	40-52N	141-36E	compass	No1-2	
3	2000.6.13	20:25	20:45	40-39N	142-64E	compass	No1-3	
4	2000.6.14	8:10	8:30	37-01N	142-08E	compass	No1-4	
5	2000.6.14	20:14	20:34	34-20N	141-21E	compass	No1-5	
6	2000.6.15	8:53	9:13	31-27N	140-21E	compass	No1-16	
7	2000.6.15	20:15	20:35	28-41N	139-59E	compass	No1-17	
8	2000.6.16	8:07	8:27	25-38N	140-00E	compass	No1-18	
9	2000.6.16	12:03	12:23	25-00N	140-00E	300m	No1-19	
10	2000.6.16	12:03	12:23	25-00N	140-00E	compass	No1-20	
11	2000.6.16	20:05	20:25	23-01N	139-59E	compass	No2-1	
12	2000.6.17	9:15	9:35	19-58N	139-59E	compass	No2-2	
13	2000.6.17	20:06	20:26	16-57N	139-59E	compass	No2-3	
14	2000.6.18	6:47	6:57	15-00N	140-00E	300m	No2-4	
15	2000.6.18	6:47	6:57	15-00N	140-00E	compass	No2-5	
16	2000.6.18	20:31	20:51	11-26N	139-59E	compass	NO2-16	
17	2000.6.19	8:16	8:36	8-55N	139-59E	compass	NO2-17	
18	2000.6.19	20:02	20:22	5-47N	140-00E	compass	NO2-18	
19	2000.6.20	11:58	12:18	7-00N	140-00E	600m	NO2-19	
20	2000.6.20	11:58	12:18	7-00N	140-00E	compass	NO2-20	
21	2000.6.21	12:20	12:40			600m	No3-1	
22	2000.6.21	12:20	12:40				No3-2	
23	2000.6.22	11:42	12:02	7-06N	140-00E		No3-3	
24	2000.6.23	12:58	13:18				No3-4	
25	2000.6.24	11:56	12:16	7-00N	140-00E	800m	No3-5	
26	2000.6.24	11:56	12:16	7-00N	140-00E	compass	No3-16	
27	2000.6.25	11:55	12:05			600m	No3-17	
28	2000.6.25	11:55	12:05			compass	No3-18	
29	2000.626	12:10	12:20			1000m	No3-19	
30	2000.6.26	12:10	12:20			compass	No3-20	
31	2000.6.27	12:08	12:20			1000m	No4-1	
32	2000.6.27	12:08	12:20	6-58N	140-06E	compass	No4-2	
33	2000.6.28	12:35	12:55			compass	No4-3	
34	2000.6.29	12:42	13:02			compass	No4-4	
35	2000.6.30	12:35	12:55			compass	No4-5	
36	2000.7.1	8:01	8:21	8-38N	140-58E	compass	No4-16	
37	2000.7.1	20:08	20:28	11-54N	141-00E	compass	No4-17	
38	2000.7.2	8:07	8:27	14-41N	141-05E	compass	No4-18	
39	2000.7.2	20:13	20:33	17-35N	141-30E	compass	No4-19	
40	2000.7.3	8:10	8:30	20-28N	141-55E	compass	No4-20	
41	2000.7.3	20:10	20:30	23-07N	142-17E	compass	No5-1	

Table 6.6.1-5: Sampling list of gases with canister.

No.	canister No.	Date	JST	latitude	longitude	weather	air	seawater	wind speed	wind d.	remarks
							℃	℃	m/s	deg	
1	4835	1996/6/12	9:23	41 ° 00.3'	141 ° 37.0'	fog	12.6	-	1.6	135	running
2	1294	1996/6/13	8:39	36 ° 54.7'	142 ° 07.5'	rainy	16.1	16.9	9.5	14	running
3	1314	1996/6/13	20:10	34 ° 19'	141 ° 20'	cloudy	21.2	24.0	3.4	218	running
4	1971	1996/6/14	8:54	31 ° 27'	140 ° 21'	rainy	20.8	24.6	9.2	50	running
5	4830	1996/6/15	8:30	25 ° 35'	139 ° 59'	fine	27.6	28.6	7.7	125	running
6	1142	1996/6/15	20:04	23 ° 01'	139 ° 59'	fine	28.1	29.1	7.1	114	running
7	1485	1996/6/16	7:52	19 ° 59.9'	139 ° 59.9'	fine	28.5	29.1	7.4	83	running
8	Y1690	1996/6/17	8:11	14 ° 41.8'	140 ° 00'	fine	28.6	29.6	3.2	101	running
9	4870	1996/6/17	20:32	11 ° 27.0'	140 ° 00'	fine	28.6	29.7	4.5	179	running
10	1306	1996/6/18	8:20	8 ° 59'	139 ° 59'	fine	28.5	29.7	4.4	117	running
11	H1246	1996/6/19	12:00	6 ° 56'	140 ° 30'	fine	28.1	29.9	3	21	kytoon
12	1277	1996/6/20	12:20	7 ° 01.7'	140 ° 03.0'	fine	28.7	29.9	3.5	30	kytoon
13	2215	1996/6/21	11:43	7 ° 00.7'	140 ° 01.6'	cloudy	27.7	29.7	7.3	123	running
14	H1219	1996/6/22	12:58	6 ° 58.7'	139 ° 51.5'	fine					running
15	1284	1996/6/23	11:58	7 ° 01.1'	140 ° 01.8'	fine	29.0	29.8	4.2	12	kytoon
16	H1255	1996/6/24	11:53	7 ° 01'	139 ° 52'	fine	29.1	29.9	5.9	83	kytoon
17	H1040	1996/6/25	12:03	7 ° 01'	139 ° 55'	fine	29.5	30.0	4.8	80	kytoon
18	H1260	1996/6/26	11:59	6 ° 55'	139 ° 56'	fine	28.2	29.6	4.2	89	kytoon
19	1056	1996/6/27	12:37	6 ° 57'	140 ° 08'	cloudy	26.8	29.6	10	119	running
20	1278	1996/6/28	12:31	6 ° 59'	140 ° 06'	rainy	27.0	29.5	7.2	180	running
21	1148	1996/6/29	12:35	6 ° 56'	140 ° 01'	fine	27.1	29.8	6.5	356	running
22	1380	1996/6/30	8:03	8 ° 39.1'	140 ° 58.4'	cloudy	27.0	29.5	8.3	155	running
23	H1221	1996/6/30	20:10	11 ° 45.7'	141 ° 00.0'	cloudy	28.6	29.6	6.6	115	running
24	1282	1996/7/1	8:08	14 ° 41.4'	141 ° 05.7'	fine	28.9	29.7	6.4	129	CTD
25	1155	1996/7/2	8:11	20 ° 26'	141 ° 54'	fine	29.0	29.4	10.2	90	running
26	1891	1996/7/2	20:11	23 ° 07'	142 ° 17'	fine	26.0	29.1	9.8	92	running
27											
28											
29											
30											

6.6.2 Chemical Properties of Atmospheric Aerosols

(1) Personnel

Mitsuo Uematsu (Ocean Research Institute, The University of Tokyo): Principal Investigator

Kiyoshi Matsumoto (Ocean Research Institute, The University of Tokyo / Japan Science and Technology Corporation)

(2) Objectives

In order to investigate the chemical properties of marine aerosols over the western Pacific Ocean, measurements and sampling of atmospheric aerosols were carried out. Simultaneously, the concentration of ozone was also measured. In addition, rainwater samples were collected to evaluate wet deposition of atmospheric chemical species to the remote ocean.

(3) Methods

The concentrations of carbonaceous species (organic carbon and elemental carbon) in aerosols were measured for every 2 hours by using an Ambient Carbon Particulate Monitor (Rupprechet & Patashnick Co. Inc., Model 5400). The concentration of ozone was measured at 12 second intervals by using an ozone monitor (Dylec, Model 1150). The inlets of air were located on the compass deck (about 17m above the sea surface).

To analyze chemical components in aerosols, atmospheric aerosols were collected by using aerosol samplers. Bulk aerosol samples were collected for about 24 hours periods on cellulose acetate filters (Whatman 41) by a high-volume air sampler (Kimoto Electric Co. Inc., Model SS-1003A). Size-fractionated aerosols were collected on quartz fiber filters (Pallflex 2500QAT-UP) by a high-volume virtual impactor (Kimoto Electric Co. Inc., Model AS9) at 3 day intervals, a low-volume impactor at 3 day intervals, and a low pressure impactor (Tokyo Dylec, Model LP-20) at about 7 day intervals. In order to avoid contamination from ship exhaust, all aerosol samplers were automatically controlled by a wind sector to start sampling only when the relative wind direction ranged from -90 ° to 90 ° of the bow and the relative wind speed was higher than 1.0m/s. The collections of aerosols were carried out on the compass deck.

Rainwater samples were collected in a PTFE bottle using a PTFE-coated funnel by each rain event basis on the compass deck. After collections, the value of pH and electrical conductivity were measured immediately. The samples were stored in both polypropylene bottles and glass bottles.

After this cruise, the samples of aerosols and rainwater will be analyzed for chemical components (major inorganic ions and organic species).

(4) Preliminary Results

As an example, temporal variation of the concentrations of particulate elemental carbon from 13 to 30 June is shown in Figure 6.6.2-1. Latitudinal gradient was clearly found, showing lower concentrations in the tropical oceanic region. Relatively higher concentrations were detected in the middle latitudinal oceanic region, suggesting anthropogenic effects to the remote marine atmosphere.

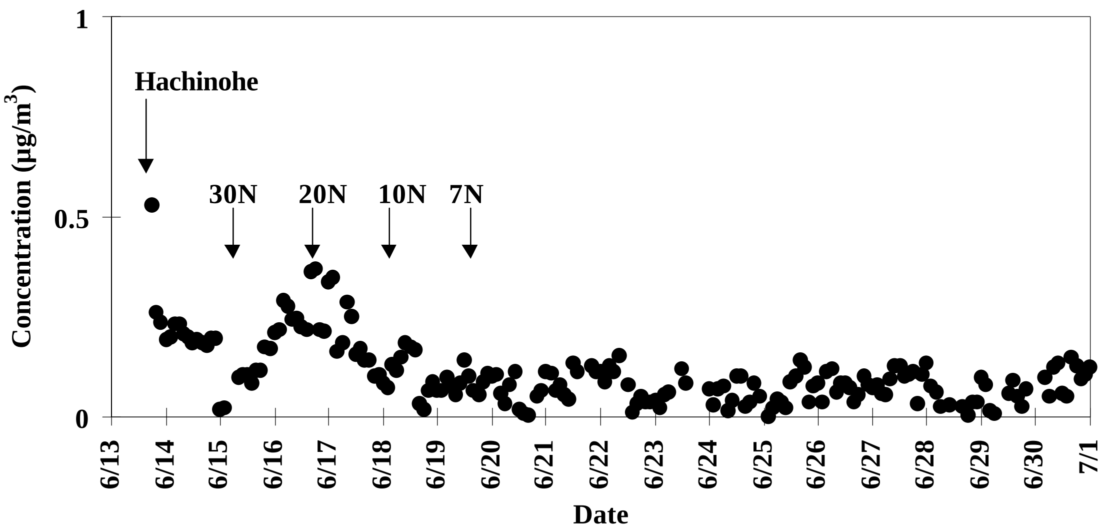

Figure 6.6.2-1 Temporal variation of the concentrations of particulate elemental carbon.

(5) Data Archives

The data of the concentrations of carbonaceous aerosols and ozone obtained in this cruise will be archived at Ocean Research Institute (ORI), the University of Tokyo. The samples of aerosols and rainwater collected in this cruise will be stored at ORI, and then analyzed for chemical components. The data and inventory of the samples are also submitted to JAMSTEC DMO.

6.6.3 Volatile and Particulate Organic Materials over the Western North Pacific and the Tropical Western Pacific

(1) Personnel

Kimitaka Kawamura (Hokkaido University)
Masahiro Narukawa (Hokkaido University)
Michihiro Mochida (Japan Science and Technology Corporation)

(2) Objectives

For studies of marine organic aerosols and volatile organic compounds (VOC's), the western North Pacific is an interesting oceanic region. A long-range transport of organic compounds from continental regions to the marine environments as well as sea-to-air flux of volatile and particulate materials from the ocean change the composition of aerosols and VOC's in the marine boundary layer. Particularly, attention has been paid to organic aerosols which may have an influence on the optical and microphysical properties of clouds in the western North Pacific. The tropical western Pacific is interesting from the viewpoint that this area would be influenced by airmass from the southern hemisphere by air mixing at ITCZ (intertropical convergence zone). Since atmosphere in the southern hemisphere is less influenced by human activities, it has different characteristics from that in the northern hemisphere. Gas-phase nonmethane hydrocarbons (NMHC's) in this area are expected to have information of mixing of airs from both hemispheres.

Regarding organic aerosols, previous studies on the marine organic aerosols have shown that water-soluble organic acids including low molecular weight dicarboxylic acids are abundant in the marine aerosols (Kawamura and Usukura, 1993). They comprise up to 18% of the total aerosol carbon in the Pacific atmosphere and their latitudinal distribution suggested that the low molecular weight diacids are produced in the marine atmosphere by photochemical oxidation of various organic compounds, mostly light hydrocarbons and oxygen-containing organic compounds (Kawamura and Sakaguchi, 1999). Furthermore, water-soluble organics alter hygroscopic behavior of atmospheric particles, suggesting that water-soluble organic compounds play an important role in controlling cloud albedo by acting as cloud condensation nuclei (CCN). The cloud activity is suggested to compensate the potential global warming caused by the increased concentrations of greenhouse gases such as carbon dioxide.

During this cruise (MR00-K04, from 6/13/2000 to 7/6/2000), aerosol samples were collected on quartz fiber filters and aluminum impaction plates to obtain spatial and size distribution of organic aerosols in the marine boundary layer over the western North Pacific and the tropical western Pacific. These samples are delivered to the laboratory in Hokkaido University and water-soluble organic compounds such as low molecular weight dicarboxylic acids are to be analyzed using capillary GC and GC/MS.

Gas samples were collected in stainless canisters to obtain spatial distribution of NMHC's and to measure their stable carbon isotope ratios ($^{13}C/^{12}C$). Isotope ratios are utilized to clarify sources of observed NMHC's and their precursors. Furthermore, we expect that their isotope ratios involve information to distinguish contribution of the oxidation process initiated by halogen atoms from that by OH radicals in the atmosphere.

In addition, rainwater samples were collected during this cruise. This is to reveal characteristics of tropical rainwater from viewpoint of organic compounds.

(3) Methods

Aerosol Analysis:

Aerosol samples were collected on the compass deck of R/V Mirai using pre-combusted (450℃, 3 hours) quartz fiber filters (Pallflex, 2500QAT-UP) using high volume air sampler (Kimoto 120F and Shibata HVC-1000N) and high volume air sampler with Andersen type 5-stage impactor (Shibata, HVC-1000N + Dylec Model AH-600Z). In addition, twelve-staged Micro-Orifice Uniform Deposit Impactor (MOUDI) (MSP corp., Model 110) with aluminum impaction plates was used for aerosol sampling. Quartz fiber filters and aluminum impaction plates after aerosol sampling were stored in pre-cleaned glass jars with Teflon-lined screw caps at –20℃ prior to analysis.

The specifications of air samplers are as follows.

1. High volume air sampler (HVS)

(Shibata, HVC-1000N)	Flow rate: 1000 L min^{-1}
(Kimoto, Model-120F)	Flow rate: 1500 L min^{-1}

2. Andersen-type high volume air sampler (AHVS) (Shibata HVC-1000N + Dylec Model AH-600Z)
   Flow rate: 1000 l min-1
   Particle diameter 50 % cut points: 5.2, 2.4, 1.5, and 0.79 μm

3. Micro-Orifice Uniform Deposit Impactor (MOUDI) (MSP corp., Model 110)
   Flow rate: 30 L min^{-1}
   Particle diameter 50 % cut points: 18, 10, 5.6, 3.2,1,8, 1.0, 0.56, 0.32, 0.18, 0.10, 0.056 μm

In order to collect aerosol samples only when relative wind direction is against the head of the ship, power supplies of these air samplers were controlled using a wind sector.

The time schedule of aerosol sampling was as follows.

6/13-6/19	HVS	6:00-18:00 and 18:00-6:00 LT
(Sekinehama – 7ºN, 140ºE)	AHVS	2 days (3 samples in this period)
	MOUDI	3 days (2 samples in this period)
6/20-6/30	HVS	1day, 2days, and 6:00-18:00 and 18:00-6:00 LT
(7ºN, 140ºE)	AHVS	1 sample in this period
	MOUDI	1 sample in this period
7/1-7/5	HVS	6:00-18:00 and 18:00-6:00 LT
(7ºN, 140ºE – Yokosuka Sinko)	AHVS	2 days (2 samples in this period)
	MOUDI	4 days (1 samples in this period)

Gas Analysis:

Gas samples were collected in stainless canisters by use of an air compressor. The gas pressure in the canister after sampling was 1.6 atm.

The time schedule of the gas sampling was:

6/13-6/19 (Sekinehama – 7ºN, 140ºE)	3:00, 6:00, and 13:00 LT

6/20-6/30 (7ºN, 140ºE)	12:00 and 21:00 LT
7/1-7/5 (7ºN, 140ºE – Yokohama Sinko)	3:00, 6:00, 13:00, and 18:00 LT

Ozone concentration was monitored by an UV ozone monitor (Dylec, Model 1150) during this cruise and obtained data (time resolution: 12 seconds) were acquired by a personal computer.

Rainwater Analysis:

Rainwater samples were collected into 250 and 500 ml glass bottles using two stainless steel rainwater collector (Effective sample collection area: ca. 0.5 m^2). The rainwater samples were stored with a small amount of $HgCl_2$ that was added as bactericide.

(4) Future Plan

Aerosol samples will be analyzed for low molecular weight diacids. Based on size distribution of diacids, we will estimate relative contribution of the continental and marine source inputs to diacids in the marine aerosols. Comparison of this study with the previous study also may characterize the aerosols in this region. Gas phase NMHC's will be analyzed, too. Their stable carbon isotope ratios ($^{13}C/^{12}C$) are measured to clarify their sources, and to obtain information of formation and removal processes over in this region. Rainwater analysis will be conducted in the laboratory, too.

(5) data archive

All samples will be archived in Institute of Low Temperature Science, Hokkaido University. The inventory information of the samples is submitted to JAMSTEC DMO.

(6) References

Peltzer, E. T. and R. B. Gagosian, Organic geochemistry of aerosols over the Pacific Ocean, in Chemical Oceanography Vol. 10, pp.281-338, Ed. J. P. Riley, R. Chester and R. A. Duce, Academic Press, London, UK, 1989.

Kawamura, K. and K. Usukura, Distribution of low molecular weight dicarboxylic acids in the North Pacific aerosol samples, J. Oceanogr., 49, 271-283, 1993.

Kawamura, K. and F. Sakaguchi, Molecular distributions of water soluble carboxylic acids in marine aerosols over the Pacific Ocean including tropics, J. Geophys. Res., 104, 3501-3509, 1999.

6.6.4 Measurement of Aerosol Optical Properties

(1) Personnel

On board scientists:
Yuji Fujitani (Graduate School of Engineering, Hokkaido University)

Co-workers not on board:
Tatsuo Endoh (Institute of Low Temperature Science, Hokkaido University)
TamioTakamura (Center of Environmental Remote Sensing Science, Chiba University)
Sachio Ohta (Graduate School of Engineering, Hokkaido University)
Teruyuki Nakajima (Center of Climate System Research, University of Tokyo)

(2) Objectives

Aerosol directly influences climate. The atmospheric net energy balance between solar radiation and emission from earth is disturbed by their optical properties i.e. single scattering albedo, optical thickness and its dependence on the wave length.. Measurement of optical properties is necessary to estimate radiative forcing for global climate.

And the data from ground based observation can give for calibration and validation remote sensing aerosol data, then providing more precise value for estimation of radiative forcing.

(3) Methods

Sky Radiometer (POM-01MKⅡ, made by PREDE) is measuring irradiating intensities of solar radiation through seven different filters with the scanning angle of 2-140 degree. These data will provide finally optical thickness, Åangstrom exponent and size distribution of atmospheric aerosols with a kind of retrieval method.

To verify value of optical thickness, there are also monitoring absorption coefficient and scattering coefficient, which need to calculate single scattering albedo, at the compass deck. Absorption coefficient is measured by Particle Soot / Absorption Photometer (made by Radiance Research), scattering coefficient is measured by Integrating Nephelometer (M903, made by Radiance Research). Furthermore aerosol sampling are also conducted to identify chemical component of aerosol particles. Teflon filter sampling is measurement for ionic and heavy metal component, and quartz filter is for carbonaceous particles. At last, ship exhausts effect is monitoring by optical particle counter (KC-01C, made by RION).

(4) Results

Operation period of data and sample obtained are summarized in Table-6.6.4-1and2. The sky radiometer has been going well owing to more calm and silent condition and circumstances about shivering problems provided by the R/V Mirai whose engines are supported by well defined cushions. Therefore, measured values will be expected to be considerably stable and provide good calculated parameters in higher quality. Absorption and scattering coefficient is extremely low, so background air mass are caught over the tropical Pacific Ocean. Filter sampling was performed with the special cautions for contamination from the ship of ourselves caused by frequent stoppages for other deep soundings. Particle number is usually extremely low because of clean air mass, but when air mass is effected by ship exhausts, the particle number increases.

(5) Data archive

All data will be archived at ILTS (Endoh) and Engineering school (Ohta), Hokkaido University after the quality check and submitted to JAMSTEC within 3-year.

Table 6.6.4-1: List of instrument operation time.

Sky radiometer	Optical Particle counter	Integrating Nephelometer			Particle Soot Absorption Photometer		
		NO.	date and time (UTC) start	date and time (UTC) end	NO.	date and time (UTC) start	date and time (UTC) end
Contiuunous measurement when the sun apperes	Contiuunous measurement	1	12Jun. 21:15	13Jun. 3:41	1	12Jun. 21:20	12Jun. 23:46
		2	13Jun. 8:38	14Jun. 9:32	2	12Jun. 23:53	13Jun. 3:39
		3	14Jun. 9:33	15Jun. 5:55	3	13Jun. 8:44	14Jun. 9:33
		4	15Jun. 6:20	16Jun. 7:15	4	14Jun. 9:49	15Jun. 5:54
		5	16Jun. 7:38	17Jun. 5:16	5	15Jun. 6:24	16Jun. 7:14
		6	17Jun. 6:18	19Jun. 8:39	6	16Jun. 7:39	17Jun. 5:15
		7	19Jun. 9:06	21Jun. 14:07	7	17Jun. 6:19	19Jun. 8:38
		8	21Jun. 14:27	22Jun. 2:07	8	19Jun. 9:05	21Jun. 14:07
		9	22Jun. 2:16	22Jun. 5:11	9	21Jun. 14:27	22Jun. 2:06
		10	22Jun. 23:36	25Jun. 4:53	10	22Jun. 2:16	22Jun. 5:11
		11	25Jun. 9:59	27Jun. 7:30	11	22Jun. 23:38	25Jun. 4:53
		12	27Jun. 7:47	29Jun. 3:36	12	25Jun. 9:57	27Jun. 7:30
		13	29Jun. 4:03	1Jul. 7:37	13	27Jun. 7:49	29Jun. 3:35
		14	1Jul. 8:07	3Jul. 5:06	14	29Jun. 4:03	1Jul. 7:36
		15	3Jul. 5:36	5Jul. 6:00	15	1Jul. 8:07	3Jul. 5:05
					16	3Jul. 5:36	5Jul. 6:00

Table 6.6.4-2: List of filter sampling parameters

Quartz fiber filter					Teflon filter				
NO.	date and time (UTC) start	date and time (UTC) end	period [min]	volume [m^3]	NO.	date and time (UTC) start	date and time (UTC) end	period [min]	volume [m^3]
1	12Jun. 23:50	13Jun. 2:34	164	3.3	1	12Jun. 23:50	13Jun. 2:34	164	3.3
2	13Jun. 8:46	13Jun. 23:01	855	17.0	2	13Jun. 8:46	13Jun. 23:01	855	17.4
~~3~~					3	13Jun. 23:50	14Jun. 23:16	1406	28.1
4	13Jun. 23:50	14Jun. 23:16	1406	28.4	4	14Jun. 23:50	15Jun. 5:52	1361	27.6
5	14Jun. 23:50	15Jun. 5:52	1361	28.0		15Jun. 7:05	15Jun. 23:44		
	15Jun. 7:05	15Jun. 23:44			5	16Jun. 0:54	16Jun. 1:50		

Table 6.6.4-2: List of filter sampling parameters. (Continued)

6	16Jun. 0:54	16Jun. 1:50	2317	45.4
	16Jun. 3:45	16Jun. 22:20		
	17Jun. 0:15	17Jun. 19:21		
7	17Jun. 23:24	18Jun. 16:30	2548	53.3
	18Jun. 21:10	19Jun. 14:58		
	19Jun. 16:20	19Jun. 23:54		
8	20Jun. 0:22	20Jun. 3:30	1664	32.9
	20Jun. 3:41	20Jun. 4:34		
	20Jun. 5:31	20Jun. 7:40		
	20Jun. 8:37	20Jun. 10:14		
	20Jun. 11:35	20Jun. 13:40		
	20Jun. 14:27	20Jun. 16:30		
	20Jun. 17:22	20Jun. 19:42		
	20Jun. 20:33	20Jun. 22:20		
	20Jun. 23:28	21Jun. 4:35		
	21Jun. 5:35	21Jun. 7:37		
	21Jun. 8:33	21Jun. 10:26		
	21Jun. 11:30	21Jun. 14:10		
9	21Jun. 14:56	21Jun. 16:34	2597	52.3
	21Jun. 17:28	21Jun. 19:23		
	21Jun. 21:14	21Jun. 22:41		
	21Jun. 23:41	22Jun. 2:01		
	22Jun. 2:37	22Jun. 4:24		
	22Jun. 5:27	22Jun. 7:40		
	22Jun. 8:32	22Jun. 10:12		
	22Jun. 11:47	22Jun. 13:51		
	22Jun. 14:40	22Jun. 16:38		
	22Jun. 17:36	22Jun. 19:58		
	22Jun. 20:29	22Jun. 22:15		
	22Jun. 23:27	23Jun. 1:52		
	23Jun. 3:21	23Jun. 7:42		
	23Jun. 8:33	23Jun. 10:15		
	23Jun. 11:30	23Jun. 13:53		
	23Jun. 14:31	23Jun. 16:26		
	23Jun. 17:32	23Jun. 19:55		
	23Jun. 20:34	23Jun. 22:19		
	23Jun. 23:28	24Jun. 4:41		
10	24Jun. 5:34	24Jun. 7:39		
	24Jun. 8:34	24Jun. 10:18		
	24Jun. 11:31	24Jun. 13:48		
	24Jun. 14:39	24Jun. 16:30		
	24Jun. 17:37	24Jun. 19:32		
	24Jun. 20:33	24Jun. 22:17		
	24Jun. 23:23	25Jun. 2:11		
	25Jun. 3:25	25Jun. 7:40		

5	16Jun. 3:45	16Jun. 22:20	1740	34.1
	17Jun. 0:15	17Jun. 9:44		
6	17Jun. 10:06	17Jun. 19:21	1880	37.6
	17Jun. 23:05	18Jun. 16:30		
	18Jun. 21:10	19Jun. 1:50		
7	19Jun. 2:11	19Jun. 14:58	1221	25.6
	19Jun. 16:20	19Jun. 23:54		
8	20Jun. 0:22	20Jun. 3:30	1664	33.3
	20Jun. 3:41	20Jun. 4:34		
	20Jun. 5:31	20Jun. 7:40		
	20Jun. 8:37	20Jun. 10:14		
	20Jun. 11:35	20Jun. 13:40		
	20Jun. 14:27	20Jun. 16:30		
	20Jun. 17:22	20Jun. 19:42		
	20Jun. 20:33	20Jun. 22:20		
	20Jun. 23:28	21Jun. 4:35		
	21Jun. 5:35	21Jun. 7:37		
	21Jun. 8:33	21Jun. 10:26		
	21Jun. 11:30	21Jun. 14:10		
9	21Jun. 14:56	21Jun. 16:34	1676	34.4
	21Jun. 17:28	21Jun. 19:23		
	21Jun. 21:14	21Jun. 22:41		
	21Jun. 23:41	22Jun. 2:01		
	22Jun. 2:37	22Jun. 4:24		
	22Jun. 5:27	22Jun. 7:40		
	22Jun. 8:32	22Jun. 10:12		
	22Jun. 11:47	22Jun. 13:51		
	22Jun. 14:40	22Jun. 16:38		
	22Jun. 17:36	22Jun. 19:58		
	22Jun. 20:29	22Jun. 22:15		
	22Jun. 23:27	23Jun. 1:52		
	23Jun. 3:21	23Jun. 7:42		
10	23Jun. 8:44	23Jun. 10:15	1774	36.4
	23Jun. 11:30	23Jun. 13:53		
	23Jun. 14:31	23Jun. 16:26		
	23Jun. 17:32	23Jun. 19:55		
	23Jun. 20:34	23Jun. 22:19		
	23Jun. 23:28	24Jun. 4:41		
	24Jun. 5:34	24Jun. 7:39		
	24Jun. 8:34	24Jun. 10:18		
	24Jun. 11:31	24Jun. 13:48		
	24Jun. 14:39	24Jun. 16:30		
	24Jun. 17:37	24Jun. 19:32		
	24Jun. 20:33	24Jun. 22:17		
	24Jun. 23:23	25Jun. 2:11		

Table 6.6.4-2: List of filter sampling parameters. (Continued)

10	25Jun. 8:48	25Jun. 10:17	2147	42.7	11	25Jun. 3:46	25Jun. 7:40	1262	25.2
	25Jun. 11:34	25Jun. 13:47				25Jun. 8:48	25Jun. 10:17		
	25Jun. 14:37	25Jun. 16:27				25Jun. 11:34	25Jun. 13:47		
	25Jun. 17:34	25Jun. 19:43				25Jun. 14:37	25Jun. 16:27		
	25Jun. 20:29	25Jun. 22:17				25Jun. 17:34	25Jun. 19:43		
	25Jun. 23:30	26Jun. 1:55				25Jun. 20:29	25Jun. 22:17		
	26Jun. 3:43	26Jun. 7:31				25Jun. 23:30	26Jun. 1:55		
	26Jun. 8:38	26Jun. 10:04				26Jun. 3:43	26Jun. 7:31		
11	26Jun. 12:05	26Jun. 13:37	2504	50.3		26Jun. 8:38	26Jun. 10:04		
	26Jun. 14:47	26Jun. 16:32			12	26Jun. 12:05	26Jun. 13:37	1484	29.7
	26Jun. 17:48	26Jun. 19:30				26Jun. 14:47	26Jun. 16:32		
	26Jun. 20:39	26Jun. 22:32				26Jun. 17:48	26Jun. 19:30		
	27Jun. 0:31	27Jun. 1:53				26Jun. 20:39	26Jun. 22:32		
	27Jun. 3:53	27Jun. 4:54				27Jun. 0:31	27Jun. 1:53		
	27Jun. 5:27	27Jun. 7:21				27Jun. 3:53	27Jun. 4:54		
	27Jun. 8:33	27Jun. 9:57				27Jun. 5:27	27Jun. 7:21		
	27Jun. 11:29	27Jun. 13:30				27Jun. 8:33	27Jun. 9:57		
	27Jun. 14:49	27Jun. 16:33				27Jun. 11:29	27Jun. 13:30		
	27Jun. 17:36	27Jun. 19:12				27Jun. 14:49	27Jun. 16:33		
	27Jun. 20:42	27Jun. 21:57				27Jun. 17:36	27Jun. 19:12		
	27Jun. 23:37	28Jun. 1:51				27Jun. 20:42	27Jun. 21:57		
	28Jun. 2:43	28Jun. 4:17				27Jun. 23:37	28Jun. 1:51		
	28Jun. 5:31	28Jun. 7:18				28Jun. 2:43	28Jun. 4:17		
	28Jun. 8:32	28Jun. 9:53				28Jun. 5:31	28Jun. 7:18		
	28Jun. 11:39	28Jun. 13:30			13	28Jun. 8:52	28Jun. 9:53	1000	20.0
	28Jun. 14:32	28Jun. 16:16				28Jun. 11:39	28Jun. 13:30		
	28Jun. 17:24	28Jun. 19:30				28Jun. 14:32	28Jun. 16:16		
	28Jun. 20:36	28Jun. 21:55				28Jun. 17:24	28Jun. 19:30		
	28Jun. 23:22	29Jun. 1:48				28Jun. 20:36	28Jun. 21:55		
	29Jun. 3:21	29Jun. 4:15				28Jun. 23:22	29Jun. 1:48		
	29Jun. 5:37	29Jun. 7:39				29Jun. 3:21	29Jun. 4:15		
	29Jun. 8:36	29Jun. 10:05				29Jun. 5:37	29Jun. 7:39		
	29Jun. 11:41	29Jun. 13:29				29Jun. 8:36	29Jun. 10:05		
12	29Jun. 14:44	29Jun. 16:13	2693	54.7		29Jun. 11:41	29Jun. 13:29		
	29Jun. 17:32	29Jun. 19:35			14	29Jun. 14:44	29Jun. 16:13	1444	29.0
	29Jun. 20:35	29Jun. 22:05				29Jun. 17:32	29Jun. 19:35		
	29Jun. 23:34	30Jun. 1:48				29Jun. 20:35	29Jun. 22:05		
	30Jun. 3:28	30Jun. 4:23				29Jun. 23:34	30Jun. 1:48		
	30Jun. 6:30	30Jun. 7:30				30Jun. 3:28	30Jun. 4:23		
	30Jun. 8:28	30Jun. 10:03				30Jun. 6:30	30Jun. 7:30		
	30Jun. 11:47	30Jun. 13:45				30Jun. 8:28	30Jun. 10:03		
	30Jun. 15:33	1Jul. 2:53				30Jun. 11:47	30Jun. 13:45		
	1Jul. 5:42	2Jul. 0:00				30Jun. 15:33	1Jul. 2:53		
	2Jul. 0:57	2Jul. 3:28			15	1Jul. 5:42	2Jul. 0:00	1249	25.2
13	2Jul. 5:51	4Jul. 6:00	1449	29.0		2Jul. 0:57	2Jul. 3:28		
14	4Jul. 6:15	5Jul. 4:00	1305	26.1	16	2Jul. 5:51	3Jul. 5:42	1431	28.6
					17	3Jul. 6:02	4Jul. 6:00	1438	28.8
					18	4Jul. 6:15	5Jul. 4:00	1305	26.1

6.7 Solar Radiation and Ocean Color Measurement

(1) Personnel

Hiroshi Ishida (Maritime University of Kobe/
Frontier Observational Research System for Global Change): Principal Investigator
Katsutoshi Kozai (Maritime University of Kobe)
Kunimitsu Ishida (Toba National College of Maritime Technology)
Masanao Kusakari (Maritime University of Kobe)
Kunikazu Nojima (Kinki University)

(2) Objectives

Characterizing aerosol optical properties and their effects on ocean color at the western equatorial Pacific Ocean are important parameters for the coupled atmosphere-ocean system. The purpose of the observation is to investigate the aerosol effects on the satellite-derived ocean color using in situ observations of aerosol optical thickness and water-leaving radiance synchronized with SeaWiFS satellite overpass.

(3) Methods

SeaWiFS is an abbreviation of Sea-viewing Wide Field-of-view Sensor onboard the SeaStar launched in 1998. The sensor has eight bands in the visible and near infrared wavelengths and the tilt mechanism to avoid sun glitter as shown in Table 6.7-1. During the research cruise SeaWiFS LAC (Local Area Coverage) scenes are received by the station onboard R/V Mirai once a day under the authorization of NASA SeaWiFS project as the temporary real-time agreement. Sunphotometer (Eiko Seiki Corp., MS120) measures the solar radiance at four wavelengths of 368, 500, 675 and 778 nm, and obtains the characteristics of the atmospheric absorption, that is the aerosol optical thickness and the Angstrom coefficient. Polarization spectral radiometer (Opto Research Corp., PSR1000) measures the atmospheric absorption of the solar radiation and the polarization degree at the 90 degrees from the sun direction at six wavelengths of 443, 490, 565, 670, 765, and 865 nm. Multi-spectral radiometer (Opto Research Corp., MSR7000) measures polarized solar radiance at every 1nm wavelength from 400 to 1000 nm, and also does the ocean color, that is the upward spectral radiance from ocean surface. Spectroradiometer (Geophysical & Environmental Research Corp., GER1500) has the same capabilities as MSR7000 without polarization for the ocean color measurements. The atmospheric depositions and rain were also sampled onboard to analyze chemical components. These data will be analyzed after the cruise. Table 6.7-2 shows the list of observation parameter and schedule.

(4) Preliminary Results

The measurements of solar radiation and ocean color were made on the fine and calm weather conditions during the whole cruise. And the atmospheric deposition was sampled once a day. The results of each observation are shown in the following tables and figures.

Table 6.7-1 Specification of SeaWiFS.

Band No.	wavelength (nm)
1	402-422
2	433-453
3	480-500
4	500-520
5	545-565
6	660-680
7	745-785
8	845-885
Equator Crossing	Local Noon(±20min), descending
Orbit type	Sun Synchronous at 705km
Spatial resolution	1.13km(LAC), 4.5km(GAC)
Swath width	2801km(LAC), 1502km(GAC)
Scan Plane Tilt	+20°,0°,-20°

Table 6.7-2 List of observation parameter and schedule.

	MSR7000		PSR1000		GER1000	Sun photometer	Remarks
day	sea	scat	direct	scat	sea	direct	
12-Jun			○	○			
13-Jun							Leave Sekinehama, Cloud cover
14-Jun							Cloud cover
15-Jun							Cloud cover
16-Jun	○				○		
17-Jun	○	○	○	○			
18-Jun	○		○	○	○	○	
19-Jun	○	○	○	○	○		
20-Jun							Arrive at 140°E, 7°N
21-Jun							Cloud cover, sensor calibration
22-Jun							Cloud cover, sensor calibration
23-Jun	○					○	
23-Jun	○	○			○	○	
24-Jun	○	○	○		○	○	
25-Jun	○		○		○		
26-Jun							Cloud cover
27-Jun							Cloud cover
28-Jun							Cloud cover
29-Jun							Cloud cover
30-Jun							Cloud cover
1-Jul							Leave 140°E, 7°N

Note: “Direct” and “scat” means the observation of solar radiation in a direct and polarized scattering mode respectively.

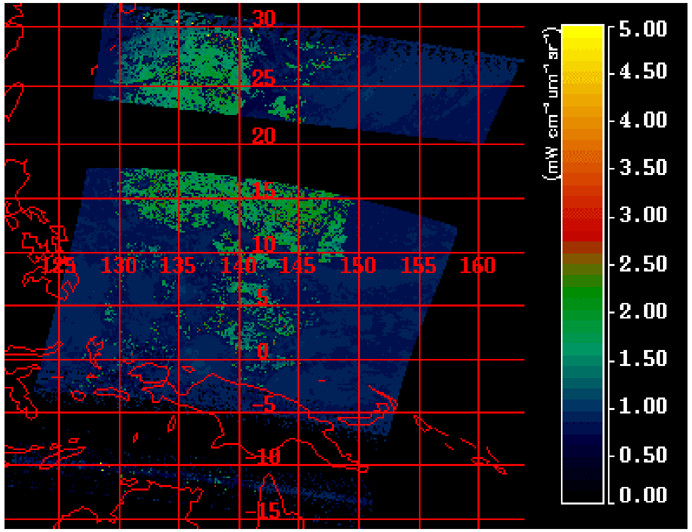

June 23 nLw 443nm

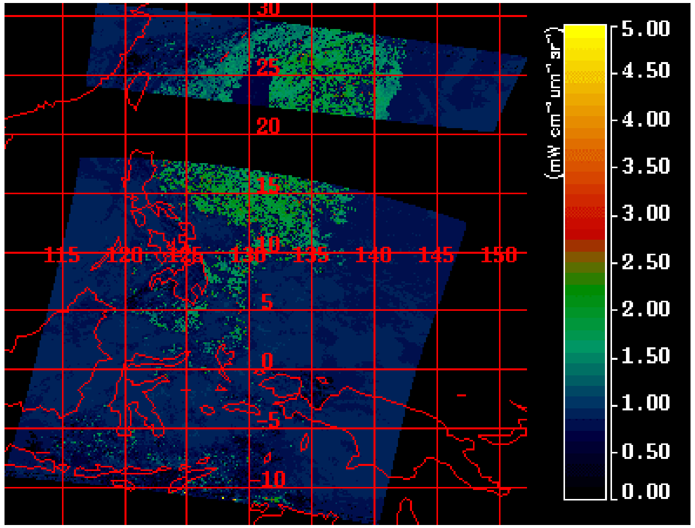

June 24 nLw 443nm

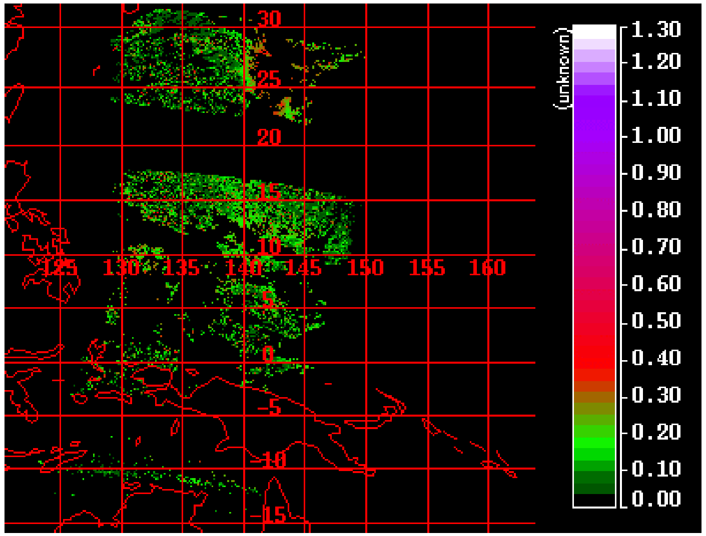

June 23 τ 865nm

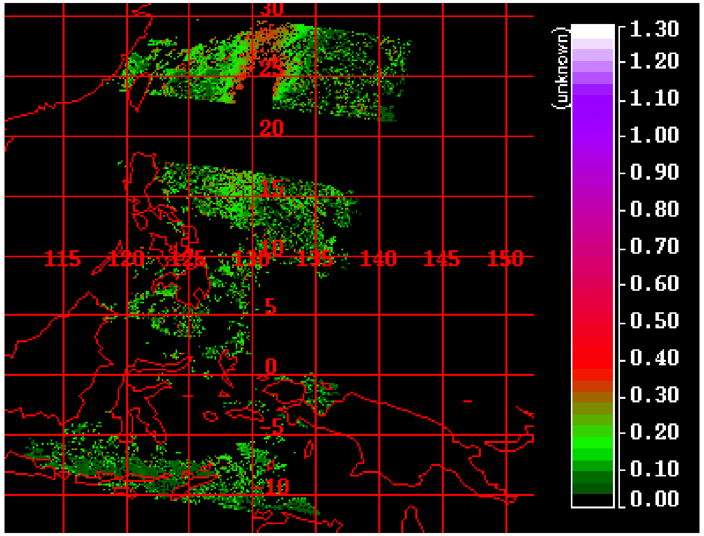

June 24 τ 865nm

Fig.6.7-1 Normalized water-leaving radiance(443nm) and aerosol optical thickness τ (865nm) derived from SeaWiFS (June 23 and 24).

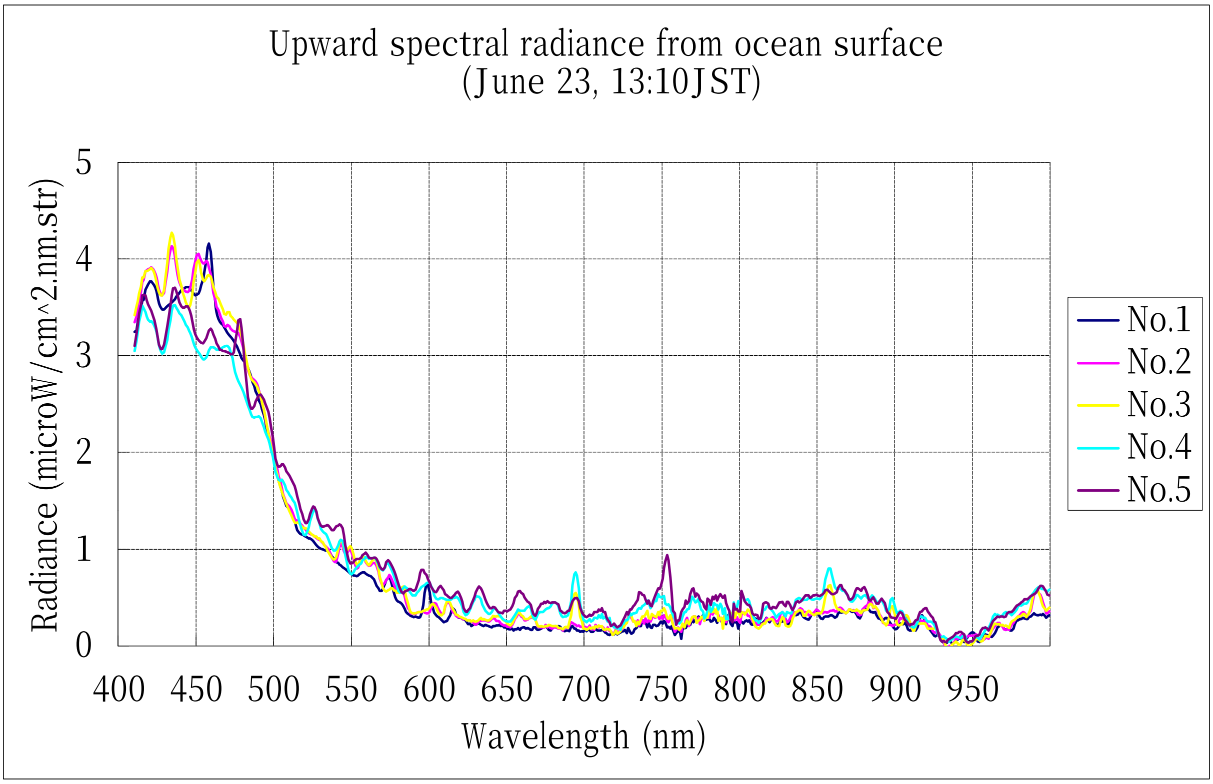

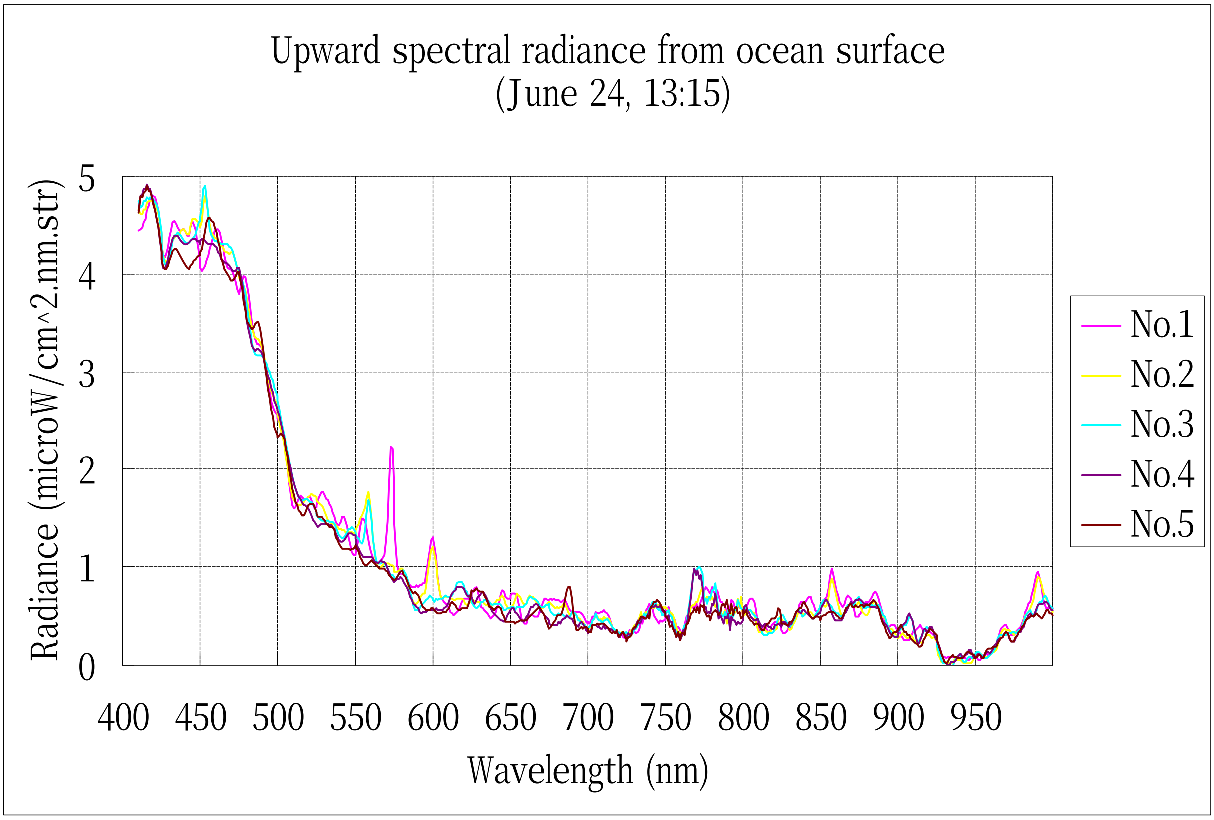

Fig.6.7-2: Upward spectral radiance from ocean surface by MSR7000 (June23 and 24).

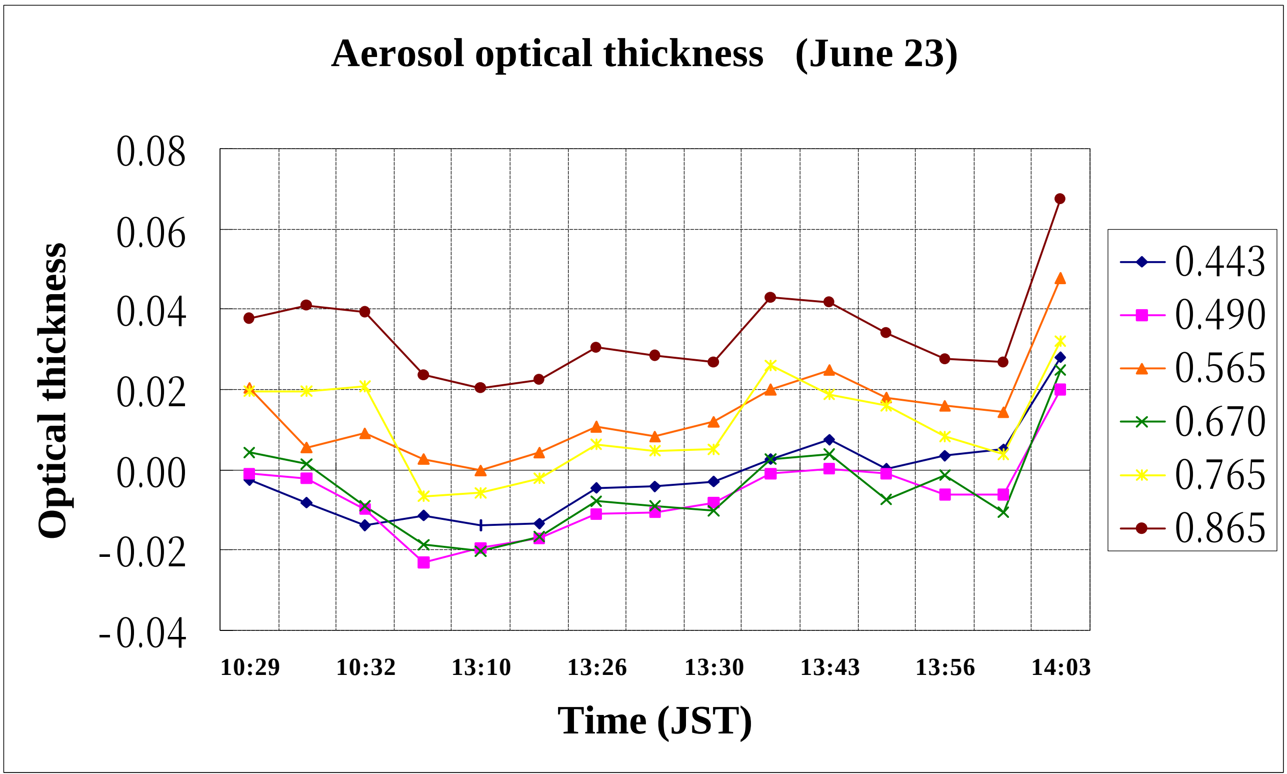

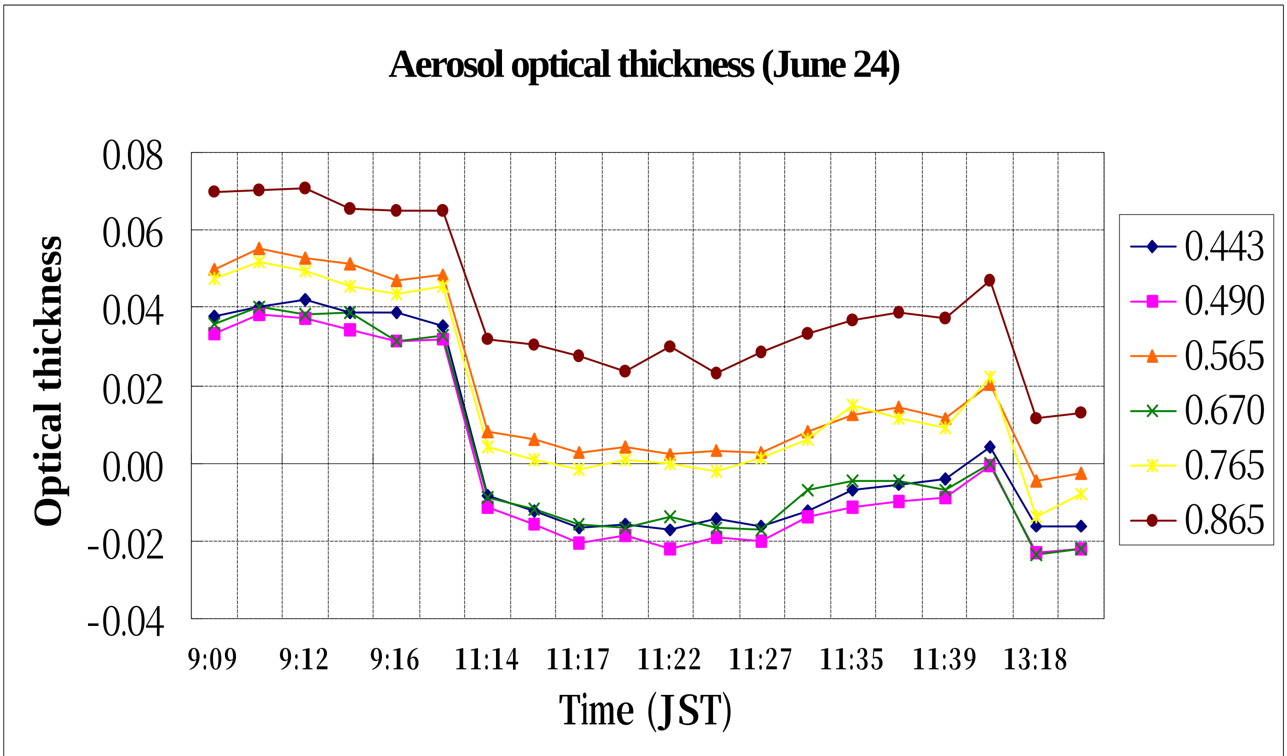

Fig.6.7-3 Variation of spectral aerosol optical thickness by PSR1000 (June 23 and 24).

(5) Data archives

The SeaWiFS raw data received by the station onboard R/V Mirai will be submitted to NASA. The other products such as spectral radiance and aerosol optical thickness derived from SeaWiFS are archived in CD-Rs. The raw data of the solar radiation are archived in floppy and optical disks. Samples of atmospheric deposition are analyzed on their chemical components etc., and the results are archived in a floppy disk. After the quality check of those data, they will be published open to public. All data will be archived at Maritime University of Kobe. The data and sample inventory information are submitted to JAMSTEC DMO.

6.8 CTD

6.8.1 CTD Observation

(1) Personal

Satoshi Ozawa (MWJ) : Operation Leader
Katsunori Sagishima (MWJ)
Ai Yasuda (MWJ)
Asako Inoue (MWJ)
Kaori Akizawa (MWJ)
Kentaro Oyama (MWJ)

(2) Objectives

Investigation of the oceanic structure and its time variation by measuring vertical profiles of temperature and salinity.

(3) Methods

We observed vertical profile of temperature and salinity by CTD / Carousel (Conductivity Temperature Depth profiler / Carousel Water Sampler). The sensor attached on CTD were temperature sensor, conductivity sensor, pressure sensor, and altimeter sensor. Salinity was calculated by measurement values of pressure, conductivity and temperature. The CTD/Carousel was deployed from starboard on working deck. Descending rate and ascending rate were kept 1.2 m/s respectively.

The CTD raw data was acquired in real time by using the SEASAVE utility from SEASOFT software (ver.4.232) provided by SBE and stored on the hard disk of an IBM personal computer. Water samplings were made during up-cast by sending a fire command from the computer. Every cast we sampled water at 1000 m to calibrate salinity data.

CTD measurements at 5 stations (30°N, 25°N,20°N,15°N,10°N,5°N) along 140°E and at stationary station (7°N,140°E) have been carried out. Basically during the stationary observation, CTD casting was conducted every 6hours (02:30, 08:30, 14:30, 20:30, UTC). Measurement depth was 1000m. In total, 48 castings were carried out (see Table 6.9.1-1).

The CTD raw data was processed using SEASOFT (ver.4.232). Data processing procedures and used utilities of SEASOFT were as follows:

DATCNV:	Converts the binary raw data to output on physical units. Output parameters are scan number, depth, pressure, temperature, salinity, sigma-theta, descent rate, conductivity. Simultaneously, this utility selects the CTD data when bottles closed to output on another file.
SECTION:	Remove the unnecessary data.
WILDEDIT:	Obtain an accurate estimate of the true standard deviation of the data. Std deviations for Pass 1: 2 Std deviations for Pass 2: 10 Points per block: 100
BINAVG:	Calculates the averaged data in every 1 db.
ROSSUM:	Edits the data of water sampled to output a summary file.
SPLIT:	Splits the data made in CNVfiles into upcast and downcast files.

Specifications of the sensors are listed below.

Under water unit: CTD 9plus (S/N 09P9833-0280, Sea-Bird Electronics, Inc.).
Calibrated Date: 02.Jan.1997
Temperature Sensor: SBE3-04/F (S/N 031524, Sea-Bird Electronics, Inc)
Calibrated Date: 05.May.2000（for all cast except cast NO.27）
Temperature Sensor: SBE3-04/F (S/N 031525, Sea-Bird Electronics, Inc)
Calibrated Date: 02.Mar.2000（for cast NO.27）
Conductivity Sensor: SBE4-04/0 (S/N 041202, Sea-Bird Electronics, Inc)
Calibrated Date: 05.May.2000（for all cast except cast NO.27）
Conductivity Sensor: SBE4-04/0 (S/N 041206, Sea-Bird Electronics, Inc)
Calibrated Date: 02.Mar.2000（for cast NO.27）
Altimeter sensor: PSA-9000 (S/N 396, Datasonics, Inc)
Deck unit: SBE11 (S/N 11P8010-0308, Sea-Bird Electronics, Inc.)
Carousel water sampler: SBE32 (S/N 329833-0026, Sea-Bird Electronics, Inc.)

(4) Results

Vertical profiles at each CTD cast are attached in the following APPENDIX. Time variations of the vertical profile of temperature and salinity at Small Triangle are shown in Fig 6.8.1-2.

Note that in these figures, the correction of salinity data by sampled water is no t applied.

(5) Trouble

It was found that spike noises for salinity are generated on cast NO.26. We exchange Temperature and Salinity Sensor which S/N is 031525, 041206 for those which S/N is 031524, 041202 respectively on next cast. But it was not troubled on cast NO.27, we exchanged original sensor once more after cast NO.27.

On cast NO.32 spike noises are found during downcast nearby 800m. Though it have not been clear that how those spike noises was appear.

(6) Data archive

All raw and processed CTD data files were copied onto magnetic optical disks (MO) and submitted to JASTEC Data Management Office (DMO) and will be under their control.

Table 6.8.1-1: CTD Cast Table

Cast No.	Cast name	Latitude	Longitude	Date (UTC)	Time (UTC)	Depth (m)
01	K4S001	30-00.10N	139-59.93E	15 June ’00	05:58	1000
02	K4S002	24-59.99N	139-59.85E	16 June ’00	02:03	1000
03	K4S003	19-59.93N	139-59.93E	16 June ’00	23:00	1000
04	K4S004	15-00.11N	139-59.93E	17 June ’00	19:32	1000
05	K4S005	09-59.98N	140-19.89E	18 June ’00	17:59	1000
06	K4S006	04-59.83N	140-00.11E	19 June ’00	14:51	1000
07	K4S007	06-58.43N	140-00.96E	20 June ’00	05:33	1000
08	K4S008	06-59.94N	139-59.18E	20 June ’00	11:34	1000
09	K4S009	06-59.47N	139-59.98E	20 June ’00	17:31	1000
10	K4S010	06-59.68N	140-00.47E	20 June ’00	23:33	1000
11	K4S011	06-59.88N	140-00.01E	21 June ’00	05:34	1000
12	K4S012	07-00.95N	140-00.77E	21 June ’00	11:36	1000
13	K4S013	07-01.32N	139-59.77E	21 June ’00	17:34	1000
14	K4S014	07-01.85N	140-00.62E	21 June ’00	23:35	1000
15	K4S015	07-01.57N	140-00.56E	22 June ’00	05:35	1000
16	K4S016	07-00.87N	139-59.43E	22 June ’00	11:39	1000
17	K4S017	07-00.57N	140-00.46E	22 June ’00	17:35	1000
18	K4S018	07-00.75N	139-59.72E	22 June ’00	23:35	1000
19	K4S019	07-01.49N	139-59.82E	23 June ’00	05:34	1000
20	K4S020	06-59.52N	139-59.43E	23 June ’00	11:43	1500
21	K4S021	06-59.44N	140-00.07E	23 June ’00	17:35	1000
22	K4S022	06-59.49N	140-00.00E	23 June ’00	23:38	1000
23	K4S023	06-59.55N	140-00.69E	24 June ’00	05:32	1000
24	K4S024	07-00.05N	139-59.46E	24 June ’00	11:35	1000
25	K4S025	06-59.06N	140-01.15E	24 June ’00	17:36	1000
26	K4S026	06-59.99N	139.59.56E	24 June ’00	23:38	1000
27	K4S027	07-01.00N	140-00.02E	25 June ’00	05:35	1000
28	K4S028	07-00.14N	139-59.67E	25 June ’00	11:32	1000
29	K4S029	06-59.42N	140-00.35E	25 June ’00	17:36	1000
30	K4S030	06-59.94N	140-00.87E	25 June ’00	23:35	1000
31	K4S031	07-00.36N	140-00.36E	26 June ’00	05:34	1000
32	K4S032	06-59.63N	140-00.31E	26 June ’00	11:35	1000
33	K4S033	06-57.36N	140-00.51E	26 June ’00	17:41	1000
34	K4S034	07-00.11N	139-59.67E	26 June ’00	23:30	1000
35	K4S035	06-59.87N	139-59.92E	27 June ’00	05:36	1000
36	K4S036	06-59.69N	139-59.94E	27 June ’00	11:29	1000
37	K4S037	06-58.56N	140.02.63E	27 June ’00	17:38	1000
38	K4S038	06-59.56N	139-59.75E	27 June ’00	23:41	1000
39	K4S039	06.58.21N	140.01.88E	28 June ’00	05:36	1000
40	K4S040	06-59.69N	139-59.61E	28 June ’00	11:33	1000
41	K4S041	06.59.57N	139-59.44E	28 June ’00	17:37	1000
42	K4S042	06-59.79N	139-59.86E	28 June ’00	23:36	1000
43	K4S043	06-58.88N	140-04.45E	29 June ’00	05:35	1000
44	K4S044	07-00.04N	139-59.51E	29 June ’00	11:27	1000
45	K4S045	07-00.63N	139-59.79E	29 June ’00	17:36	1000
46	K4S046	06-59.73N	139-59.75E	29 June ’00	23:36	1000
47	K4S047	07-00.59N	140-00.30E	30 June ’00	05:39	1000
48	K4S048	06-59.95N	139-59.43E	30 June ’00	11:46	2000

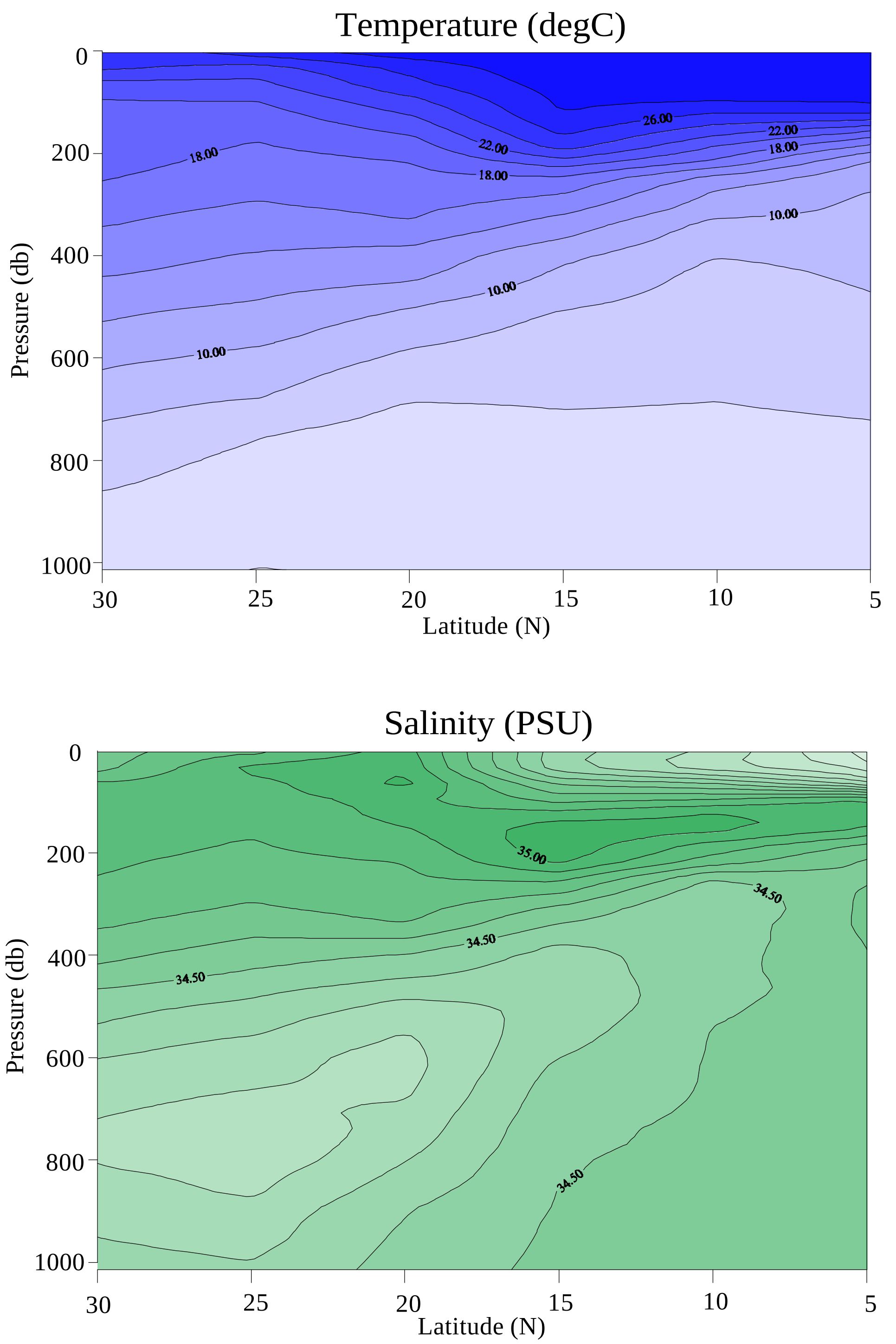

Fig.6.8.1-1: Vertical cross section of sea water temperature (upper) and salinity (lower) along 140E.

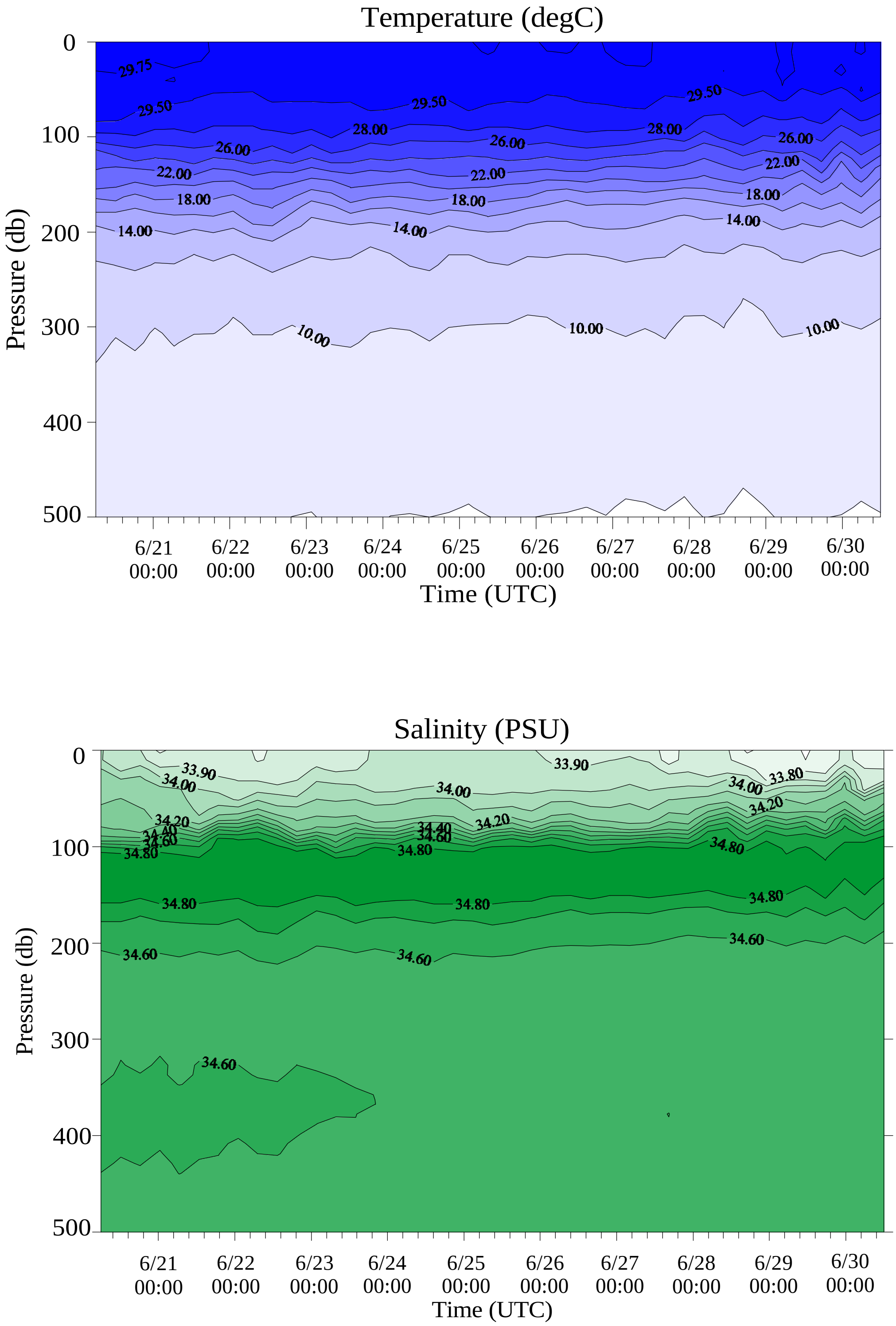

Fig.6.8.1-2: Time-depth cross section of sea water temperature (upper) and salinity (lower) at station (7N, 140E).

6.8.2 Salinity and Sea Surface Temperature Measurements by Direct Water Sampling

(1) Personal

Satoshi Ozawa (MWJ): Operation Leader
Asako Inoue (MWJ)

(2) Objectives

Calibrate the salinity data obtained by CTD, and monitoring of the variation of Sea Surface Temperature (SST) and Salinity (SSS).

(3) Method

Salinity was measured by a Guildline Autosal salinometer (model 8400B) with an Ocean Science International peristalitic-type sample intake pump and Hewlett Packard quartz thermometer (model 2804A) with two quartz probes (18111A). One probes measured at room temperature and another measured at a bath temperature. The resolution of the quartz thermometer was set to 0.001ºC. Data of both the salinometer and the temperature was collected simultaneously by a personal computer. A double conductivity ratio was defined as median of 31 times readings of the salinometer. Data collection started after 5 seconds and it took about 10 seconds to collect 31 reading by a personal computer.

The salinometer was operated in the air-conditioned ship's laboratory at bath temperature of 24ºC. Room temperature varied from approximately 22ºC to 24ºC, while a variation of bath temperature was almost within +/- 0.004ºC.

1. Salinity Sample Bottles

   The salinity samples are collected and stored in 250 ml brown glass bottles with screw caps.

2. Salinity Sample Collection and Temperature Equilibration

   Each bottle was rinsed twice with sample water and was filled to the shoulder of the bottle. Its cap was also thoroughly rinsed. Salinity samples were stored more than 24 hours in the same laboratory where the salinity measurement was done.

3. Standardization

   Autosal salinometer was standardized before and after sequence of measurements by use of IAPSO Standard Seawater batch P136 whose conductivity ratios was 0.99996.

4. Sub-Standard Seawater

   We also used deep-sea water filtered by pore size of 0.45 micrometer and stored in a 20 liter cubical made of polyethylene and stirred for at least 24 hours before measuring as sub-standerd seawater. It was measured every 10 samples in older to check and correct the trend.

(4) Preliminary Results

The difference of salinity data (at 1000 db) between CTD and directly sampled water are shown in Table 6.8.2-1. Generally two sets of salinity data agree very well except for 1 data. It supposed that the value at 1000 m of Cast No.3 were incorrect due to the personal error occurred during the measurement with Autosal or sampling was missed. The average of difference is 0.0038 PSU (CTD value is lower than that of direct sampling) with its standard deviation 0.0061 PSU. Except for the salinity data of Cast No.3, the average of difference is 0.0029 PSU with its standard deviation 0.0012 PSU.

(5) Data archive

These data are stored on a magnetic optical disk which will be kept on Ocean Research Department in JAMSTEC.

Table 6.8.2-1 Difference of salinity data between CTD and sampled water

Cast	File Name	Depth(m)	Sal.(psu)				Avg.	CTD Sal	Difference
1	K4S001	1000	34.3270	34.3274			34.3272	34.3294	0.0022
2	K4S002	1000	34.3070	34.3068			34.3069	34.3110	0.0041
3	K4S003	1000	34.3961	34.3961			34.3961	34.4403	0.0442
4	K4S004	1000	34.5235	34.5248	34.5245		34.5247	34.5258	0.0011
5	K4S005	1000	34.5441	34.5439			34.5440	34.5505	0.0065
6	K4S006	1000	34.5502	34.5506			34.5504	34.5573	0.0069
7	K4S007	1000	34.5514	34.5514			34.5514	34.5541	0.0027
8	K4S008	1000	34.5508	34.5510			34.5509	34.5522	0.0013
9	K4S009	1000	34.5512	34.5514			34.5513	34.5526	0.0013
10	K4S010	1000	34.5502	34.5508	34.5510		34.5509	34.5533	0.0024
11	K4S011	1000	34.5519	34.5516			34.5518	34.5540	0.0023
12	K4S012	1000	34.5514	34.5516			34.5515	34.5535	0.0020
13	K4S013	1000	34.5512	34.5508			34.5510	34.5535	0.0025
14	K4S014	1000	34.5492	34.5496			34.5494	34.5518	0.0024
15	K4S015	1000	34.5492	34.5488			34.5490	34.5526	0.0036
16	K4S016	1000	34.5498	34.5502			34.5500	34.5522	0.0022
17	K4S017	1000	34.5529	34.5527			34.5528	34.5547	0.0019
18	K4S018	1000	34.5518	34.5523	34.5525		34.5524	34.5545	0.0021
19	K4S019	1000	34.5504	34.5490	34.5486		34.5488	34.5510	0.0022
20	K4S020	1500	34.6020	34.6020			34.6020	34.6042	0.0022
21	K4S021	1000	34.5478	34.5480			34.5479	34.5502	0.0023
22	K4S022	1000	34.5535	34.5535			34.5535	34.5556	0.0021
23	K4S023	1000	34.5512	34.5516			34.5514	34.5548	0.0034
24	K4S024	1000	34.5486	34.5478	34.5476		34.5477	34.5513	0.0036
25	K4S025	1000	34.5537	34.5537			34.5537	34.5561	0.0024
26	K4S026	750						34.5331	
27	K4S027	1000	34.5535	34.5535			34.5535	34.5549	0.0014
28	K4S028	1000	34.5525	34.5527			34.5526	34.5549	0.0023
29	K4S029	1000	34.5508	34.5508			34.5508	34.5551	0.0043
30	K4S030	1000	34.5519	34.5521			34.5520	34.5541	0.0021
31	K4S031	1000	34.5527	34.5527			34.5527	34.5562	0.0035
32	K4S032	1000	34.5500	34.5500			34.5500	34.5526	0.0026
33	K4S033	1000	34.5549	34.5543	34.5555	34.5553	34.5552	34.5579	0.0027
34	K4S034	1000	34.5533	34.5525	34.5523		34.5524	34.5560	0.0036
35	K4S035	1000	34.5508	34.5510			34.5509	34.5555	0.0046
36	K4S036	1000	34.5512	34.5514			34.5513	34.5545	0.0032
37	K4S037	1000	34.5563	34.5569	34.5569		34.5569	34.5593	0.0024
38	K4S038	1000	34.5525	34.5519	34.5514	34.5508	34.5517	34.5555	0.0038
39	K4S039	1000	34.5543	34.5545			34.5544	34.5575	0.0031
40	K4S040	1000	34.5529	34.5535	34.5543	34.5541	34.5542	34.5571	0.0029
41	K4S041	1000	34.5539	34.5541			34.5540	34.5561	0.0021
42	K4S042	1000	34.5504	34.5506			34.5505	34.5552	0.0047
43	K4S043	1000	34.5541	34.5543			34.5542	34.5567	0.0025
44	K4S044	1000	34.5547	34.5547			34.5547	34.5575	0.0028
45	K4S045	1000	34.5557	34.5561			34.5559	34.5594	0.0035
46	K4S046	1000	34.5567	34.5561	34.5557		34.5559	34.5591	0.0032
47	K4S047	1000	34.5523	34.5529	34.5525		34.5524	34.5554	0.0030
48	K4S048	2000	34.6366	34.6368			34.6367	34.6411	0.0044
								Avg.=	0.0038
								Std=	0.0061

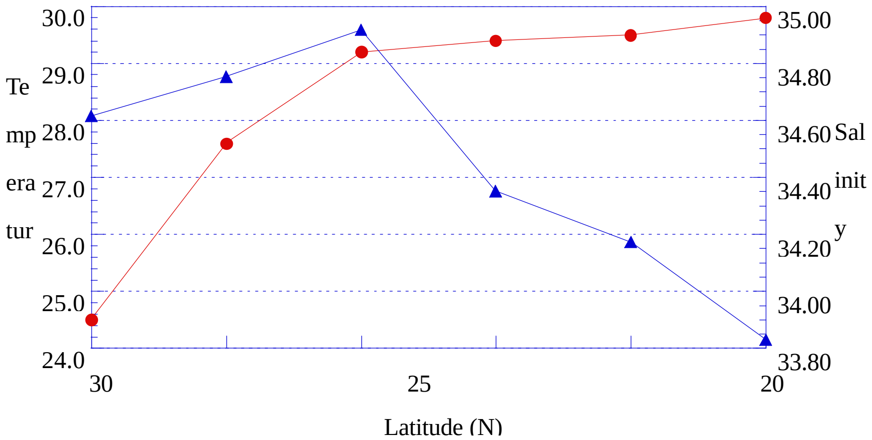

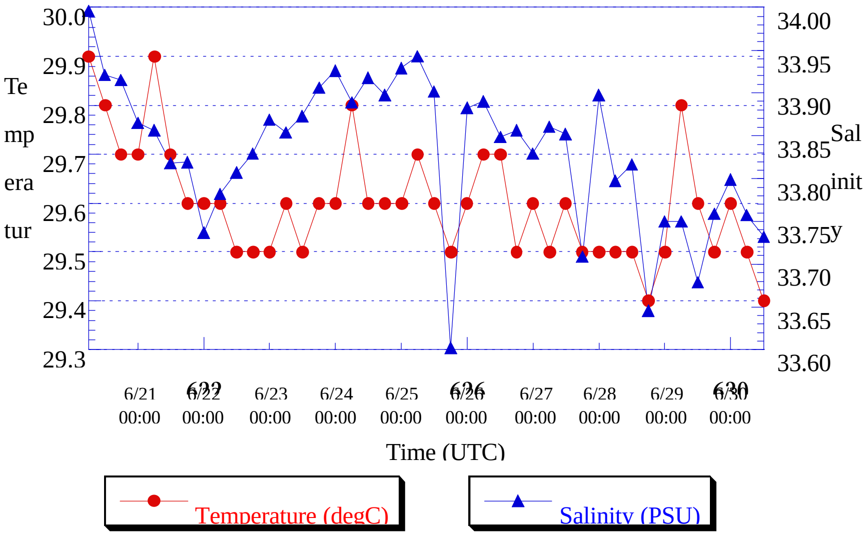

Fig. 6.8.2-1 Sea surface temperature and salinity, measured on the direct water sampling.

6.8.3 Shallow Water CTD and Chlorophyll Observation

(1) Personnel

Mitsuru Hayashi (Maritime University of Kobe): Principal Investigator
Satoshi Ozawa (MWJ)
Katsunori Sagishima (MWJ)
Ai Yasuda (MWJ)
Asako Inoue (MWJ)
Kaori Akizawa (MWJ)
Kentaro Ooyama (MWJ)

(2) Objectives

We carried out the shallow water observation to understand the spatial and temporal variations of temperature, salinity and chlorophyll in the euphotic layer.

(3) Methods

We observed vertical profiles of temperature, conductivity and chlorophyll by the shallow water observation unit (Chlorothec ACL-200DK, Alec Electronics Co. Ltd.) from surface to 150 m depth every 0.1 m as shown Table 6.8.3-1. Chlorophyll was output as the raw data (N value : 0 to 4095), and should be calibrated by the pigment analysis. Accuracy of sensors is as follows ;

Depth : ±0.2 m
Temperature :±0.05 deg-C
Conductivity : ±0.05 mmho

At the same time, transparency was also observed by the Secchi Disk in day time.

(4) Preliminary Results

Depth-Latitude cross sections of temperature, salinity, sigma-T and chlorophyll along the 140E line are shown in Fig. 6.8.3-1. There is a front between 20N and 15N, like a thermohaline front.

Fig. 6.8.3-2 shows Depth-Time cross sections of (a) temperature, (b) salinity, (c) sigma-T and (d) chlorophyll in 7N, 140E. The depth of the mixing layer is about 80 m in depth, and the chlorophyll maximum layer exists just below the mixing layer.

(5) Data archives

The data are archived in a floppy disk and will have a quality check in Maritime University of Kobe, and will be distributed to the public later. The raw data are submitted to the JAMSTEC DMO.

Table 6.8.3-1: The shallow water observation table.

Stn.	Cast	LMT=UTC-9h month	day	hour	Lat. deg.	min.		Long. deg.	min.		File name *.raw	Transparency m
1	1	6	15	16	30		N	140		E	30N140E	24
2	1	6	16	12	24	00.0	N	139	59.8	E	25N140E	33
3	1	6	17	9	19	59.8	N	139	59.5	E	20N140E	30
4	1	6	18	5	15	00.4	N	139	59.6	E	15N140E	34
5	1	6	19	4	10	00.2	N	140	19.9	E	10N140E	N/A
6	1	6	20	1	4	59.1	N	140	00.2	E	5N140E	N/A
A	1	6	20	15	6	58.3	N	140	00.6	E	Acast1	40
A	2	6	20	21	7	00.1	N	139	59.1	E	Acast2	N/A
A	3	6	21	3	6	59.6	N	139	59.7	E	Acast2	N/A
A	4	6	21	9	7	00.0	N	140	00.4	E	Acsat4	38
A	5	6	21	15	6	59.8	N	140	00.0	E	Acast5	44
A	6	6	22	21	7	01.1	N	140	00.7	E	Acast6	N/A
A	7	6	22	3	7	01.3	N	139	59.7	E	Acast6	N/A
A	8	6	22	9	7	01.9	N	140	00.9	E	Acast8	N/A
A	9	6	22	15	7	01.7	N	140	00.6	E	Acast9	41
A	10	6	23	21	7	01.1	N	139	57.3	E	Acast10	N/A
A	11	6	23	3	7	00.5	N	140	00.2	E	Acast10	N/A
A	12	6	23	9	7	00.8	N	139	59.4	E	Acast10	46
A	13	6	23	15	7	01.5	N	139	59.7	E	Acast13	45
A	14	6	23	21	6	59.5	N	139	59.1	E	Acast13	N/A
A	15	6	24	3	6	59.3	N	139	59.9	E	Acast13	N/A
A	16	6	24	9	6	59.5	N	139	59.6	E	Acast13	41
A	17	6	24	15	6	59.6	N	140	00.5	E	Acast13	50
A	18	6	24	21	7	00.0	N	139	59.2	E	Acast18	N/A
A	19	6	25	3	6	59.0	N	140	01.0	E	Acast18	N/A
A	20	6	25	9	6	59.9	N	139	59.6	E	Acast20	53
A	21	6	25	15	7	01.0	N	139	59.9	E	Acast21	48
A	22	6	25	21	7	00.2	N	139	59.6	E	Acast22	N/A
A	23	6	26	3	6	59.3	N	140	00.4	E	Acast22	N/A
A	24	6	26	9	6	59.9	N	139	60.0	E	Acast22	45
A	25	6	26	15	7	00.5	N	140	00.4	E	Acast25	45
A	26	6	26	21	6	59.6	N	140	00.4	E	Acast26	N/A
A	27	6	27	3	6	59.6	N	140	00.8	E	Acast26	N/A
A	28	6	27	9	6	59.8	N	139	59.5	E	Acast28	49
A	29	6	27	15	6	59.7	N	140	00.1	E	Acast29	37
A	30	6	27	21	6	59.6	N	139	59.9	E	Acast29	N/A
A	31	6	28	3	6	58.5	N	140	02.6	E	Acast29	N/A
A	32	6	28	9	6	59.6	N	139	60.0	E	Acast29	25
A	33	6	28	15	6	58.3	N	140	01.8	E	Acast29	25
A	34	6	28	21	6	59.8	N	139	59.3	E	Acast34	N/A
A	35	6	29	0	6	59.6	N	139	59.2	E	Acast34	N/A
A	36	6	29	9	6	59.8	N	139	59.7	E	Acast34	40
A	37	6	29	15	6	58.8	N	140	04.5	E	Acast37	45
A	38	6	29	21	7	00.2	N	139	39.3	E	Acast38	N/A
A	39	6	30	3	7	00.0	N	140	00.0	E	Acast38	N/A
A	40	6	30	9	6	59.7	N	139	59.8	E	Acast38	38
A	41	6	30	15	7	00.6	N	140	00.3	E	Acast38	40
A	42	6	30	21	7	00.1	N	139	59.7	E	Acast38	N/A

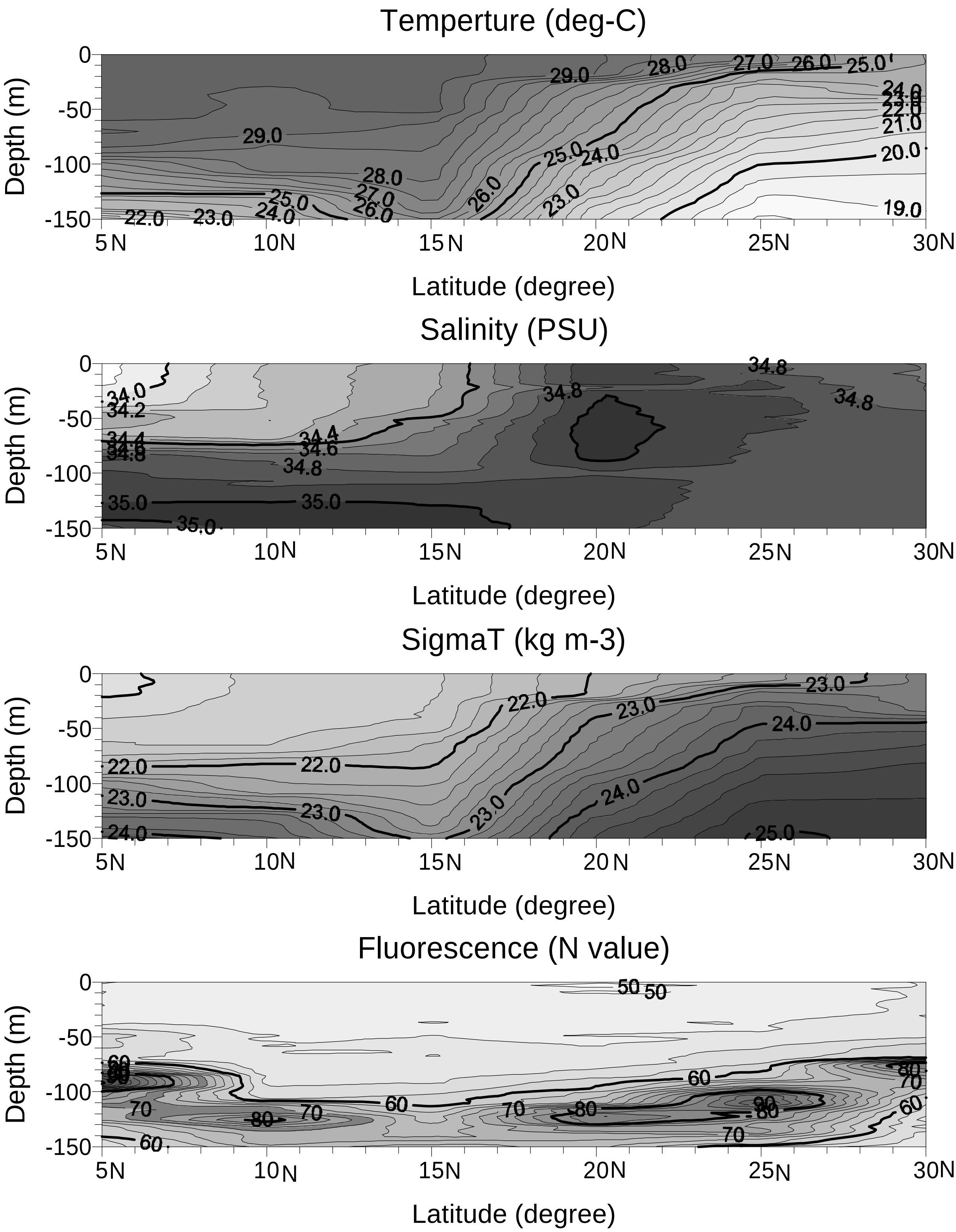

Fig. 6.8.3-1: Depth-latitude cross section of temperature, salinity, sigma-T and chlorophyl along the 140E line.

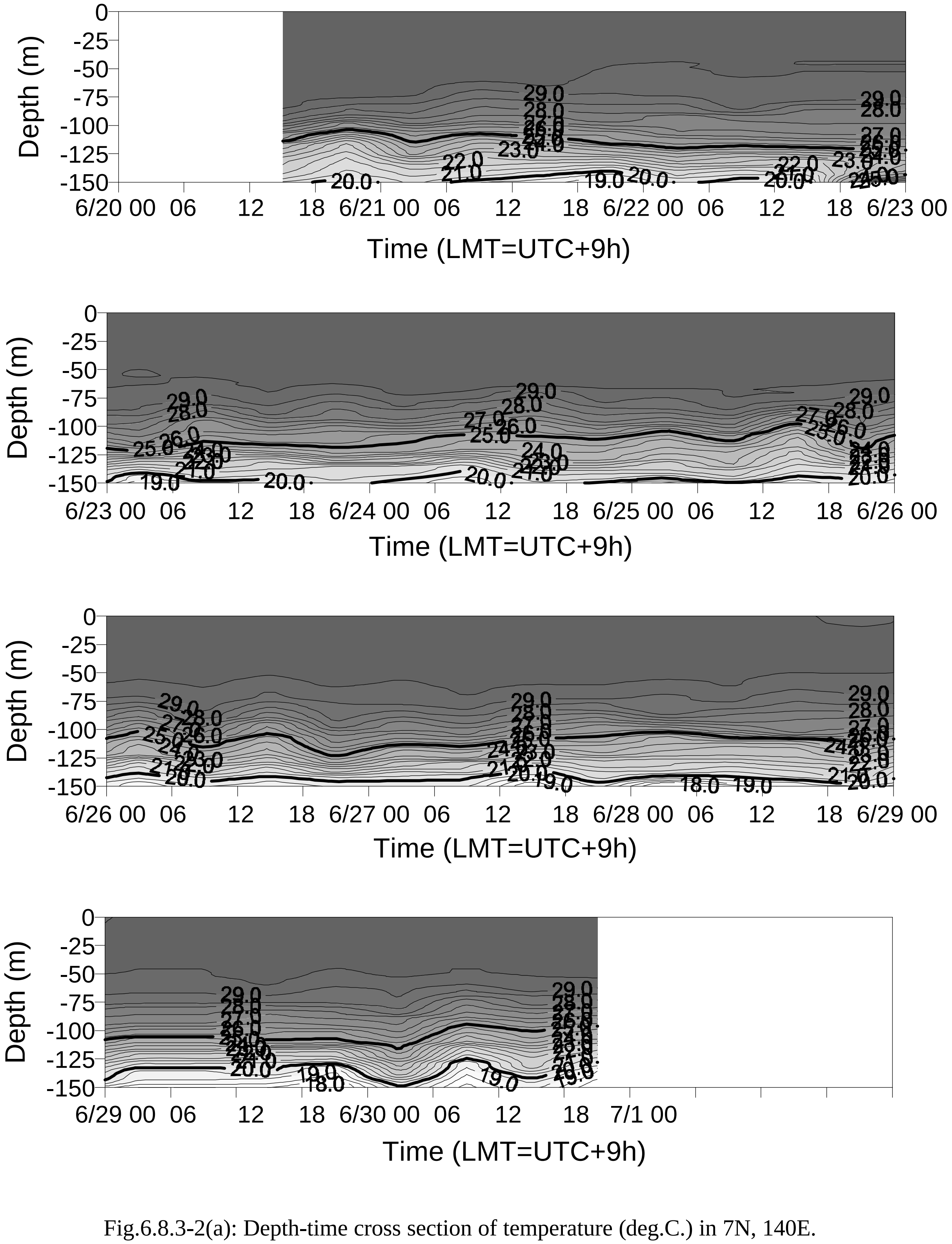

Fig.6.8.3-2(a): Depth-time cross section of temperature (deg.C.) in 7N, 140E.

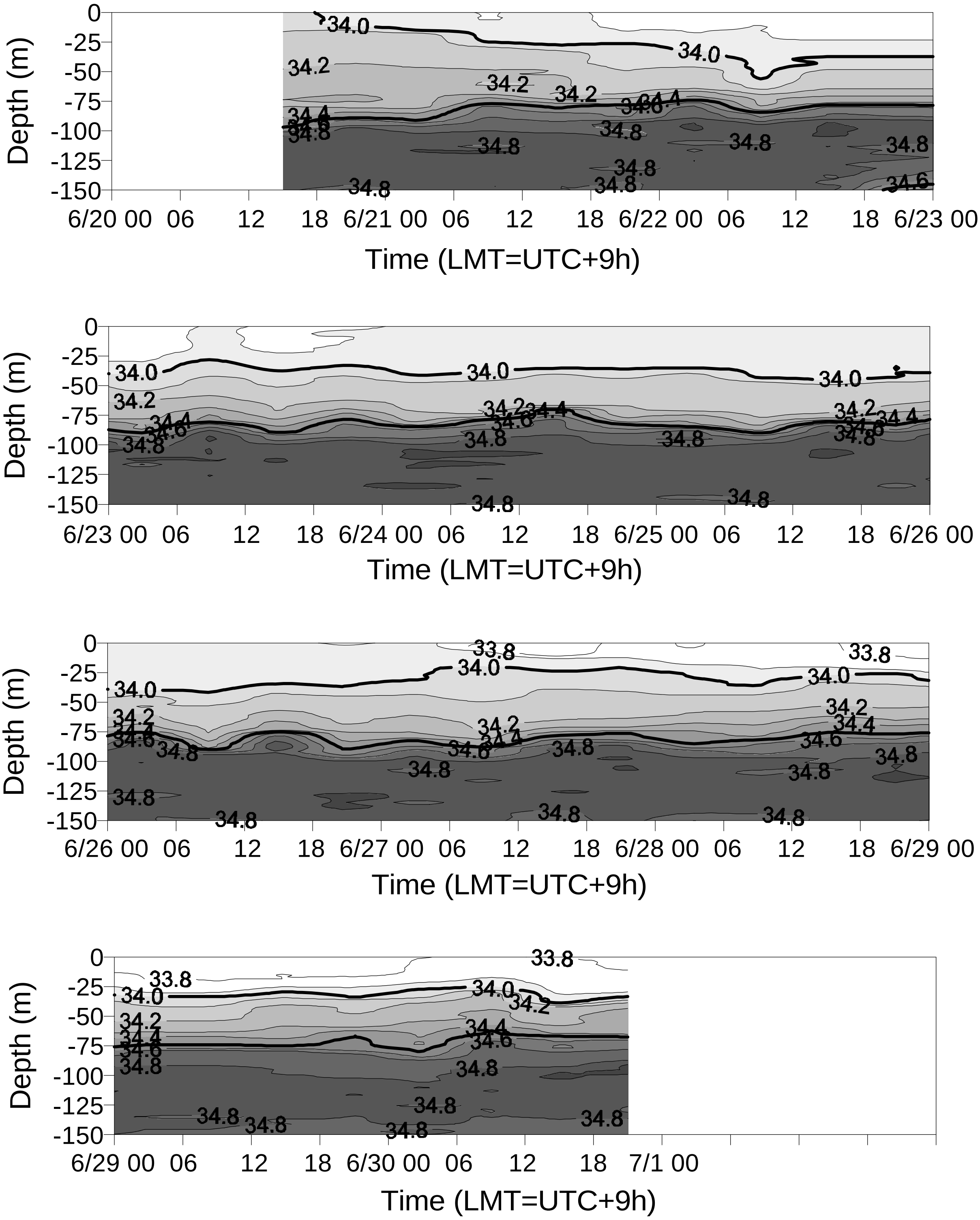

Fig.6.8.3-2(b): Depth-time cross section of salinity (PSU) in 7N, 140E.

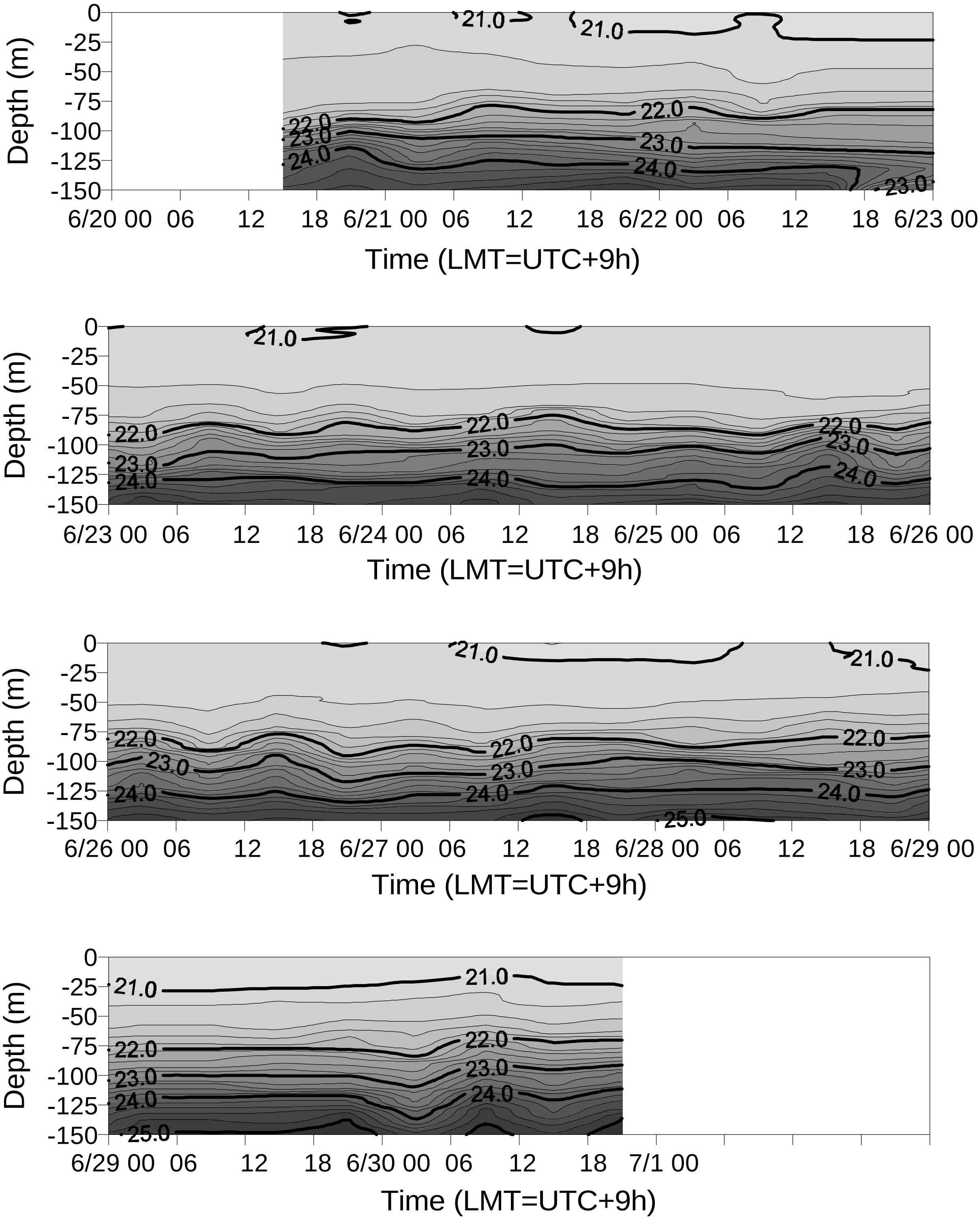

Fig. 6.8.3-2(c): Depth-time cross section of sigma-T (kg/m^3) in 7N, 140E

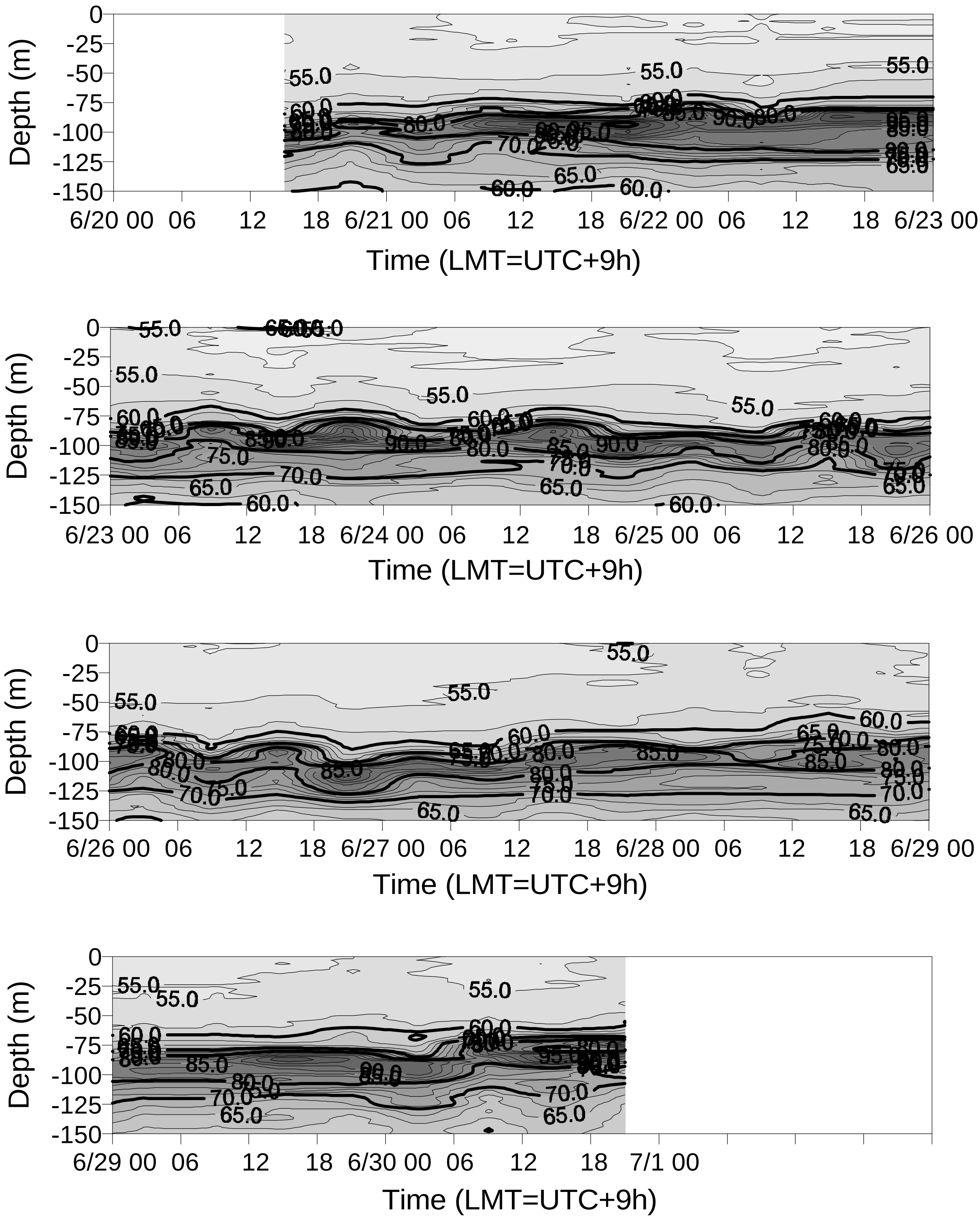

Fig. 6.8.3-2(d): Depth-time cross section of chlorophyl (N vale) in 7N, 140E.

6.9 Shipboard ADCP

(1) Personnel

Masaki Hanyu (GODI): Operation Leader
Kiyotake Kouzuma (GODI)
Fumitaka Yoshiura (GODI)
Souichiro Sueyoshi (GODI)

(2) Objectives

The ocean current profiles are measured for the use of large fields of oceanography, as the basic dataset.

(3) Methods

We measured current profiles by VM-75 (RD Instruments Inc. U.S.A.) shipboard ADCP (Acoustic Doppler Current Profiler) throughout MR00-K04 cruise from departure of Sekinehama, Japan on 13 June 2000 to the arrival of Yokosuka, Japan on 6 July 2000. The N-S (North-South) and E-W (East-West) velocity components of each depth cell [cm/s], and echo intensity of each cell [dB] are measured.

Major parameters for the measurement configuration are as follows:

Frequency:	75kHz
Averaging:	every 300 sec
Depth cell length:	1600cm
Number of depth cells:	40
First depth cell position:	30.9m
Last depth cell position:	654.9m
Ping per ADCP raw data:	16

(4) Preliminary Results

Hourly current vectors of 2-hour running mean averaged data are plotted along the ship's track for 30.9m-layer (Fig.6.9-1) and 206.9m-layer (Fig.6.9-2) respectively. Fig.6.9-3 shows the time-depth current vectors during the IOP.

(5) Data Archives

ADCP data obtained in this cruise will be submitted to the DMO (Data Management Office), JAMSTEC and will be under their control.

(6) Remarks

We used Nav_track data to make RDI_ASCII data file.

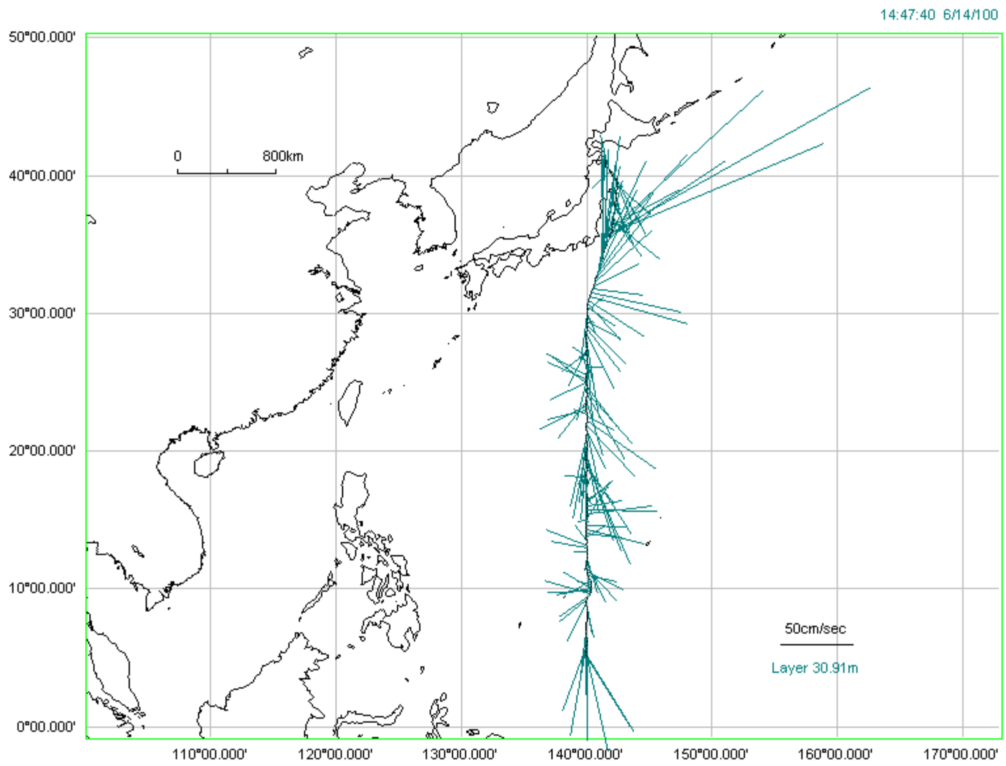

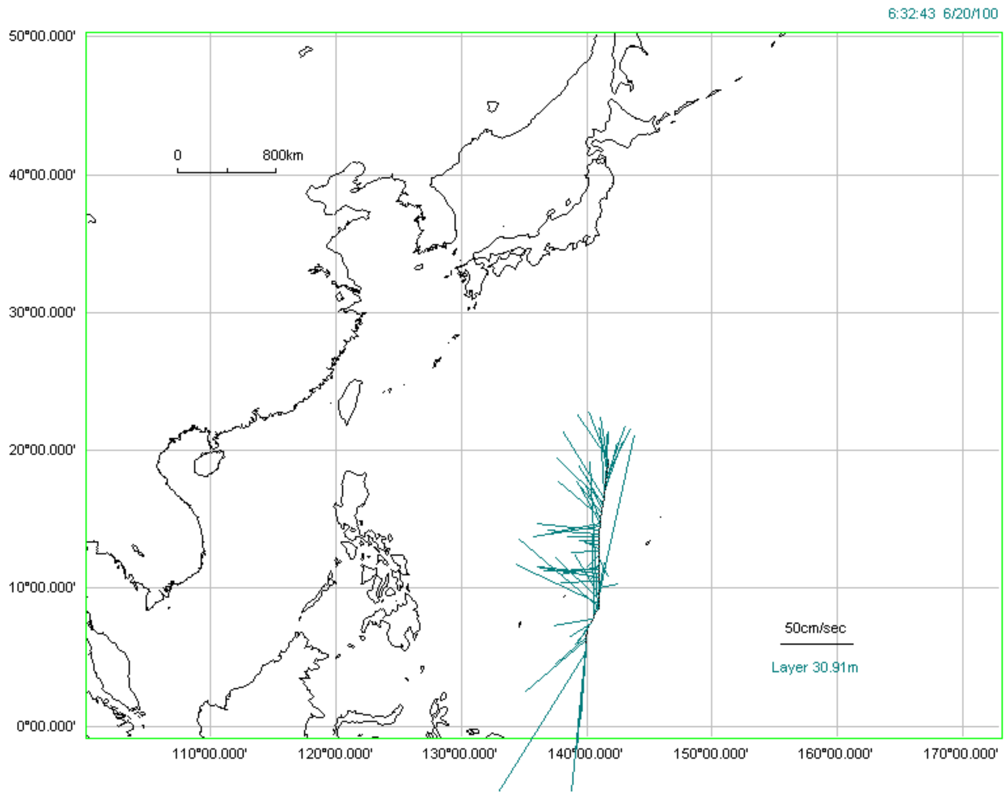

Fig.6.9-1: Two-hour averaged current vectors for every hour along the ship track, at 31m depth (upper: Jun.13-Jun.19, lower: Jun.30-Jul.4)

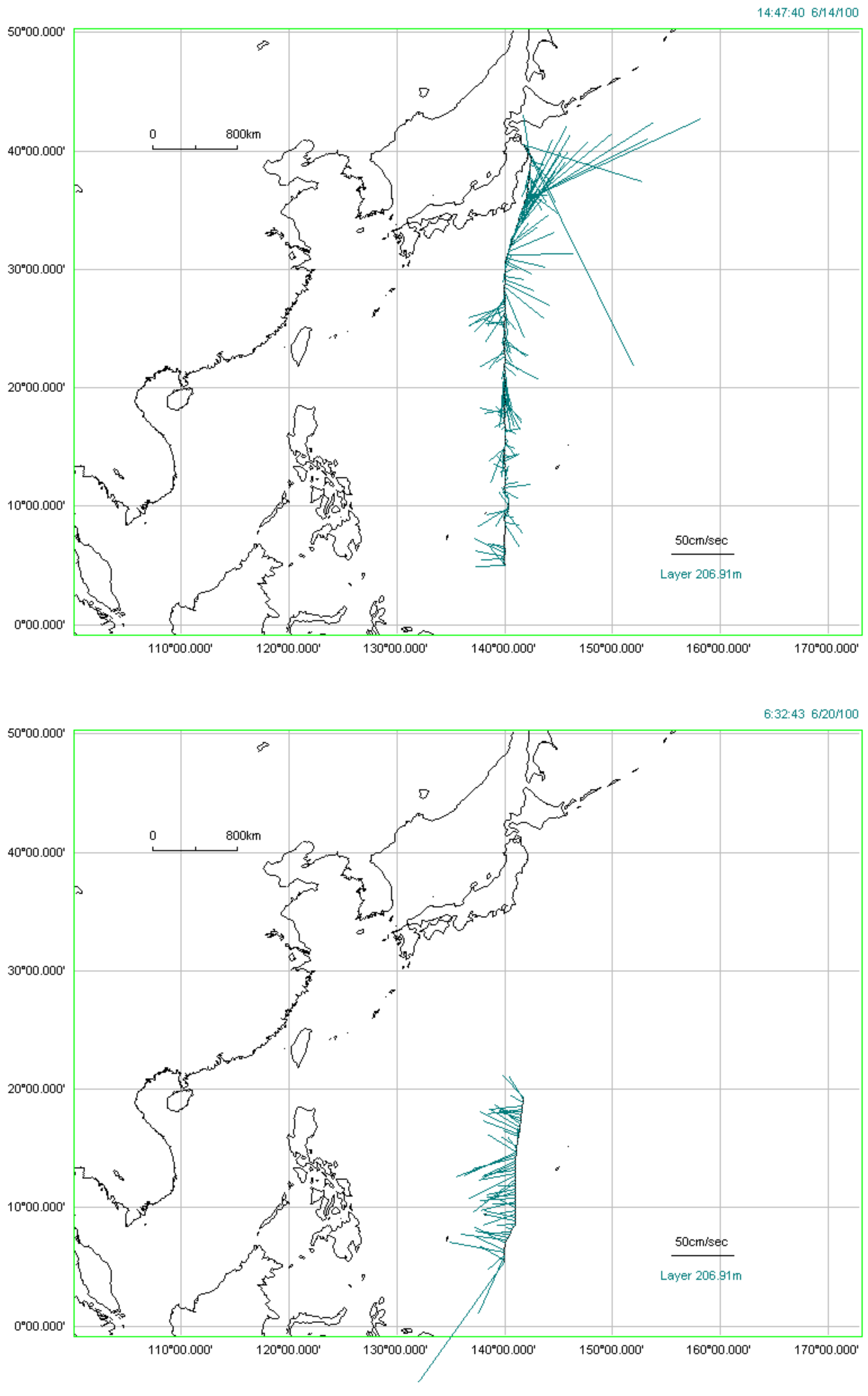

Fig.6.9-2: Same as Fig.6.9-1, except at 207m depth.

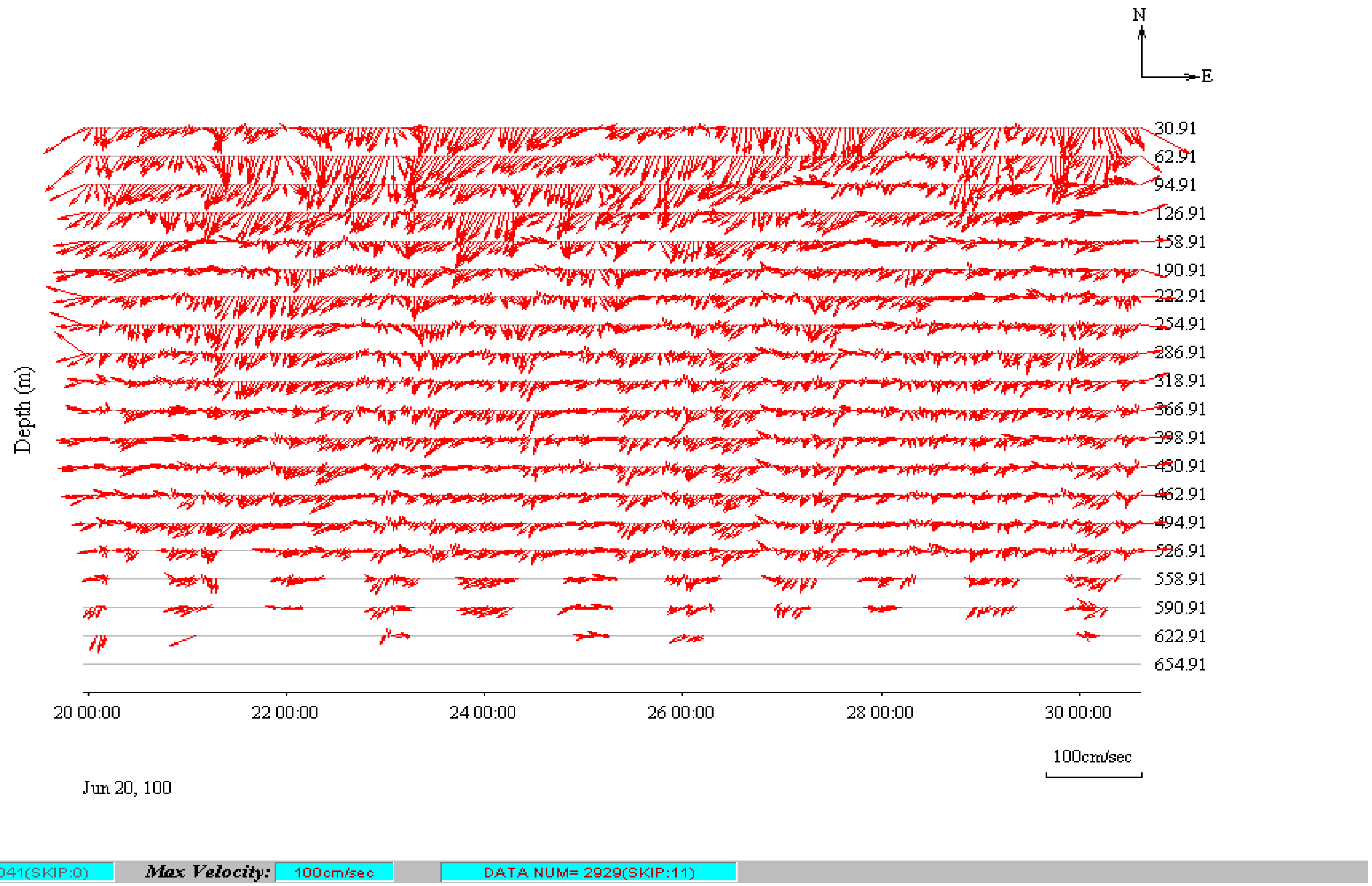

Fig.6.9-3: Time-depth current vectors during the IOP

6.10 Sea Surface Water Monitoring

(1) Personnel

Katsunori Sagishima (MWJ) : Operation Leader
Ai yasuda (MWJ)
Kaori Akizawa (MWJ)

(2) Objective

Continuous monitoring of the physical, chemical and biological characteristics of near-sea surface water.

(3) Methods

The *Continuous Sea Surface Water Monitoring System* (Nippon Kaiyo co., Ltd.) is located in the "*sea surface monitoring laboratory*" on R/V Mirai. It can automatically measure temperature, salinity, dissolved oxygen, fluorescence and particle size of plankton in the near-surface water every 1-minute. Measured data are saved every one-minute together with time and the position of ship, and displayed in the data management PC machine. This system is connected to shipboard LAN-system and provides the acquired data for p-CO_2 measurement system, etc.

The uncontaminated seawater intake is 4.5m below the sea surface. Near-surface water was continuously pumped up about 200L/min from the intake to the laboratory and then flowed into *the Continuous Sea Surface Water Monitoring System* and p-CO_2 measurement system etc. through a steel pipe. The flow rate of surface water for this system was 12L/min, which controlled by some valves and passed through some sensors except with fluorometer (about 0.3L/min) through vinyl-chloride pipes.

The Continuous Sea Surface Water Monitoring System has six kinds of sensors, which TSG comprises of two SBE sensor modules. Sea surface temperature is measured by a ship bottom oceanographic thermometer situated on the suction side of the uncontaminated seawater supply in the forward hold. Specification and calibration date of the each sensor in this system of listed below.

a-1) Temperature and salinity sensors
SEACAT THERMOSALINOGRAPH
Model: SBE-21, SEA-BIRD ELECTRONICS, INC.
Serial number: 2113117-2088
Measurement range: Temperature -5 to +35 deg-C, Salinity 0 to 6.5 S/m
Accuracy: Temperature 0.01 deg-C/6month, Salinity 0.001 S/m/month
Resolution: Temperature 0.001 deg-C, Salinity 0.0001 S/m
Calibration date: 28-Jun-00 (mounted on 29-Apr.-00 in this system)

a-2) Ship bottom oceanographic thermometer (mounted at the back of the pump for surface water)
Model: SBE 3S-A, SEA-BIRD ELECTRONICS, INC.
Serial number: 032607
Measurement range: -5 to +35 deg-C
Initial Accuracy: 0.001 deg-C per year typical
Stability: 0.002 deg-C per year typical
Calibration date: 23-Jan.-00 (mounted on 29-Apr.-00 in this system)

b) Dissolved oxygen sensor
Model: 2127, Oubisufair Laboratories Japan INC.
Serial number: 31757
Measurement range: 0 to 14 ppm
Accuracy: ±1% at 5 deg-C of correction range
Stability: 1% per month
Calibration date: 13-Jun-00

c) Fluorometer
Model: 10-AU-005, TURNER DESIGNS
Serial number: 5562 FRXX
Detection limit: 5 ppt or less for chlorophyll a
Stability: 0.5% per month of full scale

d) Particle size sensor
Model: P-05, Nippon Kaiyo LTD.
Serial number: P5024
Accuracy: ±10% of range
Measurement range: 0.02681mm to 6.666mm
Reproducibility: ±5%
Stability: 5% per week

e) Flowmeter
Model: EMARG2W, Aichi Watch Electronics LTD.
Serial number: 8672
Measurement range: 0 to 30 L/min
Accuracy: ±1%
Stability: ±1% per day

The monitoring periods (UTC) during this cruise are listed below.
13-Jun.-'00 13:15 to 30-Jun.-'00 15:00 (UTC)

(4) Preliminary Result

a) Calibration
Temperature and salinity sensor
We compared salinity values of the water samples and those from SBE21 sensor of the system (Fig 6.10-1).
Almost salinity values of the sensor were lower than those of water samples. This trend is as well as during the former cruise. We calculated the Root Mean Squares (R.M.S.) of differences of values was 0.0096 (one sigma).

References:
Porra R. J., W. A. Thompson and P. E. Kriedemann (1989) Biochem. Biophys. Acta, 975, 384 – 394.

b) Result
Every 10 minutes data are plotted along the ship's track in the period of June 13 – 19 (fig. 6.10-2), and time series at stationary observation site at (7°N, 140°E) are shown in Fig.6.10-3, respectively.
Both figures showed the respective trend of temperature, salinity, dissolved oxygen and fluorescence distributions.

(5) Other remarks
Equation was to obtain values of temperature (IPTS-68) converted into ITS-90 as follows.
$T_{90} = 0.99976 * T_{68}$
2) Period of maintenance flow cell on fluorometer was from 29-Jun-2000 04:24 to 05:37

(6) Data archive
Format of raw data files was ASCII, calibration values of salinity and temperature (IPTS-68, ITS-90) were Microsoft excel files and ASCII format files, were stored on a magnetic optical disk (M.O.disk). All the data will be submitted to the DMO at JAMSTEC.

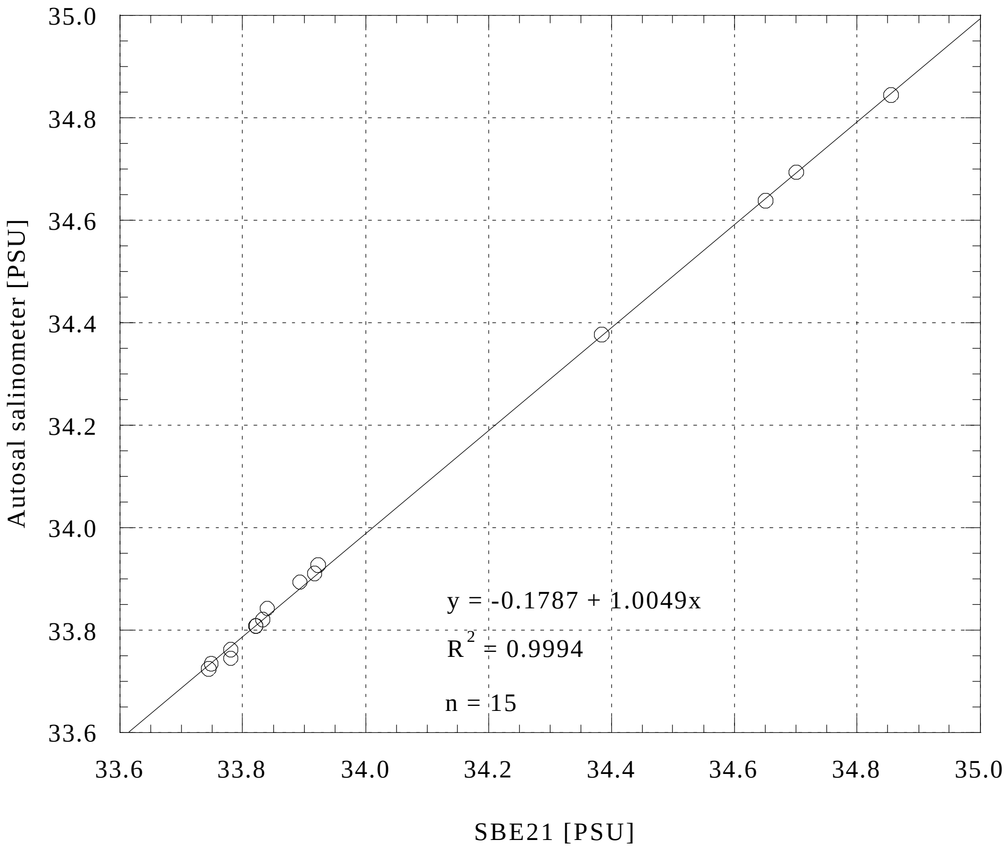

Fig. 6.10-1: Comparison between the salinity values measured by SBE21 of the Sea Surface Monitoring Ssytem and Autosal salinometer for 15 samples. (Note: Salinity in this figure is not corrected).

(a)

(b)

(c)

(d)

(e)

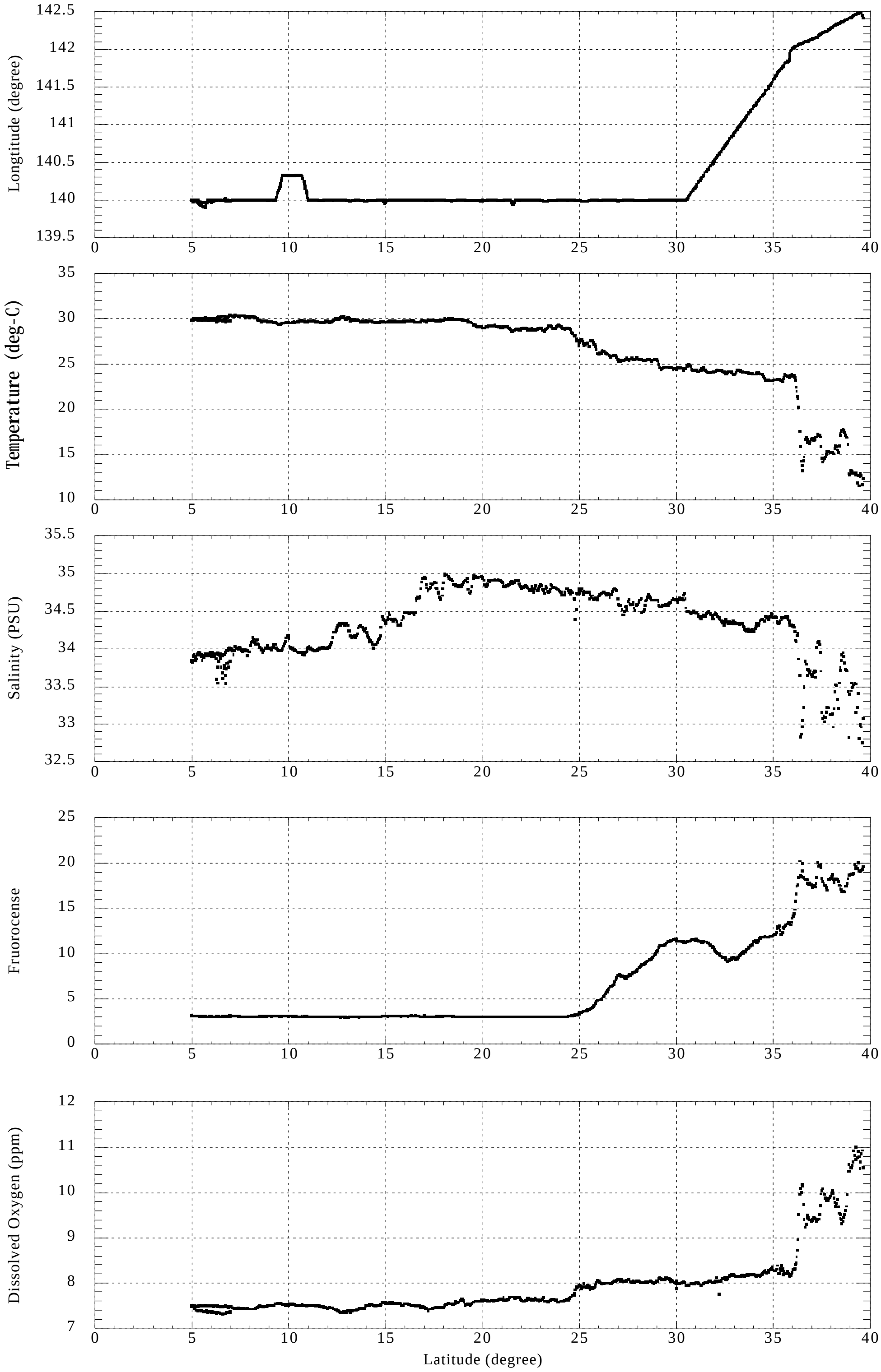

Fig. 6.10-2: Observed spatial variation of (a) ship track, (b) temperature, (c) salinity, (d) fruorocense and (e) dissolved oxygen from 40N to 5N.

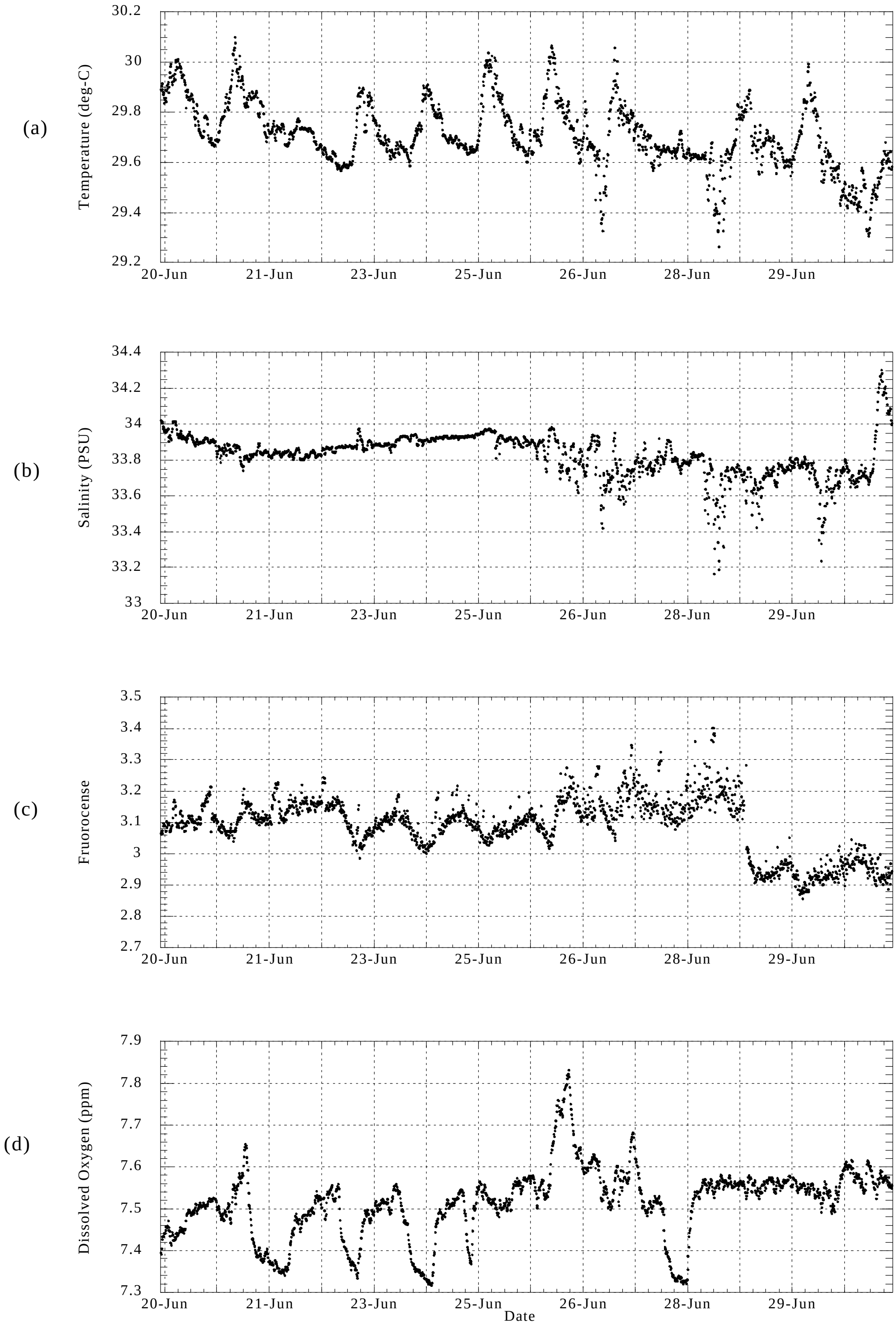

Fig. 6.10-3: Observed temporal variation of surface water on (a) temperature, (b) salinity, (c) fruorocense and (d) dissolved oxygen from Jun.20 to Jun.30.

6.11 N_2O and CO_2 Measurements

(1) Personnel

Hiroshi Ishida
(Maritime University of Kobe / Frontier Observational Research System for Global Change): Principal Investigator

Mitsuru Hayashi (Maritime University of Kobe)

Kenichi Shibayama (University of Osaka)

Kaichi Moriwaki (University of Osaka)

Kunimitsu Ishida (Toba National College of Maritime Technology)

Ayako Nakanishi (Okayama University)

(2) Objectives

N_2O (Nitrous oxide) and CO_2 (Carbon dioxide) gasses play important roles and functions of the global warming. It is required to get more accurate information of those gas exchanges between the sea and the atmosphere in order to understand the mechanism of the global warming process. The measurements of those gas concentrations in the atmosphere and sea water were made during the navigational/observational periods toward/at the observational point in the Equatorial Western Pacific, 07 N and 140 E, for two weeks from 16 June to 30 June in 2000. The observational period, date and position are listed in Table 6.11.1.

Table 6.11.1 Observational period, date and position

Period (June)	Position	Measurement (Surface water/Vertical distribution)
16 – 20	25N, 140E to 7N, 140E	6 hourly measurement of N_2O and CO_2 in surface sea water
26 – 28	7 N, 140 E	3 hourly measurement of N_2O and CO_2 in surface sea water
23	7 N, 140 E	Measurement of vertical distribution of N_2O (0, 50, 150, 200, 300, 500, 1000 m)
24	7 N, 140 E	Measurement of vertical distribution of N_2O (0, 50, 100, 150, 250, 750, 1000 m)
25	7 N, 140 E	Measurement of vertical distribution of N_2O (0, 100, 200, 300, 400, 500, 750 m)
30	7 N, 140 E	Measurement of vertical distribution of N_2O (1000 m; N_2O measurement only)

(3) Methods

The sample air was intaken at the foremast about 11m height above the sea level, and surface sea water was intaken from the bottom of the R/V MIRAI at about 5 m depth. Sea water for the vertical distribution measurement was sampled by the niskin sampler. N_2O and CO_2 concentrations were measured with N_2O and CO_2 infrared gas analyzers. Both gas concentrations in sea water were obtained by the babbling method.

Specification of analyzer is as follows;

CO_2 Infrared Gas Analyzer
- Model: VIA-510 (HORIBA Ltd.)
- Accuracy: 0.5 % of full scale

N_2O Infrared Gas Analyzer
- MODEL: 46C (Thermo Environmental Instruments Inc.)
- Accuracy: 2 % of full scale < 50 ppm

(4) Preliminary Results

6 hourly time series of N_2O and CO_2 concentrations in the atmosphere and surface sea water from June 16 to 20 and 3 hourly time series from June 26 to 28 are shown in Figs 6.12.1 and 6.12.2, respectively. N_2O and CO_2 concentrations in the atmosphere are higher than those in surface sea water.

The vertical distributions of the N_2O concentrations in sea water from 50 to 1,000 m in depth are shown in Fig. 6.12.3. The concentration increases from surface water to 300 m and tends to be constant in deep sea water from 400 to 1,000 m depth. The maximum peak is found in 300 m depth. All observational data will have a quality check and be analyzed in detail later.

(5) Data archives

The data are archived in a floppy disk and will have a quality check in Maritime University of Kobe, and will be distributed to the public later. The raw data are submitted to the JAMSTEC DMO.

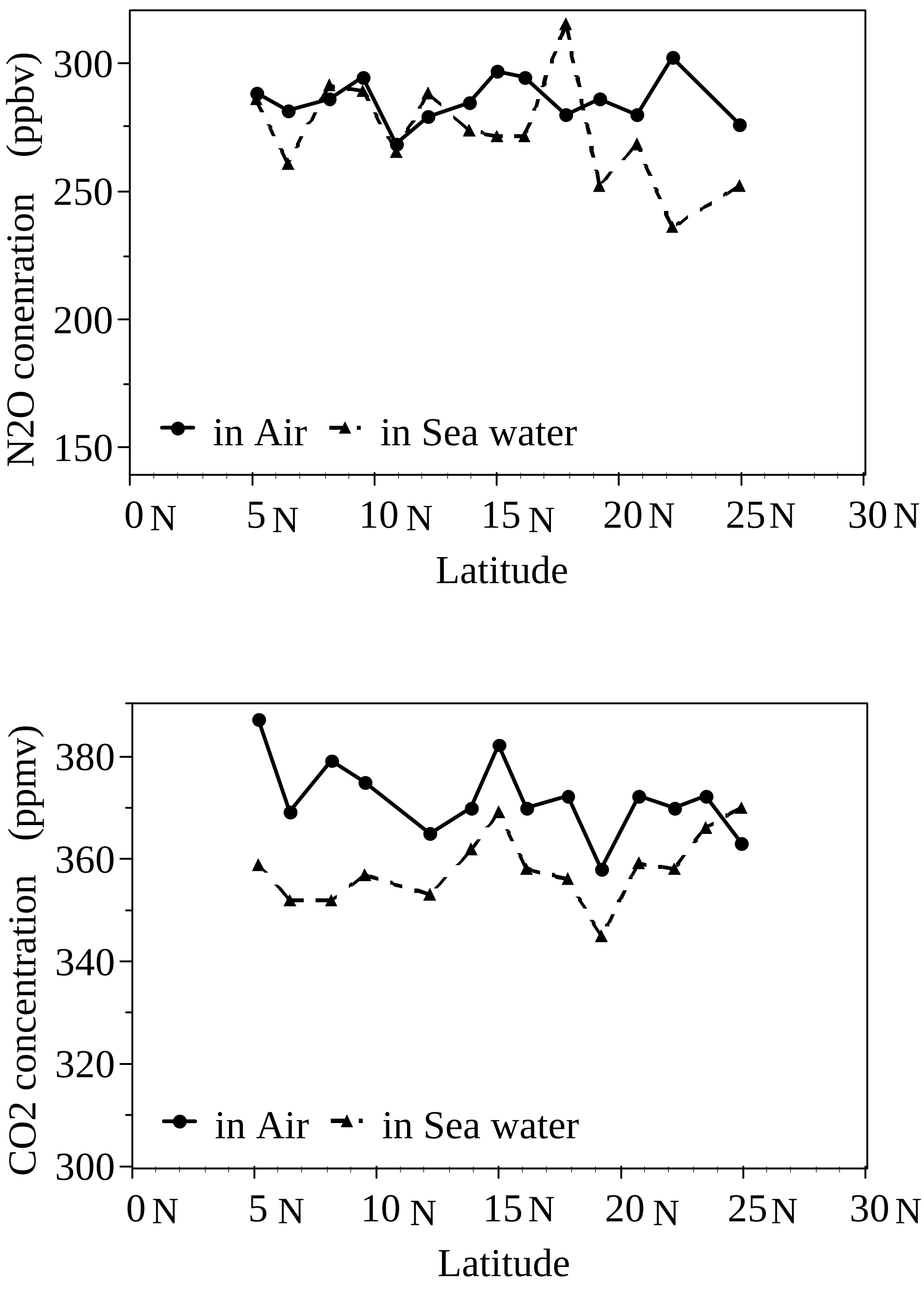

Fig. 6.11-1: Spatial variations of N2O and CO2 concentrations in air and surface sea water along the 140E line.

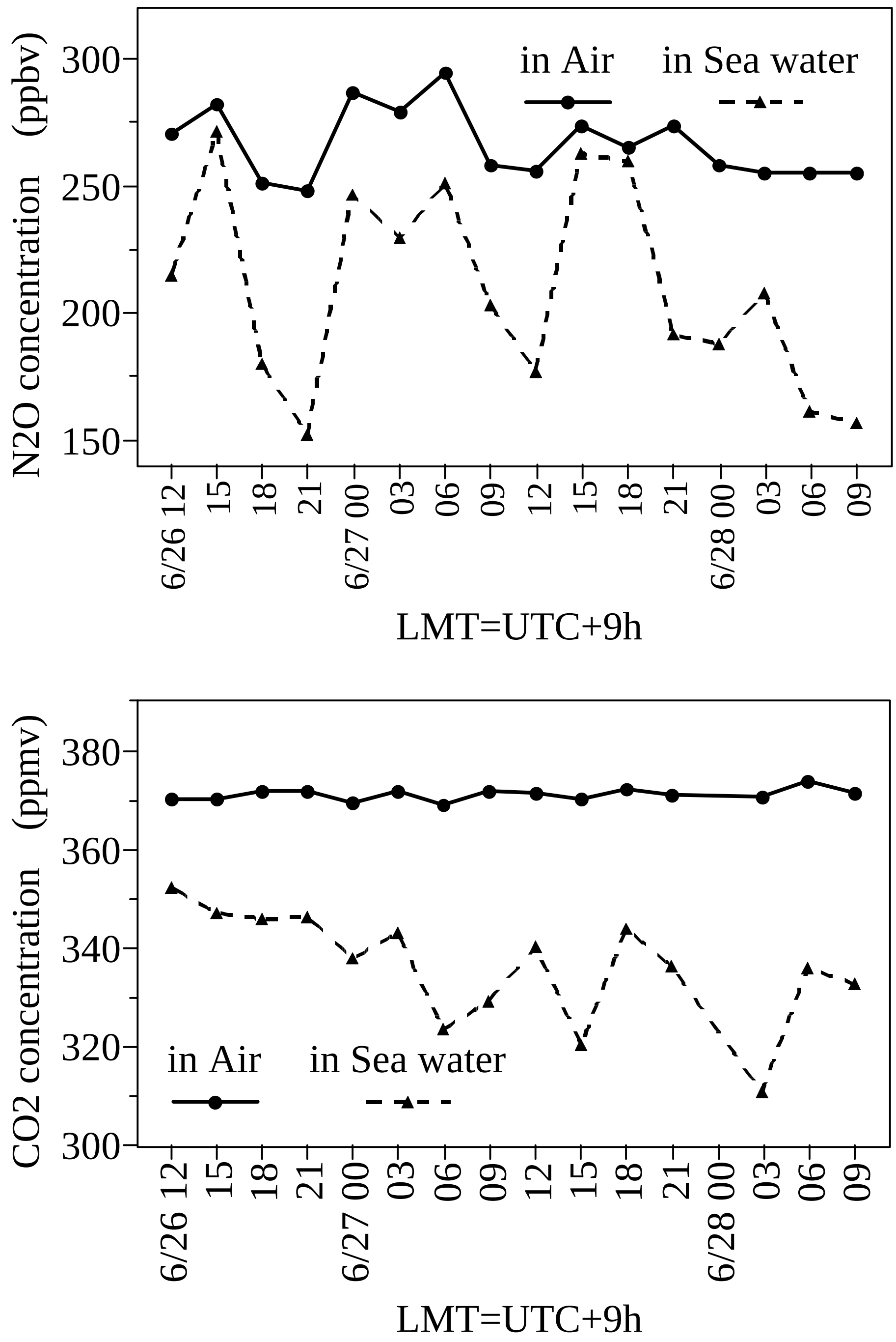

Fig. 6.11-2: Temporal variations of N2O and CO2 concentrations in air and surface sea water in 7N, 140E.

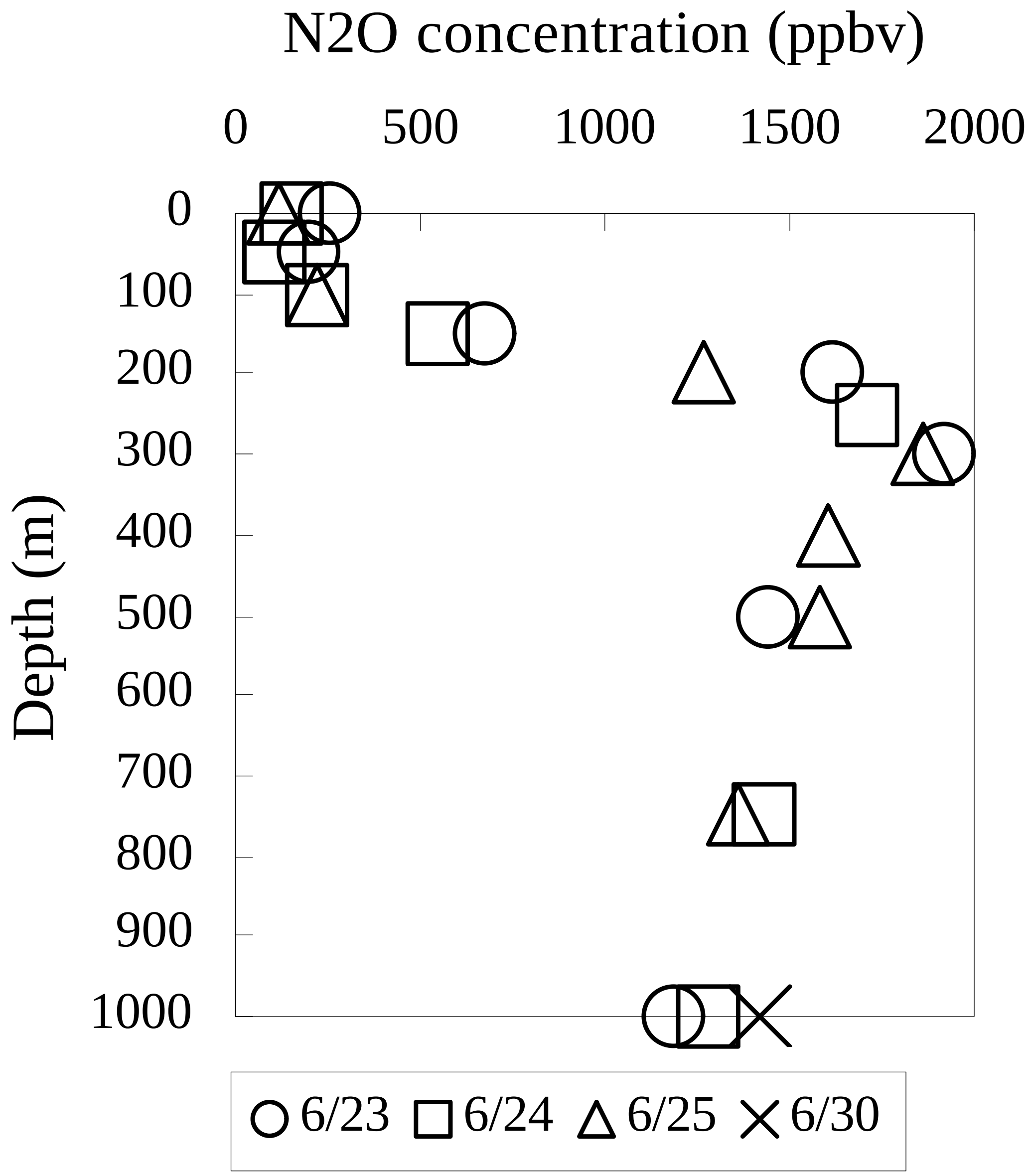

Fig. 6.11-3: Vertical distributions of N2O concentration in 7N, 140E.

6.12 pCO_2/PCO_2 Measurement

(1) Personnel

Eiji Yamashita (Okayama University of Science) ： Observation leader
Takehiko Kono (Okayama University)
Jun Iwata (Okayama University of Science)

(2) Objective

Latitudinal distribution of pCO2 and PCO2 between Sekinehama and the equatorial station(5.00°N, 140.00°E).

Time variation of pCO2 at the equatorial station(7.00N,140.00E).

Vertical distribution of pCO2 at station A(30.00°N, 140.00°E), B(25.00°N, 140.00°E), C(20.00°N, 140.00°E), D(15.00°N, 140.00°E), E(10.00°N, 140.00°E), F(7.00°N, 140.00°E) and G(5.00°N, 140.00°E).

(3) Methods

Carbon dioxide in the sea water and carbon dioxide in the atmosphere were measured using the measurement system which is made by the S-ONE company.

The present CO_2 instrument only requires a small amount of sea water sample to measure pCO_2. 500 ml sea water is enough to determine pCO_2.

It located in the sea surface laboratory on this ship.

Surface sea water was pumped up to the laboratory and deep sea water was obtained by CTD-RMS sea water sampling system. Sample air was introduced from foremast.

We had measured from June 13 to July 4, 2000. We checked the system everyday.

Specification of the carbon dioxide measurement system was listed below.

Unit 1: CO2 analyzer
  Model: LI-6252 LI-COR ,INC.
  Serial number: IR-62-286
  Measurement range: 0-5V
Unit 2: Gas mixing unit
  Model: SO96NL-T, S-ONE, INC.
Unit 3: Equilibrumeter
  Model: SO96NL-T, S-ONE, INC.
Unit 4: Data processing equipment (personal computer)

(4) Results

Fig. 6.12-1 shows the latitudinal distribution of pCO_2 and PCO_2 during Sekinehama(41.20°N, 140.42°E) to Sta. A(30.00°N, 140.00°E), from June 13 to June 15, 2000. The pCO_2 concentrations are higher than pCO_2 during Sekinehama to Sta. A. This result is support that during this period, this area is found to be a CO_2 sink.

Fig .6.12-2 shows the time variation of pCO_2 from June 23 to June 30, 2000 at the equatorial station F (7.00°N, 140.00°E). The raw pCO_2 concentrations show that low value in nighttime and high value in daylight hours. The PCO_2 concentrations are higher than pCO_2. This result is support that during this period, equatorial station F (7.00°N, 140.00°E) is found to be a CO_2 sink.

Fig .6.12-3 shows the vertical profile of carbon dioxide in the sea water (pCO_2) at the Sta. A(30.00N, 140.00E), D(15.00N, 140.00E), G(5.00N, 140.00E) in June 15, June 18, June 20, 2000, respectively. As a whole, pCO_2 increased with increasing the depth. The pCO_2 values of 1000 m depth were above 2000ppmv. However, the large inflection point of Sta. A, D and G were differed, respectively.

Fig .6.12-4 shows the vertical profile of pCO2, pH and dissolved oxygen(DO) in the sea water at the Sta. D(15.00N, 140.00E) in June 18, 2000. Contrary to the pCO_2 profile, pH and dissolved oxygen decreased with increasing the depth. The phenomenon of pCO_2 increase with depth is caused by the biological pump. A maximum peak of dissolved oxygen was observed at 100 m.

(5) Data archive

The raw data were stored on a magnetic optical disk which will be kept on Ocean Research Department, JAMSTEC. The raw data were corrected and will be published.

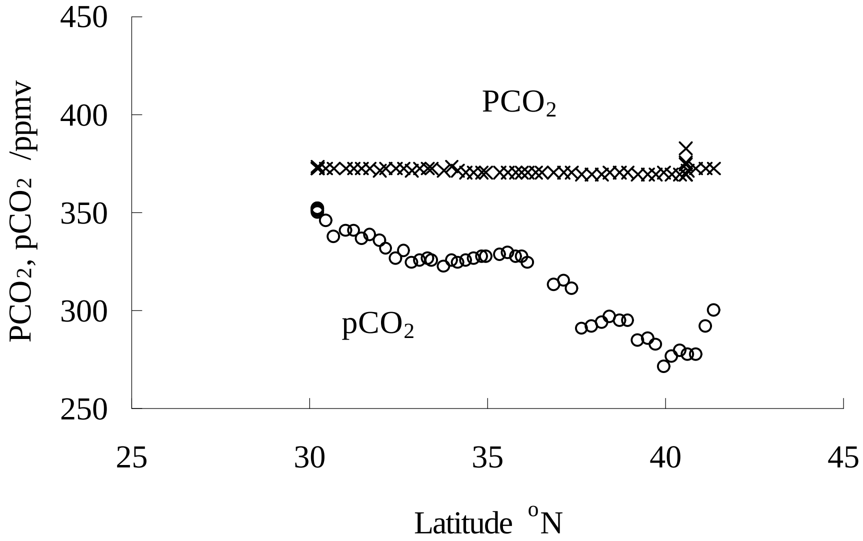

Fig.6.12-1 Latitudinal distribution of carbon dioxide in the sea water (pCO_2) and carbon dioxide in the atmosphere (PCO_2) during Sekinehama to the Sta. A(30.00°N, 140.00°E) from June 13 to June 15, 2000.

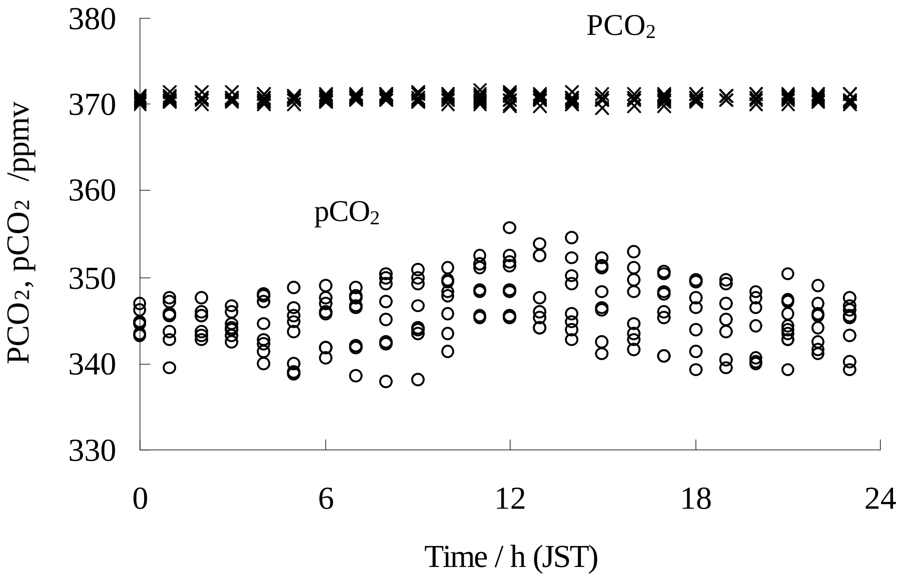

Fig.6.12-2 Time variation of carbon dioxide in the sea water (pCO_2) and carbon dioxide in the atmosphere (PCO_2) from June 23 to June 30, 2000 at the Sta. F(7.00ºN, 140.00ºE).

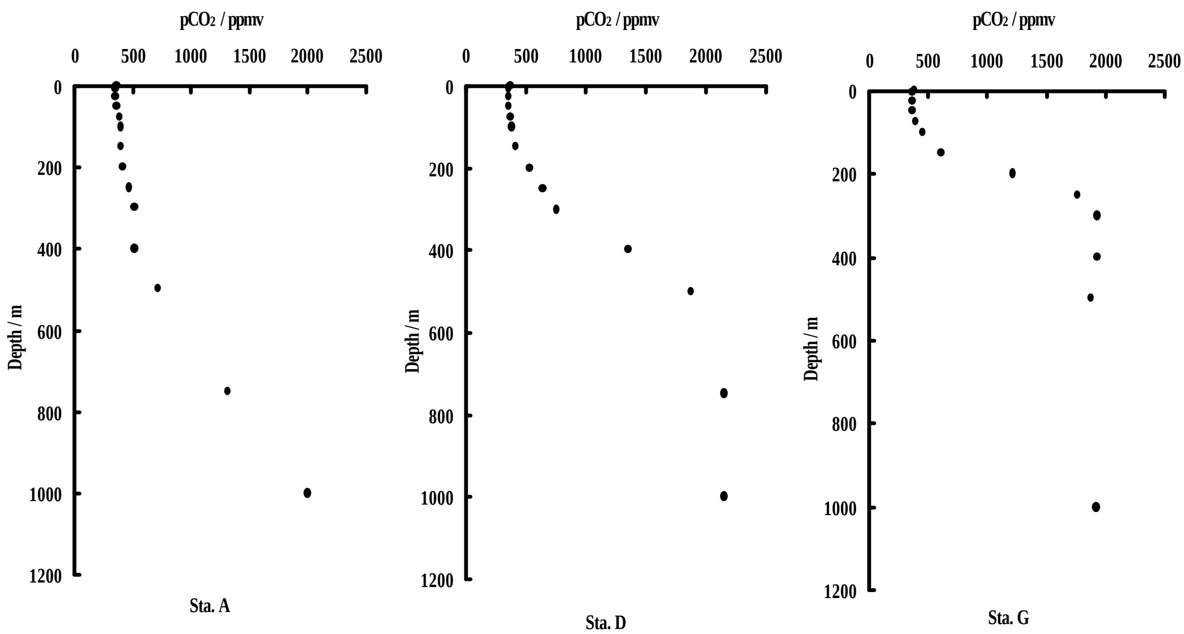

Fig .6.12-3 Vertical profile of carbon dioxide in the sea water (pCO_2) at the Sta. A(30.00N, 140.00E), D(15.00N, 140.00E), G(5.00N, 140.00E) in June 15, June 18, June 20, 2000, respectively.

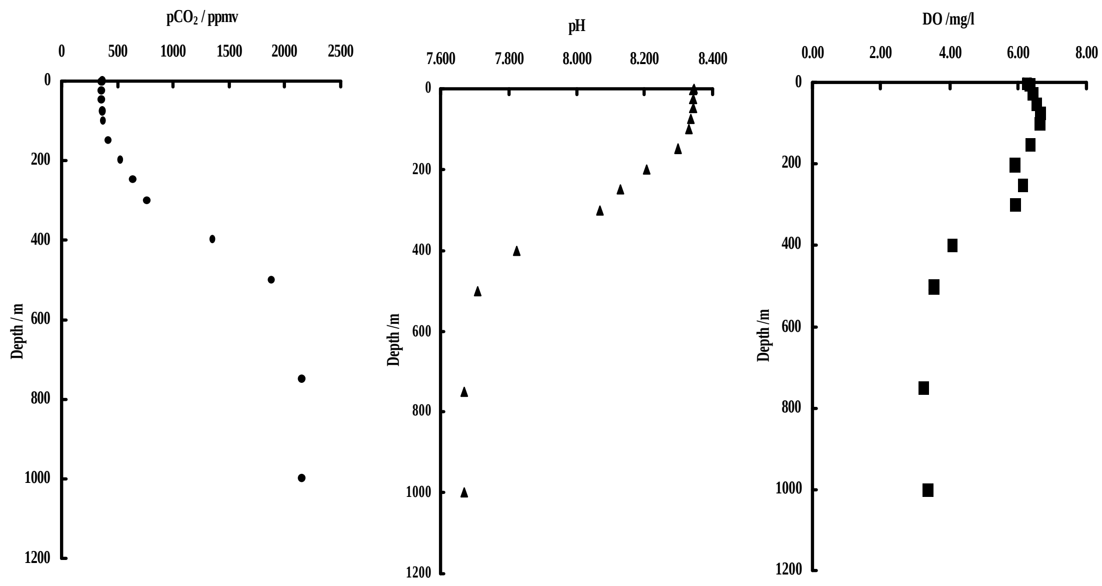

Fig .6.12-4 Vertical profile of pCO_2, pH and dissolved oxygen(DO) in the sea water at the Sta. D(15.00N, 140.00E) in June 18, 2000.